Strategies for improving the genetic toolbox in *Aedes aegypti* mosquito

by

Ivan Hok Yin Lo

B,Sc. Hons (Animal Biology), University of British Columbia, 2021

A THESIS SUBMITTED IN PARTIAL FULFILLMENT OF
THE REQUIREMENTS FOR THE DEGREE OF

MASTER OF SCIENCE

in

The Faculty of Graduate and Postdoctoral Studies

(Zoology)

THE UNIVERSITY OF BRITISH COLUMBIA

(Vancouver)

April 2024

The following individuals certify that they have read, and recommend to the Faculty of Graduate and Postdoctoral Studies for acceptance, the thesis entitled:

Strategies for improving the genetic toolbox in *Aedes aegypti* mosquito

submitted by Ivan Hok Yin Lo in partial fulfilment of the requirements for

the degree of Master of Science

in Zoology

Examining Committee:

Ben Matthews, Assistant Professor, Zoology, UBC
Supervisor

Kota Mizumoto, Associate Professor, Zoology, UBC
Supervisory Committee Member

Kevin Wei, Assistant Professor, Zoology, UBC
Additional Examiner

Additional Supervisory Committee Member:

Nozomu Yachie, Professor, School of Biomedical Engineering, UBC
Supervisory Committee Member

Abstract

The yellow fever mosquito, *Aedes aegypti*, is a prevalent vector that spreads transmissible diseases in human populations. In the past few decades, increasing effort have been made to study these fascinating animals. The rising research in CRISPR/Cas9 technology has allowed the potential for gene editing to be done in *Ae. aegypti*. This thesis focuses on three novel applications of CRISPR/Cas9 in *Ae. aegypti* that focus on improving gene editing efficiency and expanding the mosquito genetic toolbox.

In the first chapter, germline gene promoters (*zpg* and *nanos*) are used to promote the expression of Cas9 proteins. We hypothesized that germline gene promoters can bias Cas9 expression in space and time to favor Homology Directed Repair (HDR). We discovered that transient tail expression of fluorescence markers in injected mosquitoes successfully predicted integration of transgene into the germline. This transgene was able to be passed on to the next generation. The use of germline gene promoters can reduce efforts in creating transgenic mosquitoes, as it increases mosquito survival rate and reduce time needed to screen fluorescence.

In the second chapter, a sgRNA and donor template cassette was inserted into the mosquito genome through *piggyBac* transposon integration to create a split CRISPR system. We hypothesized that the endogenous expression of CRISPR components in a split system can favor HDR. We found no offspring that had a stable integration of transgene through HDR, while most strains exhibited Mendelian inheritance of

fluorescence genes. Our results show that split systems in gene editing should test multiple candidates to ensure Cas9 activity.

In the third chapter, we aimed to create a novel balancer chromosome in *Ae. aegypti* through utilizing CRISPR/Cas9 to generate a large chromosomal inversion. We applied methods of CRISPR gene editing at two target sites simultaneously, which has the potential for HDR repair to invert the chromosome segment between these sites. Future work will validate the sequences of putative G_0 founders. These are the first steps towards creating a novel balancer chromosome.

Lay Summary

Yellow fever mosquitoes are dangerous vectors that take bloodmeals from humans. Many attempts have been made to control their population worldwide, with some using the power of genetics. To create a genetically modified mosquito, a long time and a lot of effort must be invested by researchers. The work done in this thesis presents various attempts to improve what we can do in mosquito genetics. We used different strategies to tackle current problems with CRISPR gene editing in mosquitoes. We also plan to create a new tool that can help reduce the effort needed to breed mosquitoes. Some of my results show that certain strategies fail to work due to mosquitoes being weaker when genetically modified. We provide some suggestions for future work in this field, as well as present evidence for exciting first steps in generating a novel tool.

Preface

The work completed in this thesis is primarily done by the author, Ivan Lo. All experiments were completed by Ivan Lo at the Ben Matthews Lab. The work done to validate sgRNA activity was previously published by me and Dr. Benjamin Matthews. This thesis is an extension of a previous thesis done during my Honors work as a B.Sc. student in UBC.

In Chapter 2 – Helper Plasmid, embryo microinjections and the initial screening of helper plasmid strains were completed by our collaborators, the members of the McMeniman Lab. The idea behind Chapter 2 and Chapter 3 were conceived through collaboration of Dr. Ben Matthews, Dr. Conor McMeniman, Dr. Andrew Hammond and me. In Chapter 4, the strategy for creation of a novel balancer chromosome was suggested by one of my committee members, Dr. Kota Mizumoto.

The illustration of *Aedes aegypti* was done by a fellow graduate student in the Ben Matthews Lab, Leisl Brewster. All figures and data analysis were completed by Ivan Lo with the use of Microsoft Excel, GraphPad Prism, R studios and Adobe Illustrator. The embryo microinjection set up was done with the help of Cassidy Mark and Nicholas Tochor. The creation of helper plasmid was done with the help of Jonathan Chiang and the validation of gene targets for balancer chromosome was done with the help of Dania Samara. Both students completed their work under the direct supervision of Ivan Lo.

All transgenic mosquito strains were kindly provided to us by the McMeniman Lab, Johns Hopkins University.

Table of Contents

List of Tables

List of Figures

List of Abbreviations

Ae. aegypti: Aedes aegypti

An. gambiae: Anopheles gambiae

C. elegans: Caenorhabditis elegans

CRISPR: Clustered Regularly Interspaced Short Palindromic Repeats

D. melanogaster: *Drosophila melanogaster*

DIPA-CRISPR: Direct Parental CRISPR

HDR: Homology Directed Repair

ITR: Inverted terminal repeat

LVP: Liverpool

NHEJ: Non-Homologous End Joining

PCR: Polymerase Chain Reaction

ReMOT Control: Receptor-Mediated Ovary Transduction of Cargo

RIDL: Release of Insects Carrying a Dominant Lethal Gene

RNP: Ribonucleoprotein

sGD: split Gene Drive

sgRNA: single-guide RNA

SIT: Sterile Insect Technique

ssODN: single-stranded oligodeoxynucleotide

TC: Transposon Transgene Cassette

TE: transposable elements

WT: Wildtype

Acknowledgements

I offer my gratitude to Dr. Benjamin Matthews and the members of the lab at UBC, who have helped me achieve my goals to study gene editing and push the frontiers of CRISPR. I owe my gratitude to my fellow lab members, Orna, Leisl, Elsa, Jonathan, Nick, Cassidy and Bridget who have all contributed to my academic career.

Special thanks to members of the McMeniman Lab for allowing me to collaborate with them on studying the fascinating mosquitoes. Thank you to Dr. Conor McMeniman, Dr. Margaret Wohl and Dr. Andrew Hammond for taking time to teach me the basics of embryo microinjection.

I am inspired to continue contributing to the world of science.

1 Introduction

1.1 Introduction to CRISPR/Cas9 and *Aedes aegypti*

1.1.1 Introduction to *Aedes aegypti* mosquito

The yellow fever mosquitoes *Aedes aegypti* cause significant mortality in humans annually by the transmission of pathogens (Dong et al., 2015; Scott & Takken, 2012). When infected by arboviruses, these mosquitoes become vectors that can carry yellow fever, dengue, chikungunya and zika (Barrett & Higgs, 2007; S. B., 2008). Specifically, *Ae. aegypti* are anthropophilic mosquitoes that prefer human as blood source, as females require nutrients from blood meals for energy and egg development (Scott & Takken, 2012). Once females bite an infected human, arboviruses can stably infect and harbor in the mosquito. These females can spread viruses when they take subsequent bloodmeals, thereby spreading throughout a human population. (Fuller, 1961; McBride et al., 2014). Combined with their ability to lay large numbers of eggs in small bodies of fresh water (Fuller, 1961; Matthews, Younger & Vosshall, 2019), this makes yellow fever mosquitoes dangerous organisms that must be carefully controlled and studied.

1.1.2 Methods in traditional mosquito population control

Mosquito population control has traditionally relied on chemical insecticides, but the effectiveness of pesticides has waned due the development of resistance to chemicals. As an improvement to traditional strategies, genetic controls have been steadily implemented worldwide in the last decade. These genetic controls can prevent viral infections, cause mosquito sterility, or introduce genetic disruptions (Alphey, L., 2014). To control the spread of arboviruses by *Ae.* aegypti, strains of mosquito with a

stable infection of intracellular bacteria *Wolbachia pipientis* has been deployed in the field to limit viral infections (Moreira et al., 2009; Tantowijoyo et al., 2022). To reduce *Ae. aegypti* populations, Sterile Insect Technique (SIT) makes use of the mass release of sterile male mosquitoes. If effective, female mosquitoes that mate with sterile males will fail to develop viable offspring (Phuc et al., 2007; Krafsur, 1998). The male determining factor *Nix* in *Ae. aegypti* can also be expressed to convert females into males, or even cause females to die off. This creates a male bias in the population and reduces the overall population (Adelman & Tu, 2016). SIT has been further developed into the Release of Insects Carrying a Dominant Lethal Gene (RIDL) system, which is a cassette carrying dominant lethal genes, causing the population to crash when males mate and spread this transgene to the offspring (Labbe et al., 2012). Traditional SIT uses irradiation to sterilise males but induce high fitness costs and require separating males from females; the RIDL system uses genetic insertion of a lethal cassette that can sometimes help differentiate male and female phenotypes (Labbe et al.,2012; Wang et al., 2021). These traditional methods suppress mosquito populations through the mass release of lab mosquito strains, without causing genetic modifications to wild populations.

1.1.3 Summary of genetic manipulation techniques

Targeting genetic factors in the mosquito requires molecular techniques that have been developed in recent years. Using *in vivo* genetic manipulation, gene editing has been introduced to help alter mosquito populations. Genetic manipulation of *Ae. aegypti* aims to introduce transgenic elements into the mosquito to alter their genotypes and phenotypes. Transposable elements (TE) like *Mariner* (Coates et all., 1998), *Hermes*

(Jasinskiene et al., 1998) and *piggyBac* transposons (Kokoza et al., 2001; Lobo et al., 2006) were used to insert transgenes at random into the *Ae. aegypti* genome. These inserted elements can range from visual markers to lethal constructs. Manipulation later involved the cleavage of DNA using Homing Endonuclease Genes (HEG) and synthetic *Medea* element to bias inheritance of genes of interest (Alphey, 2014; Burt, 2003; Hay et al., 2010). These methods then further developed into targeted gene knockout using Zing Finger Nucleases (ZFN) (DeGennaro et al., 2013; McMeniman et al., 2014) or Transcription Activator-Like Effector Nucleases (TALEN) (Aryan et al., 2013; Aryan, Myles & Adelman, 2014), which gave researchers the opportunity to accurately disrupt target genes. These methods make use of multiple DNA-binding domains to target a specific target site, which require careful design and lengthy cloning processes before their implementation (Dong et al., 2015; Sentmanat et al., 2018). With the establishment of Clustered Regularly Interspaced Palindromic Repeats (CRISPR) systems as a staple in the field of biology, CRISPR/Cas9 has been adapted by researchers in *Ae. aegypti* to great success.

1.1.4 Introduction to CRISPR/Cas9

CRISPR/Cas9 system provides a relatively straightforward process from designing to implementing genetic disruption in organisms. Originally discovered in the *Streptococcus pyogenes* bacterial immune system, it serves as an RNA-guided nuclease that cleaves viral DNA and plasmids (Barrangou et al., 2007; Barrangou & Pijkeren, 2016; Doudna & Charpentier, 2014). Previous work has established a chimeric single-guide RNA (sgRNA), which combines the trans-activating crRNA (tracrRNA) with the precursor crRNA (pre-crRNA) to direct the Cas9 nuclease protein (Cong et al., 2013;

Jinek et al., 2012; Ren et al., 2013; Wang et al., 2013). The sgRNA can be designed as a 20 - 23 bp sequence that includes and recognizes the Protospacer Adjacent Motif (PAM) sequence in the target (5'-NGG-3'). Combined with homology sequence binding to another ten to twelve nucleotides through Watson-Crick base pairing, the sgRNA can easily target most genetic sequences in a genome (Li et al., 2017a; Ma et al., 2016; Sternberg et al., 2014). The Cas9-sgRNA complex then cleaves the DNA on both strands and create a Double-Strand Break (DSB).

This DSB is repaired by two distinct and conserved pathways in the eukaryotic cell machinery (Tang et al., 2019). The more frequent pathway is Non-Homologous End Joining (NHEJ), which ligates the DSB ends with the use of DNA Ligase IV and other protein complexes. This process is error-prone and can generate insertion/deletion (indel) mutations. The less frequent pathway is Homology Directed Repair (HDR), which is a faithful repair of the DSB according to any homologous DNA sequence present (Chen et al., 2021b; Nambiar et al., 2022; Paix et al., 2017; Sekelsky, 2017). Genetic manipulation in organisms can be done using the HDR pathway. An exogenous source of DNA with homology sequence to the DSB is provided to the cell, so that HDR repair can alter the genic sequence according to this donor template (Chang et al., 2013; Richardson et al., 2016; Song & Stieger, 2017). The activity of the two pathways during the cell cycle and efforts in optimising CRISPR/Cas9 HDR repair is further discussed in **Chapter 1 Helper Plasmid – Introduction**.

1.1.5 CRISPR/Cas9 in organisms

The utilization of CRISPR/Cas9 for precise genetic editing has been widely adapted to model and non-model organisms. HDR editing was first adapted to

traditional model organisms including mice (Xue et al., 2014), zebrafish (Chang et al., 2013) and *Caenorhabditis elegans* (Friedland et al., 2013). In arthropods, HDR editing was first shown to be successful in *Drosophila melanogaster* (Bassett et al., 2013; Gratz et al., 2013; Ren et al., 2013). Mosquito gene editing was later developed in *Anopheles gambiae* (Hammond et al., 2016) and *Aedes aegypti* (Kistler, Vosshall & Matthews, 2015), and has moved on to be adapted in many insects (Sun et al., 2017; Taning et al., 2017; Yan et al., 2023). Application of CRISPR/Cas9 in *Ae. aegypti* is wide ranging and can create transgenic lines for many purposes. To study mosquito physiology and attraction to humans, mutants have been created using CRISPR/Cas9 to target key genes. Some notable examples include *Op1* and *Op2* mutations to study vision during host seeking (Zhan et al, 2021) and *ppk301* mutation to study egg laying in fresh water (Matthews, Younger and Vosshall, 2019). Others have created novel genetic tools in *Ae. aegypti* using precise CRISPR genetic knock-in, like the creation of strains that allow pan-neuronal calcium imaging (GCaMP) and the Q binary expression system to study neurons (QF2/QUAS) (Zhao, Tian and McBride, 2021).

1.1.6 Overall project approach and chapter summaries

Although CRISPR/Cas9 is a widely adaptable system to be used in *Ae. aegypti*, much effort is still needed to further optimize the mosquito genetic toolbox. This thesis aims to improve genetic manipulation in *Ae. aegypti* using three strategies. In **Chapter 2**, helper plasmids were designed with germline gene promoters to express the Cas9 protein during developmentally optimal timing, which can bias DSB repair to HDR.

In **Chapter 3**, the sgRNA and donor template were integrated into the *Ae. aegypti* genome using efficient but random transposase-mediated mutagenesis to create a

transgenic line, which can be later crossed with a Cas9 transgenic line. The meeting of the CRSPR/Cas9 components could lead to HDR repair according to an endogenous donor template. This can hopefully reduce the number of mosquitoes needed to establish a stable edited line as compared with direct embryo microinjection of Cas9 components.

Finally in **Chapter 4**, we made use of CRISPR/Cas9 to make DSBs at two locations of the chromosome. These DSBs can be repaired by HDR through a “bi-genic” donor template, which induces the chromosomal inversion across the two DSB junctions. Once a chromosomal inversion occurs, it can be the first step towards creating a valid balancer chromosome for *Ae. aegypti*. The ability of balancer chromosomes to prevent gene recombination is further discussed in **Chapter 3 Balancer Chromosome – Introduction**.

Not only is *Ae. aegypti* a potent vector, it is also a growingly popular non-model organism in the fields of neurobiology and physiology. The improvement to CRISPR/Cas9 gene editing and creation of novel genetic tools can help reduce efforts in mosquito rearing and research. The result of this work can be widely adaptable from the genetic manipulation of *Ae. aegypti* to creating transgenic lines for reverse genetics.

2 The use of germline gene promoters to express Cas9 in helper plasmids

2.1 Introduction

2.1.1 Developmental Timing and Efforts in Improving HDR Repair

CRISPR/Cas9 generated DSBs are repaired by NHEJ and HDR pathways in the cell. Although the choice between pathways is currently an active area of research, it is known that NHEJ happens predominantly compared to HDR in mammalian cells (Savic et al., 2018). In NHEJ, the activity of various recruited protein complex restricts the DSB and ligate the ends together (Chen et al., 2021b; Liu et al., 2019). This creates mutations and errors in repairing DSBs. In HDR, the Rad51 protein searches for homologous sequences to the DSB, which is usually the sister chromatid. This allows the repair to be “error-free” and faithful to the original sequence before DSB (Krejci et al., 2012; Liu et al., 2019). While NHEJ is active during all parts of the cell cycle (Iyama & Wilson, 2013), HDR is mainly active during the S- and G2- phase (Gutschner et al., 2016; Howden et al,, 2016). This cell machinery is conserved in *Drosophila melanogaster* (Sekelsky, 2017) and *Ae. aegypti* (Mota et al., 2019). When an exogenous donor template is provided to the cell, HDR can repair DSBs according to this donor and edit the gene of interest.

As gene editing relies on HDR, previous work has sought to bias the HDR pathway through various approaches (Liu et al., 2019). One approach is to target the NHEJ pathway and reduce its efficiency, which includes DNA Ligase IV inhibition

(Srivastava et al., 2012) and small interfering RNA (siRNA) inhibition of NHEJ protein expression (Li et al., 2018). Others have shown that Cas9 delivery during cell cycle arrest in the S and G2 phase can bias HDR in mammalian cells (Lin et al., 2014 ; Yang et al., 2016). While these methods can successfully bias HDR, most of these methods have yet to be explored *in vivo* in *Ae. aegypti*. In other mosquito systems, it has been shown that Cas9 maternal deposition is a main source of NEHJ mutations. Cas9 protein deposited into germline cells of *Anopheles gambiae/coluzzi* females cause DSBs and NHEJ repair in the offspring (Gantz et al., 2015; Hammond et al., 2017; Hammond et al., 2020). The higher efficiency of NHEJ lowers the possibility of HDR events, and thus decrease efficiency of gene editing. To overcome maternal Cas9 effects, the use of germline gene promoter to express Cas9 can restrict the timing of DSB repairs to bias HDR. The avoidance of maternal Cas9 and NHEJ effects is specifically important in gene drive settings.

2.1.2 Introduction to gene drives

CRPSR gene drive is one of the most actively researched areas in mosquito genetics, due to its potential to use HDR editing to affect mosquito populations. This technology relies on the homing of selfish genetic elements that can copy itself into the genome and allows it to be passed on throughout a population (Burt, 2003). These genetic elements spread by integrating their copies into the genome, which can spread in subsequent offspring and alter an entire population. With the rise of CRISPR/Cas9 systems, homing based gene drives have been developed in *Drosophila melanogaster* (Champer et al., 2017; Marshall et al., 2017), *Anopheles stephensi* (Gantz et al., 2015), *Anopheles gambiae* (Hammond et al., 2016) and *Aedes aegypti* (Anderson et al., 2023;

Reid et al., 2022; Li et al., 2020). Through the inheritance of a CRISPR/Cas9 construct, transgenes are passed on a higher rate than the expected Mendelian inheritance of alleles (Champer, Buchamn & Akbari, 2016). This spread of transgenes relies on HDR editing to continuously introduce transgenic elements into the parental germline cells. NHEJ mutations to the target site can cause mutations and make the target unavailable for gene drive, which is known as gene drive resistance (Champer, Buchamn & Akbari, 2016; Hammond et al., 2020). Therefore, it is beneficial for gene editing to not only increase HDR rate, but also decrease NHEJ events.

2.1.3 Previous methods in optimising CRISPR/Cas9 in *Ae.aegypti*

Delivery of CRISPR/Cas9 into the mosquito system relies on the direct microinjection of various forms of Cas9 and CRISPR components into the pre-blastoderm embryo of *Ae. aegypti* (Wohl & McMeniman, 2023). Cas9 can be injected in the forms of recombinant Cas9 protein (Kistler, Vosshall & Matthews, 2015), Cas9 mRNA (Dong et al., 2015) or Cas9 plasmids (Reid et al., 2022). Direct injection of recombinant Cas9 protein, along with sgRNA and Donor DNA plasmid resulted in a G_0 survival of 9.6% and HDR repair rate of 0.71% (Kistler, Vosshall & Matthews, 2015). Cas9 protein can also be delivered into adult mosquitoes. Receptor-Mediated Ovary Transduction of Cargo (ReMOT Control) involves the direct delivery of Cas9 ribonucleoportein (RNP) into the adult female ovaries to carry out germline gene editing (Chaverra-Rodriguez et al., 2018). Most recently, direct parental-CRISPR (DIPA-CRISPR) has been shown to be effective via injection of Cas9 sgRNA RNP into the haemocoel of blood fed *Ae. aegypti* females (Shira et al., 2023).

Although both methods show great promise in reducing the time and effort required for embryo microinjection, they are currently restricted to generating NHEJ mutations only. Without the co-delivery of donor template, HDR editing have not been adapted in both ReMOT control and DIPA-CRISPR. Components of CRISPR/Cas9 can also be endogenously expressed, as previously mentioned in gene drive scenarios. Transgenic, endogenous expression of Cas9 has previously been created in Li et al. (2017). This approach allows Cas9 to be expressed in transgenic mosquitoes that can then be injected with sgRNA or crossed with other transgenic strains (Sun et al., 2022). (Use of transgenic strains for CRISPR/Cas9 system components is further discussed in **Chapter 3 Transposon Transgene** – **Introduction).** Our approach to improve HDR editing in *Ae. aegypti* will be to focus on increasing HDR editing rate and increasing the survival rate for embryo microinjection.

2.1.4 Helper Plasmid Project Approach and Significance

As previously discussed in Lo (2021), this project builds upon the work done by Hammond et al. (2021) to improve HDR editing in *An. gambiae*. In summary, they investigated three germline genes to promote Cas9 activity and found up to 99.6% transmission in some gene drive constructs. We used gene orthologs of the germline genes *zpg* (*AGAP007365* in *An.* gambiae; *AAEL006726* in *Ae.* aegypti) and *nos* (*AGAP006098* in *An.* gambiae; *AAEL012107* in *Ae.* aegypti), and constructed Cas9 expression plasmids with the proposed regulatory regions of each gene. We compared HDR rates from the plasmid injections with an established transgenic strain *Exu*-Cas9, which expresses Cas9 with an *exuperentia* (*AAEL010097*) promoter and is integrated stably into the genome (Li et al., 2017). These embryos were provided via direct

microinjection with a separate source of sgRNA and donor template encoding a fluorescent marker to test for HDR integration efficiency (hereby known as HDR rate). We hypothesized that if germline gene promoters express Cas9 in developmentally optimal timing, more *Ae. aegypti* larvae will gain eye fluorescence through HDR. The results generated in this study can help reduce the time needed to generate a novel targeted transgenic line, which often requires lengthy screening and microinjection processes. If survival rate of G0s increase, less efforts can be invested in multiple rounds of embryo microinjections. Improvement towards HDR can also help elucidate the mechanism of DSB repair within *Ae. aegypti*, which could have implications for future gene editing work. As gene drive is increasingly contemplated as key mosquito control strategies across the world, improvement to HDR can improve fundamental mechanisms behind these genetic manipulation strategies.

2.2 Methods

2.2.1 Mosquito Rearing and Maintenance

Aedes aegypti mosquitoes were maintained according to standard protocol as described (Sun et al., 2022; Wohl & McMeniman, 2023). Mosquito eggs were hatched in a vacuum chamber (20 – 25 Psi) and kept in containers of dechlorinated water until pupation. All adult mosquito strains were kept at 25 – 28 °C in mesh cages (Bugdorm, 4M3030), with constant relative humidity of 70-80% and 12 : 12 light : dark photoperiod. 10% sucrose solution was provided in the mesh cages of mixed sex for strain maintenance. All females were blood fed on defibrillated sheep blood (Cedarlane Labs, DSB250) via a glass mosquito feeder (Chemglass, Cat# CG1836) with a layer of parafilm spread across the feeder. Blood inside the feeder was warmed to 37.5°C. Blood fed mosquito cages were given 30% sucrose solution to minimize egg laying on 10% sucrose solution sugar wicks.

I utilised two different strains in this chapter. Wild-type laboratory Liverpool strain (LVP) was reared and maintained at the McMeniman Lab. Exu-Cas9 strain had a stable integration of *Exuprentia* promoter region expressing Cas9 sequence and a DsRed fluorescence body marker (Li et al., 2017). Both strains were kindly provided and reared by Dr. Connor McMeniman and colleagues (Johns Hopkins Malaria Research Institute).

2.2.2 Establishment of Helper Plasmid

All cloning and Hifi assembly procedures were previously described in (Lo, I. 2021).

2.2.3 Embryo Microinjection of Helper Plasmids

Two helper plasmids expressing Cas9 (*nanos* and *zpg*) were previously created via commercial HiFi assembly kit (Lo, I. 2021). Helper plasmids were injected into Wildtype *Liverpool (LVP)* strain mosquito embryos with sgRNA targeting *Ir8a* and *Ir8a*$^{3xP3\ dsRed}$ donor template at the McMeniman Lab, as described in (Raji et al., 2019). *Ir8a* sgRNA and *Ir8a*$^{3xP3\ dsRed}$ donor template were also injected into *ExuCas9* strain. Embryo microinjection procedures were done according to Sun et al. (2022).

2.2.4 Fluorescence screening

Injected embryos were hatched and screened under a fluorescence microscope at the 3rd-4th instar stage. Larvae were separated individually on an 8-well glass slide. Small droplets of water were provided to prevent larval desiccation during fluorescence imaging.

2.2.5 Pooled and Individual Egg laying of Transgenic Mosquitoes

Injected embryos were raised to adulthood and kept as virgins. To find individuals that carry the *IR8a*$^{3xP3\ dsRed}$ transgene, G0 adult mosquitoes were crossed to the opposite sex. G0 Males were mated individually with multiple WT females (>2), while G0 females were group mated with WT males. Crosses were done in small mosquito mesh cages (Bugdorm, 4M1515). Details of mating scheme were previously described (Sun et al., 2022). Pooled egg laying refers to a batch of blood fed females that are given wet filter paper to lay eggs, which allows screening for founding individuals within the pool of adults. Individual egg laying refers to blood fed females that were separated

into individual vials to ensure parentage of eggs. Individual egg laying allows identification of parental genotypes through fluorescence screening of larvae.

2.2.6 Statistical Analysis

R studio (Version 4.1.1) was used to analyze data in this chapter. Scatterplot was generated with the ggplot() function. All comparisons of hatch rate, transient rate and pooled G1 transgenic rates were made with χ^2 test. GraphPad Prism 10 was used to plot bar graphs for hatch rate and transient rate. One-way ANOVA was done in Prism.

2.2.7 Software Availability and Data Availability

DNA sequences were obtained from Vectorbase v. 66 (https://vectorbase.org/vectorbase/app/), Ensembl Metazoa v. 58 (https://metazoa.ensembl.org/index.html) and FlyBase FB2023_06 (https://flybase.org/). Genome Assembly AaegL5.0 was the reference genome for all analysis in this thesis (Matthews et al., 2018). All genic components were manually annotated on Benchling Vol. 12 (http://benchling.com).

Data is available upon request, contact: Benjamin Matthews (ben.matthews@zoology.ubc.ca)

2.3 Results

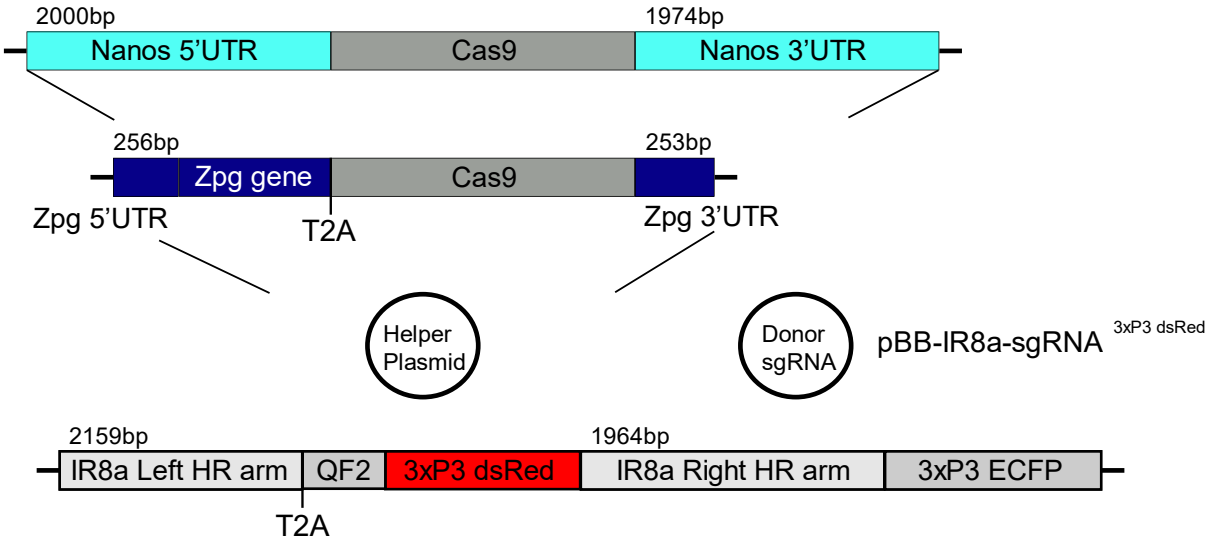

Figure 1. Helper Plasmid Design Schematic
Schematic representation of helper plasmid designs, as shown in Lo (2021). *Zpg-Cas9* and n*anos-Cas9* plasmids were co-injected into *Ae. aegypti* embryos with *pBB-IR8a-sgRNA*$^{3xP3\ dsRed}$ (Shankar et al., 2020). Donor template carried left and right homology arms with *IR8a*, where *3xP3 dsRed* served as the marker for HDR repair. sgRNA was expressed by a U6 promoter, and a *3xP3 ECFP* served as a transformation marker for unsuccessful HDR repair. T2A is the ribosomal skip sequence, while QF2 is a transcription factor that is a remnant of the previously generated donor template.

2.3.1 Design of Helper plasmids and generation of G0s

To compare the efficacy of germline gene promoters to express Cas9, *zpg-Cas9* and *nanos-Cas9* were designed as helper plasmids. For *zpg*, the 5' and 3' untranslated regions (UTR) were captured by our design as regions with possible gene promoter activity. This design also included exon 1 to exon 3, but with a 78 amino acid deletion to render the gene non-functional. We hypothesised that promoter activity is likely to be found in the non-repetitive sequences in the genome, which was present in the 5'UTR

and the introns included in this design. For *nanos*, 2000bp upstream and downstream of the gene was captured as the 5' and 3'UTR respectively as they included non-repetitive sequences. The *nanos* 3'UTR has been shown to form a mRNA structural element that is essential for their germline activity in flies and mice embryos (Crucs, Chatterjee & Gavis, 2000; Suzuki et al., 2010). Both helper plasmid designs were assembled via Hifi assembly kit and sequence verified via Sanger sequencing (further discussed in Lo, 2021). These designs were compared to *exuCas9* (Li et al., 2017), which was created using *piggyBac* transposon mediated insertion of this Cas9 cassette. They included only the 2132 bp sequence upstream (5') of *exu* and did not include any downstream (3') sequence. The *IR8a-sgRNA*$^{3xP3\ dsRed}$ was injected with the helped plasmids, which carries a donor template for *IR8a* and a sgRNA targeting this gene (**Fig 1a**). *IR8a* is involved in human odour detection and was chosen as the target of integration based on the work by Shakar et al. (2020). The use of *IR8a-sgRNA*$^{3xP3\ dsRed}$ was shown to be successful in generating *3xP3 dsRed* integration into *IR8a.* We made use of a previously validated donor and sgRNA plasmid for our work. *3xP3* is a widely used promoter that restricts fluorescence in the eye (Kokoza et al., 2001) (**Fig 2b**). A *3xP3 eCFP* marker carried by the plasmid backbone served as a transformation marker. Expression of both *3xP3 eCFP* with *dsRed* suggests plasmid expression instead of HDR repair, while successful HDR repair of *3xP3 dsRed* should exclude the *eCFP* sequence. No G_1 offsprings were observed to have *eCFP* expression throughout the following experiments. Both helper plasmids were co-injected with *IR8a-sgRNA*$^{3xP3\ dsRed}$ in embryos. For *exuCas9*, embryos were collected from a single generation outcross to *LVP* strain and injected with *IR8a-sgRNA*$^{3xP3\ dsRed}$ only.

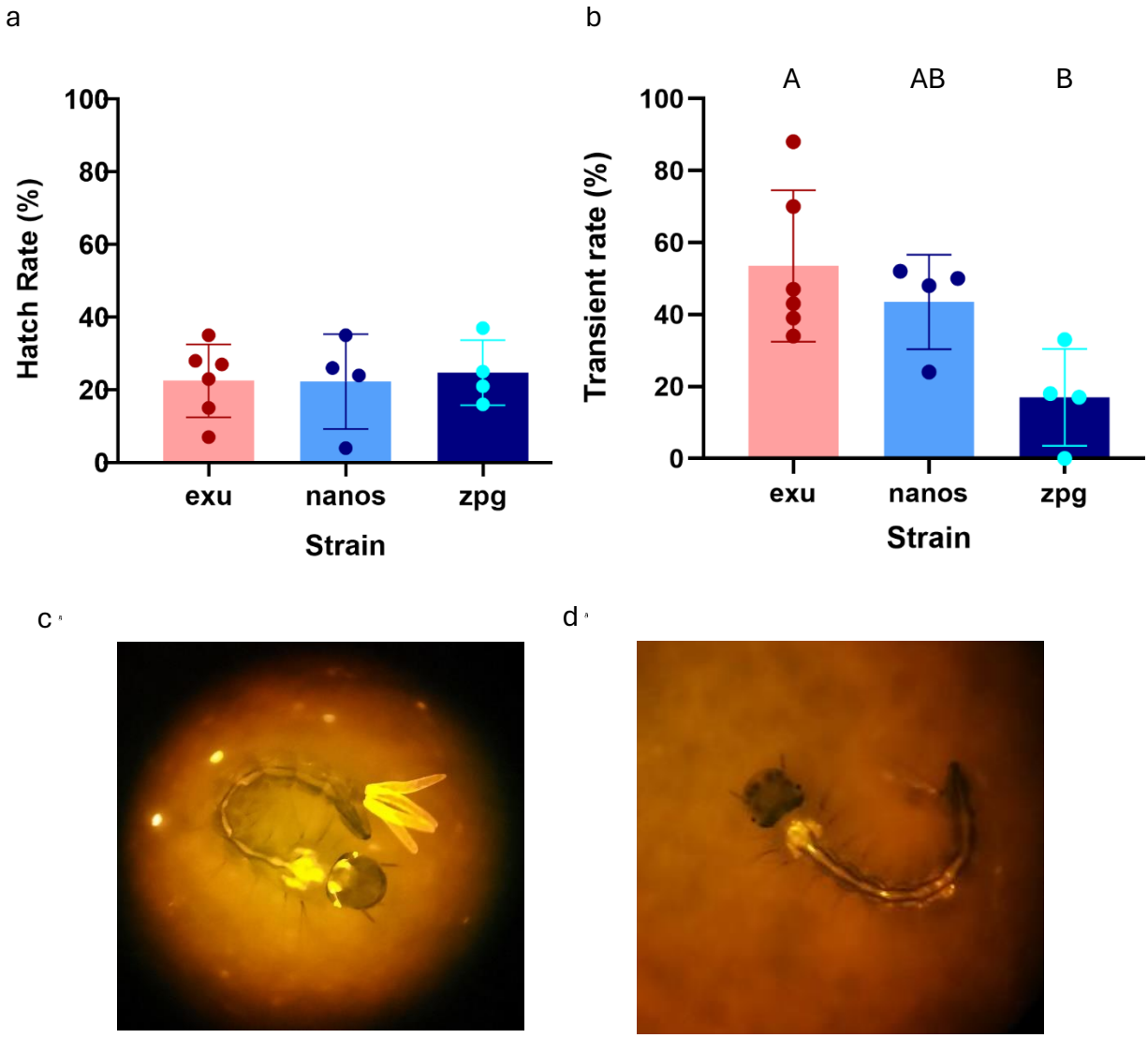

Figure 2. Hatch rate and transient tail expression rate of helper plasmids and *exuCas9* G_0s.
(a) Hatch rate of injected G_0s across all three strains. Hatch rate was measured by the number of surviving larvae over total number of eggs laid. Error bars represent standard deviation. **(b)** Transient tail expression rate of G_0s over total hatched larvae. Transient rate was measured by the number of larvae with fluorescence in the tail out of the overall number of larvae. Error bars represent standard deviation. The letters A and B on the bar graph represent the Tukey post-hoc test, with difference in letters showing statistically significant difference in comparison. **(c)** Representative *Ae. aegypti* larvae showing *dsRed* fluorescence in the eye (arrow) and a tail transient pattern of *dsRed*. **(d)** Representative *Ae. aegypti* larvae in the *exu-Cas9* strain showing body *dsRed* fluorescence pattern.

2.3.2 *ExuCas9* strain and *nanos-Cas9* helper promoted tail transience despite similar hatch rates of injected G_0s

Injected G_0s were hatched five days post injection and counted for larval hatch rates. In *ExuCas9* strain, 160 larvae hatched from 683 eggs in six rounds of injection, which gave a hatch rate of 23.43%; For *nanos* helper, 129 larvae hatched from 492 eggs in four rounds of injections, which gave a hatch rate of 26.22%; For *zpg* helper, 119 larvae hatched from 443 eggs in four rounds of injections, which gave a hatch rate of 26.86%. A χ^2 test was done to test for association between hatch rate in all three strains, with a χ^2 value of 2.0598 (p = 0.357). The hatch rate was not associated to G_0 strain used. An ANOVA was done to test for differences between the mean hatch rate of all three strains, which also found no statistically significant difference (F = 0.06970, p = 0.933). The hatch rate between the three strains was not statistically significantly different (**Fig. 2a; Supp. Table 2**).

Tail transient rate was counted in hatched G_0 larvae, where the tail of larvae shows red fluorescence marker from expressing *dsRed* template (**Fig. 2c; Supp. Table 2**). In *ExuCas9*, 82 out of 160 larvae had positive fluorescence, which gave a transient rate of 51%; in *nanos* helper, 60 out of 129 larvae had positive fluorescence, which gave a transient rate of 47%; in *zpg* helper, 24 out of 119 larvae had positive fluorescence, which gave a transient rate of 20%. A χ^2 test was done to compare the average transient rates from all three strains, with a χ^2 value of 29.972 (p <0.001). This shows that transient rates were associated with the strains used for G_0. An ANOVA was done to compare the mean transient rate of all three strains (F = 5.485, p < 0.05), which was statistically significant. The transient rate between strains is significantly different, with

exu and *nanos* giving more tail transient larvae than *zpg*. A Tukey post-hoc test was done for pairwise comparisons between the mean transient rate of each strain. Only the comparison between *exu* and *zpg* was statistically significantly different (p <0.05) (**Fig. 2b**).

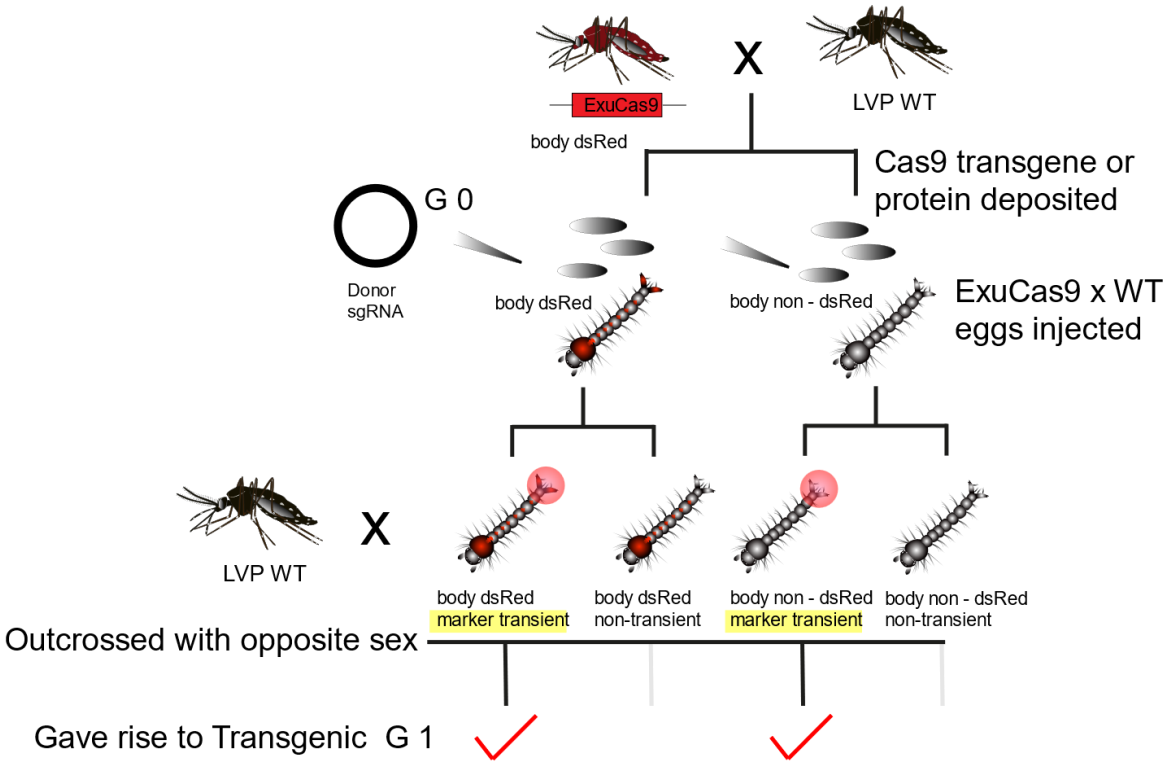

Figure 3. Schematic representation of *exuCas9* G_0 cross that gave rise to transgenic G_1s. *ExuCas9* adults were outcrossed to *LVP WT* adults prior to egg laying. G_0 embryos were injected with *IR8a* donor template and sgRNA plasmids. Larvae could either be body *dsRed* due to inheritance of *exuCas9* transgene, or body *non-dsRed* with the possibility of maternal deposition of Cas9 protein from their parents. All injected larvae were screened for tail transient expression of the donor template. Larvae were either marker transient or non-transient. G_0 adults were outcrossed to *LVP WT* to screen for transgenic G_1s. Only marker transient parents were able to give rise to transgenic G_1s, regardless of Cas9 transgene inheritance from their parents.

Table 1. Number of Transgenic G_1s generated (*3xP3 dsRed* +) in *zpg-Cas9*, *nos-Cas9* helper plasmid injections compared to *exuCas9* strain in the first pooled egg laying cycle. Transient refers to positive expression for tail fluorescence in G_0 parent, while Transgenic refers to positive expression of *3xP3 dsRed* from integration of the donor template in G_1 larvae. (n) refers to number of mosquitoes in each cross.

exuCas9 G1	G1 Transgenic	G1 Non Transgenic	Percent Transgenic (%)
non-*dsRed* , Non Transient G0 female (5) x WT male (50)	0	228	0.00
non-dsRed, **Transient** G0 female (9) x WT male (50)	3	351	0.85
dsRed , Non Transient G0 female (16) x WT male (50)	0	409	0.00
dsRed , **Transient** G0 female (22) x WT male (50)	7	1189	0.59
non-dsRed, Non Transient G0 male (2) x WT female (30)	0	704	0.00
non-dsRed, **Transient** G0 male (4) x WT female (20)	47	145	24.48
dsRed , Non Transient G0 male (26) x WT female (50)	0	1173	0.00
dsRed , **Transient** G0 male (27) x WT female (50)	28	1376	1.99
TOTAL	85	5575	1.50

nanos-Cas9 helper G1	G1 Transgenic	G1 Non Transgenic	Percent Transgenic (%)
Transient G0 male (25) x WT female (50)	1	450	0.22
Transient G0 female (18) x WT male (50)	0	600	0.00
TOTAL	1	1050	0.10

zpg-Cas9 helper G1	G1 Transgenic	G1 Non Transgenic	Percent Transgenic (%)
Transient G0 male (7) x WT female (50)	0	330	0.00
Transient G0 female (10) x WT male (50)	0	720	0.00
TOTAL	0	1050	0.00

2.3.3 *ExuCas9* male G_0s with transient marker expression were most likely to give rise to transgenic progeny

All G_0s from *exuCas9, zpg* and *nanos* helper were raised to adulthood and outcrossed to *LVP WT* mosquitoes of the opposite sex. These G_0s were batch mated (pooled egg laying), and G_1s were scored for inheritance of *3xP3 dsRed*. The presence of *3xP3 dsRed* eye marker expression indicates successful integration of the marker via HDR repair. Transgenic G_1s would indicate the presence of founders in the parental pool, but not the individual identities of the founders.

Before injection of donor and sgRNA plasmid into the *exuCas9* strain, adults were outcrossed to *LVP WT* mosquitoes to produce eggs. The expression of the dsRed marker in the body of the larvae indicates the inheritance of the *exuCas9* transgene, while those that do not have body dsRed expression could have inherited Cas9 protein maternally. These injected G_0s were further screened for a transient expression of the donor template in their tails (**Fig. 2d**; **Fig. 3**). This created four possible phenotypes of *exuCas9* G_0s, which were “non-dsRed, non transient”, “dsRed, transient”, “non-dsRed, transient” and “dsRed, non-transient” (**Table 1**).

G_1s were counted as transgenic with the eye expression of the *3xP3 dsRed* marker. In *exuCas9,* 85 out of 5674 G_1s were transgenic, which gave a 0.015% HDR rate in the pooled egg laying. This indicates that there were founders in the G_0s, but the actual HDR rate would be higher if founders were counted individually. Regardless of parental expression of body *dsRed*, transgenic G_1s were found if their parents had transient expression of the marker. Specifically, male *exuCas9* parents gave rise to

more transgenic G_1s than females. Transient males gave rise to 75 transgenic G_1s out of 1596 larvae (4.70%) while transient females gave rise to 10 transgenic G_1s out of 647 larvae (1.55%). A χ^2 test was done to compare the G_1 transgenic rates between male and female parents, which had a χ^2 value of 11.708 ($p < 0.001$). *ExuCas9* male G_0s were significantly more likely to give rise to transgenic G_1s compared to females. It should be noted that the cross that generated the most transgenic G_1s was from a "*non-dsRed"*, transient male. The transgenic rate was 24.48% despite a lower number of G_1s compared to *exuCas9* crosses with other sgRNA / donor template (**Table 1**).

For *nanos*, 1 out of 1051 larvae (>0.001%) gave rise to transgenic G_1 to a male parent G_0. For *zpg*, no G1 larvae were observed to be transgenic (**Table 1**). As *exuCas9* was the only strain successful in producing transgenic G_1s with potential improvements in HDR rate, the following work was done only in this strain.

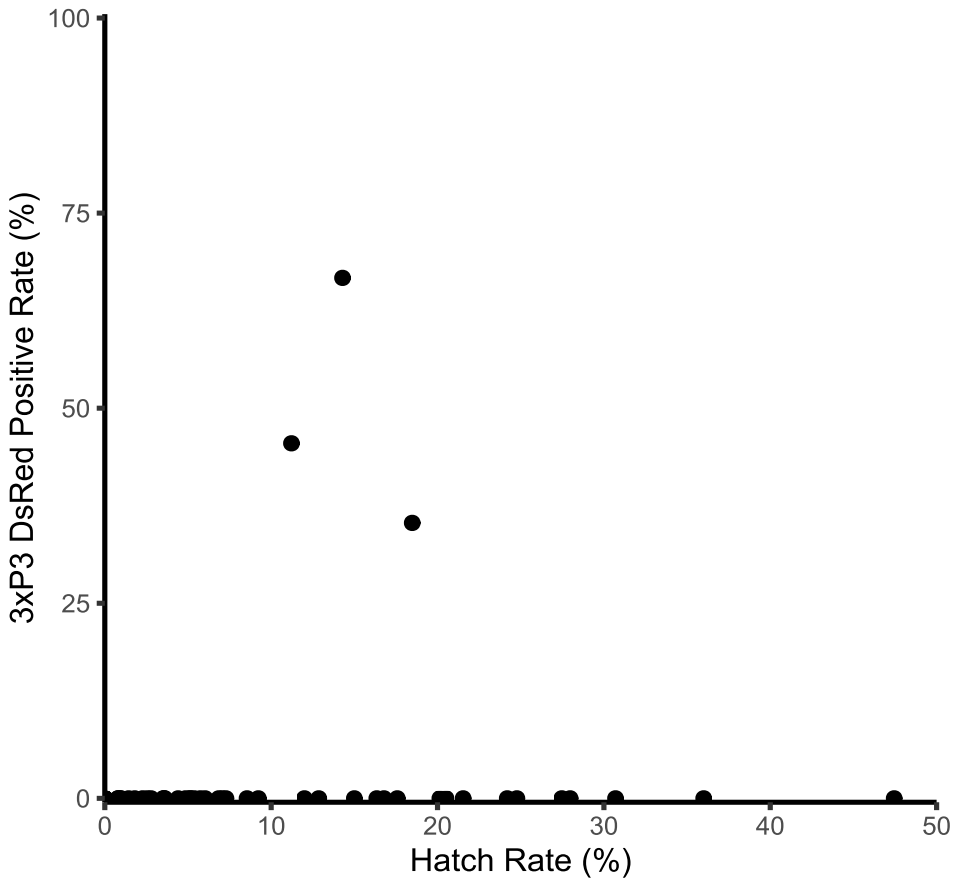

Cross Identity	Eggs	Hatched	DsRed +	Hatch rate (%)	Positive rate (%)
3	98	11	5	11.22	45.5
6	92	17	6	18.48	35.3
8	21	3	2	14.29	66.7

Figure 4. Identification of the number of founders in the second egg laying cycle through positive fluorescence rate and hatch rate of 63 outcrosses. Crosses are labelled from 1 to 63. G_1 *3xP3 dsRed*-positive rate were counted against hatch rate of each individual outcross. Table provided for 3 crosses with positive transgenic G_1s. *DsRed+* represents larvae with positive expression for *3xP3 dsRed.*

2.3.4 At least three *exuCas9* founders identified with successful HDR repair events

A second outcross was done by separating each individual G_0 to identify the total number of founders. *ExuCas9* G_0 parents were crossed again with *LVP WT* mosquitoes of the opposite sex and allowed to lay eggs individually. Lineage of G_1s were tracked to identify the number of founders with HDR repair of *3xP3 dsRed* (**Supp. Table 3; Supp. Table 4**)**.** Out of 63 crosses, three G_0s gave rise to transgenic G_1s. The overall HDR rate of G_0s was counted as the number of founders divided by total number of crosses, which was 4.7%. All three G_0s were "*non-dsRed*, transient" G_0 *exuCas9* males that were crossed to *LVP* females. The G_1 transgenic rates in these three crosses labelled 3, 6 and 8 were 45.5%, 35.3% and 66.7% respectively (**Fig. 4**). It should be noted that 19 of the G_0 crosses did not have any eggs laid or did not have any larvae hatch from eggs (**Supp. Table 3; Supp. Table** 4). It is possible that some founders were unable to lay eggs again in the second outcross, so we conclude that the number of founders in G0 was more than or equal to three.

2.4 Discussion

2.4.1 Improvements in survival rate of injected G_0s

The result of using helper plasmid and *exuCas9* shows improvement to both the survival and HDR rates, compared to the work that this project is built upon (Kistler, Vosshall and Matthews, 2015). Previous recommendations for generating HDR transgenic mosquito relies on injection of Cas9 recombinant protein with sgRNA and donor DNA plasmid, which resulted in a hatch rate of 9.6% G_0 embryos and 0.71% HDR rate. Both helper plasmid strains and *exuCas9* tested here resulted in higher survival rates (23.43% - 26.86%), which could reduce the amount of embryo microinjections needed to generate a stable transgenic line. It is possible that an endogenous source of Cas9, including those expressed from injected plasmid, is relatively less toxic to the mosquito than Cas9 protein (toxicity of Cas9 is further discussed below in **2.4.8**).

Of these three strains, the transgenic strain containing an *exuCas9* cassette showed the most promise in improving HDR rates and generating transgenic offspring. 4.7% of G_0s from *exuCas9* successfully generated transgenic G_1s through HDR. This number is likely an underestimate due to the low number of eggs laid by each female and poor hatch rates. All three identified founders had a less than 20% hatch rate of eggs but with high positive transgenic rates. Pooled egg laying was used to search for presence of any G_0 founders, while a second round of individual outcross allowed specific founders to be identified. Founders identified during pooled egg laying of G_0s were not found in individual egg laying, suggesting that some founders were not able to lay eggs during their second outcross. As 19 individual outcrosses did not give progeny,

we were not able to identify all G_0 founders. Although the rate of founders cannot be directly compared to the HDR rate of 0.71% in Kistler, Vosshall and Matthews (2015), *exuCas9* showed the highest rate of HDR across all three strains.

2.4.2 Discussion of *nanos* helper design

At the time of completing this project, Reid et al. (2022) tackled helper plasmid designs in *Ae. aegypti* for both *nanos* and *zpg*. Surprisingly, they found relatively high HDR transmission rates for their homing constructs. The following sections will compare the differences between our designs and possible explanations as to why our helper plasmids did not result in improvements to HDR.

Our *nanos* helper was designed to restrict expression of Cas9 to early embryonic development of the mosquito. It was previously shown that *nanos* function in female ovaries, where it localizes to the oocytes and posterior pole of early embryos across mosquito species (Adelman et al., 2007; Calvo et al., 2005). In *An. gambiae*, *nanos* driving Cas9 expression was able to promote HDR in up to 99% of G1s (Hammond et al., 2021).

In our work, *nanos* helper had a HDR rate of less than 0.1% (only one G1 was found to be transgenic out of 1051 total G1s). Our design of *nanos* helper was an indiscriminate 2kb region up and down stream of the genic regions, in hopes of capturing *nanos* promoter activity. Reid et al. (2022) designed a 1.1kb 5’ promoter and 594bp 3’UTR, which is smaller than our design. However, they reported a 16% HDR rate of their gene drive construct. The design of our *nanos* helper should have captured this proposed promoter regions, but failed to produce similar results. During embryo

microinjection of helper plasmids, Reid et al. co-injected recombinant Cas9 protein and sgRNA for editing activity. Therefore, HDR activity could have been driven not only by the helper plasmid, but the Cas9 protein in the injection mix. They further noted a strong gene drive transmission of the *nanos* construct in subsequent generations, which suggests that HDR repair was still active for their gene promoter design. As *nanos* should be active during germline cell development, one possibility is to test for Cas9 expression in embryos to ensure *nanos* promotes gene expression in the embryos. Our result could not rule out *nanos* as a possible candidate for improving HDR rates.

2.4.3 Discussion of *zpg* helper design

Both helper plasmids were designed to capture the germline promoter regions of these genes and restrict expression of Cas9 to germline cell development. In *Drosophila*, *zpg* (also known as *innexin* 4) is a gap junction gene that has been shown to be function in early germ cell differentiation and localizes in the surface of germ cells (Tazuke et al., 2002). Hammond et al. (2021) tested this approach of *zpg* Cas9 expression in *An. gambiae* and found remarkable HDR rates (> 93.5% HDR in G_1s). HDR repair in *An. gambiae* has been found to be much more efficient than *Ae. aegypti* (Hammond et al., 2016), so HDR rates are not directly comparable across mosquito systems.

In our work, *zpg* helper produced no transgenic G_1s. The design of our *zpg* helper was relatively small, and only included around 250 base pairs of the 5’ and 3’ UTR. We also included part of a truncated *zpg* gene, including the first intron, that should render it non-functional. This design included non-repetitive sequences that could have regulatory activity, which was found only in the small UTR regions and the

first intron. It is possible that this design did not capture the promoter region of *zpg*, so Cas9 was not expressed appropriately in the germline cells. Reid et al. (2022) included 1.7kb upstream of *zpg* (5' promoter) and 1.3kb downstream (3' UTR) for their version of *zpg* helper. They found a 7.9% transmission rate of a homing construct that includes Cas9 and sgRNA in the G1s. Our *zpg* helper design could have failed to include enough of the sequences that leads to promoter activity of Cas9. Similar to *nanos*, the co-injection of recombinant Cas9 protein and sgRNA could have improved their reported HDR rate.

One limitation of our study is that NHEJ mutations were not accounted for, which can act as a proxy for Cas9 activity. The number of mutations at the target site can show the active cutting of Cas9 and creation of DSBs. Our result could not definitively rule out *zpg* as a possible candidate for germline promotion of Cas9.

2.4.4 Advantages of *exuCas9* strain

The generation of *exuCas9* strain by Li et al. (2017) allowed for an *Ae. aegypti* strain with stable integration of Cas9. In summary, the *exuperentia* gene was shown to have increased transcript expression when the female blood feeds, particularly in the ovary. Out of six promoter Cas9 cassettes generated through *piggyBac* random insertion, *exuCas9* resulted in the highest survival and mutation rates. Therefore, it is likely that *exu* promoter activity can most effectively restrict Cas9 expression to germline cell development. Another possibility for testing *zpg* and *nanos* is to use similar methods as Li et al. (2017) and insert these Cas9 promoter cassettes into the genome. We further hypothesized that a source of CRISPR/Cas9 components integrated into the

genome can increase HDR rates, which is further explored in the following chapter (**Chapter 3**).

2.4.5 Transient tail expressions of fluorescence marker in larvae can act as an indicator of HDR events

All transgenic G_1 offspring came from G_0s with transgenic tail expression of the donor template, which has not been reported in other studies. While both *exuCas9* and *nanos* showed similar transient rates, *exuCas9* had a higher HDR rate of at least 4.7%. During embryo microinjection, a mix of sgRNA and donor template were injected into the posterior pole of the pre-blastoderm embryo. There are two possible explanations for this transient tail expression. One possibility is that donor template concentrations were sequestered at high enough levels in the posterior cells of the embryo, which later gave rise to the cells in the tail. In other words, *dsRed* fluorescence could be expressed through the leftover plasmid that persist into larval development. Another possibility was the stable integration of donor template due to HDR in the tail. G_0 mosaicism can be observed in adults (Li et al., 2017; Hammond et al., 2021), where only parts of the cells in the organisms had successful edits. However, this explanation is unlikely the case for *exuCas9* as the tail transient pattern was repeated across many G0s without other mosaic patterns. Therefore, transient tail expression is likely the result of a high concentration of donor template within the tail cells. This could indicate a particularly successful injection event in which a higher dose of injection mix was directed to the appropriate compartments within the developing embryo.

With only three founding *exuCas9* individuals captured, we cannot definitively conclude that transient expression of the donor template leads to HDR repair. However,

screening of larvae can prioritize these transient larvae which can be an improvement to current research protocols. To reduce the time and effort needed to sort through G0s in the creation of a transgenic line, we recommend future work to only select G0s with transient tail expression as possible founders. This could help alleviate the time needed to outcross all G0s regardless of phenotype.

2.4.6 Males gave rise to more transgenic offspring than females

Our results showed that male *exuCas9* G_0s were significantly more likely to give rise to transgenic G_1s compared to female parents. Specifically, "*non*-dsRed" males had the highest G_1 transgenic rate. This result was surprising as previous work done with *exuCas9* did not report this degree of male bias, including the work that characterized this strain (Li et al., 2017; Li et al., 2020). In our work, *exuCas9* was outcrossed to wildtype before egg laying for G_0 injections. Maternally inherited Cas9 protein is highly effective in generating mutations with sgRNA presence in the *exuCas9* strain (Li et al., 2020). As parental genotypes were not considered, we could not establish the inheritance of Cas9 proteins in male and female G_0s. Thus, we cannot definitively conclude that this male bias for transgenic rate is due to maternal deposition of Cas9.

It is well established by previous work that maternal deposition of Cas9 is a major source of NHEJ mutations for gene drives (Champer et al., 2017; Kandul et al., 2019; Li et al., 2017; Lopez Del Amo et al., 2020). Cas9 protein deposited in germline cells can make DSBs with the presence of sgRNAs. Subsequent repair of DSBs in the early stages of embryo development favors NHEJ over HDR pathway, resulting in mutations instead of donor template repair (Kandul et al., 2019). Thus, gene drive components in males are not affected by Cas9 deposited in the female germline cells. However,

maternal Cas9 deposition does not fully explain the results observed in our work. As our focus is on the HDR events in the G_0 germline cells, successful HDR editing would have happened in the G_0s with their Cas9 activity. Transgenic G_1s are the result of HDR editing in G_0s before maternal deposition of Cas9 could be accounted for.

In the search for G_0 founders, it is possible that the few male founders gave rise to more offspring. This could lead to an over representation of transgenic G_1s in the data, despite being from a small number of founders. While male transgenic rates were normalized to the total number of offspring, this is only one measure of transgenic rates for individual founders. We cannot definitively conclude whether male *exuCas9* have higher HDR rate and are more likely to give rise to transgenic G_1s. As Cas9 expression is toxic to the organism, one possibility is that "*non-dsRed*" males simply had higher fecundity and male founders gave rise to more transgenic G_1s. Specifically, only 9 out of 38 G_0 males failed to give offspring (24%) when compared to 10 out of 25 G_0 females that failed to lay eggs (40%). This suggests that fecundity of G_0 females could have been heavily impacted by Cas9 toxicity, resulting in less offspring and less possibilities of transgenic of G_1s. Overall, males could have given rise to a higher proportion of offspring due to batch mating of G_0 males with wildtype females.

2.4.7 Fitness and Cas9 toxicity

The gene target *Ir8a* and sgRNA donor template design chosen for HDR repair was previously validated by our collaborators in Raji et al., (2019). The sgRNA targets exon 2 of *Ir8a* and inserts a *3xP3 dsRed* into this target site. Disruption to this gene caused a lack of attraction to human odor, which is essential for host seeking behavior for females during blood feeding (Raji et al., 2019). As the target site for HDR editing

had biological relevance to blood feeding, G_0 females with disruption to *Ir8a* could have lowered fitness. It is also established in previous work that Cas9 expression can be toxic. Cas9 expression and activity causes lethality in bacterial and algal systems (Cobb et al., 2015; Jiang et al., 2014; Wendt et al., 2016). In the *exuCas9* strain, Li et al. also noted lowered fecundity in females (Li et al., 2020). This could explain the high number of G_0 crosses in the second gonotrophic cycle that did not lay eggs. Cas9 toxicity could impact future work done in *Ae. aegypti,* as transgenic G_0s could simply be unable to pass on transgenes to G_1s. This is especially relevant in the work done in the following chapters, where Cas9 expression and editing seemed to cause lowered survival in progeny.

2.4.8 Future work and limitations

As noted above, germline gene promoter designs can vary greatly depending on the regions of interest. Both *zpg* and *nanos* genes could have promoter activity that was not captured in our plasmid design, which led to lowered expression of Cas9. Possible ways to identify activity of Cas9 in the embryo include *in situ* hybridization for Cas9 mRNA in the G_0 embryos and checking NHEJ mutations at the target site as a proxy for Cas9 activity. Due to the toxicity of Cas9 and lowered fecundity, we were unable to conclude the actual number of founders in the G0s. Another improvement for our work could be to target more than one gene, which could elucidate if the low activity of helper plasmids was target specific. Building upon these results, we hypothesized that endogenous expression of components in the CRISPR/Cas9 system is beneficial for increased HDR rate. In the next chapter (**Chapter 3**), we created a transgenic strain

expressing sgRNA and donor template. This strain is then crossed to *exuCas9* to allow HDR editing to happen.

2.4.9 Conclusions

In this chapter, we established that *exuCas9* shows the most promise in generating transgenic *Ae. aegypti* when compared to Cas9 expression driven by two germline gene promoters. To improve current standards to generating transgenic strains, we seek to improve the survival rate and HDR rate of G_0s. Embryo microinjection of *zpg* helper, *nanos* helper and *exuCas9* all improved the survival rate of G_0s compared to injection of recombinant Cas9 protein. Specifically, screening transient tail expression of the donor transgene can reduce time and effort required to outcross all surviving G_0s. Due to possible flaws in the design of helper plasmids, Cas9 expression could have been restricted. Overall, we cannot conclusively reject our hypothesis that germline gene promoters can express Cas9 in developmentally optimal timing in *Ae. aegypti*, which in turn could lead to more HDR events. We noted the advantages of using *exuCas9* due to the ease of generating transgenic G_1s. This strain improved on HDR rates compared to other strategies. We also recommend using male *exuCas9* as the prime candidate for passing on stable integration of donors and selecting G_0 individuals with transient expression of the transformation marker in their tails for further outcrossing efforts.

3 Use of transposon mediated integration to create a split CRISPR/Cas9 system

3.1 Introduction to transposon transgene

3.1.1 Transposon mediated transfer of genetic material

Aside from CRISPR/Cas9, genetic sequences can also be randomly inserted into the *Ae. aegypti* genome using transposons. The *piggyBac* transposon genetic element was first identified in cabbage looper moth *Trichoplusia ni*, and subsequently used to transform *D. melanogaster* (Handler and Harrell, 1999). It was then shown to be effective in *Ae. aegypti* germline transformations, creating transgenic mosquitoes via embryo microinjections (Kokoza et al., 2001; Lobo et al., 2002). The *piggyBac* transposase recognizes genomic TTAA sequences as insertion sites. It then recognizes inverted terminal repeats (ITR) from an exogenous plasmid and inserts a copy of the genetic sequences between ITRs into the host genome. Transformation of *Ae. aegypti* can be done successfully by allowing *piggyBac* to randomly insert transgenes into the genome (Lobo et al., 2002; Kokoza and Raikhel, 2011). A key difference between transposon mediated gene editing and CRISPR/Cas9 is the target specificity. While CRISPR/Cas9 inserts via HDR only at the target gene, transposons insert transgenes in random locations and can also result in multiple insertions.

3.1.2 Background of HACK system and split gene drives

Aside from integrating Cas9 into the genome, other components of the CRISPR/Cas9 systems can also be stably integrated to provide an endogenous source of sgRNA and donor templates. The sgRNA is often expressed by U6 promoter (U6 is a RNA polymerase III promoter) which was first used to express RNA in *Drosophila* cells ubiquitously at high levels (Wakiyama, Matsumoto and Yokoyama, 2005). The U6 promoter regions have been utilized to express sgRNA for creating transgenic *D. melanogaster* strains, from germline Cas9 systems (Kondo and Ueda, 2013) to tissue specific Gal4 lines (Koreman et al., 2021). Various versions of U6 promoter have been adopted in *An. gambiae* (Hammond et al., 2016) and *Ae. aegypti* (Li et al., 2020), becoming a staple in the insect genetic toolbox as a means of expressing sgRNAs at high levels.

Our approach to creating a split CRISPR/Cas9 transgenic system was first used in *D. melanogaster* in the Homology Assisted CRISPR Knock-in (HACK) system by Lin and Potter (2016). In summary, HACK used random insertion of a donor template and sgRNA to create a donor stock. This line is crossed to a line expressing Cas9, which allows for all components of CRISPR/Cas9 system to meet in the offspring generation. HDR repair can then convert the target gene without the need for further efforts in embryo microinjection. Thus, HDR repair was shown to be able to knock-in gene of interest in as few as two genetic crosses (Lin and Potter, 2016).

This system of split CRISPR/Cas9 was then further developed into split gene drive (sGD) systems, which can pass on a sgRNA cassette as a donor template. By

crossing this line to a Cas9 line, a sgRNA cassette is able to be passed on by HDR repair and propagate through a population. sGD has been shown to be effective in *D. melanogaster* (Lopez Del Amo et al., 2020; Terradas et al., 2021) and *Ae. aegypti* (Anderson et al., 2024; Kandul et al., 2020; Li et al., 2020). This system is less likely to spread in a population than a full gene drive, as both lines need to be active for gene drive components to propagate. Escape of only one sGD line should, in theory, be able to limit the possible ecological impact of gene drive research (Champer et al., 2019; Lopez Del Amo et al., 2020).

By combining previous research on germline expression of Cas9 and transposon mediated transgenesis, a split system has the potential of generating HDR repairs in higher efficiency compared to current systems. Donor template designs can vary greatly depending on the needs of the researcher, while sgRNAs can be multiplexed in the genome to allow simultaneously editing in multiple target genes.

3.1.3 Project approach and significance

Building upon our results from **Chapter 2 Helper Plasmid**, we adapted the HACK system and sGD approach for *Ae. aegyti* in a transgenic context. Instead of the spread of sGD elements, we tested if this strategy can improve HDR editing. The Transposon Transgene strategy makes use of *piggyBac* transposon to randomly insert a Transposon Transgene Cassette (TC) that carries sgRNA and donor template with a fluorescent transformation marker. A TC-carrying transgenic line is first established and outcrossed for three generations. This line is then crossed with *exuCas9* strain, which we previously showed had great promise for high HDR repair efficiency. We hypothesized that if an endogenous, genomic source of sgRNA and donor template are

present in developmentally optimal timing, more HDR will occur in *Ae. aegypti* larvae. While Cas9 will be expressed in the germline with the *exu* promoter, sgRNA and donor template are ubiquitously present in the cell. We utilized the U6 promoter to drive a strong expression of sgRNA, while insertion of donor template ensured its presence early in the development of the germline cells (albeit at single copy insertion instead of high concentration of DNA templates in embryo microinjections). With the co-expression of *exuCas9*, this created a possible window in development that could favor HDR over NHEJ. In comparison, injection of Cas9 protein or Cas9 expression plasmids would result in these components meeting later in the germline cells, which could favor NHEJ instead. The cross between *exuCas9* and TC carrier allows the split components to meet in the organism, and repair target gene with HDR. This strategy can reduce the time and effort spent in creating transgenic lines by taking advantage of transposon mediated transgenesis, compared to the high number of embryos needed for CRISPR/Cas9 mediated gene integration. Results from this work can help elucidate if the source of CRISPR/Cas9 components can help bias HDR in *Ae. aegypti*.

3.2 Methods

3.2.1 Design of Transposon Transgene Cassette

The Transposon Transgene Cassette (TC) contained (1) an integration marker, (2) sgRNA sequence and (3) a HDR donor template, in between two *piggyBac* inverted terminal repeats (ITR). The overall design of TC included pBAC-ECFP-U6sgRNA-*ppk301*$^{3xP3\ dsRed}$. Sequences between ITR were randomly inserted into the genome in the presence of the *piggyBac* transposase.

3.2.2 Hifi Assembly and Cloning

pBAC-ECFP-15xQUAS_TATA-SV40 (Addgene #104875) was used as a backbone to create TC, which includes a *3xP3 eCFP* as the integration marker. This plasmid contained a *15x QUAS* sequence, which was cut out using MluI and BsmFI double restriction enzyme digestion in 37°C for 1 hour. The backbone was re-ligated using HiFi Assembly kit, following recommendations from the NEBuilder Assebmly Tool.

Other components of TC, including (2) sgRNA targeting exon 2 of *ppk301* and (3) *3xP3 dsRed* donor template, were previously designed (Kistler et al., 2015). (2) U6 promoter driving *ppk301* sgRNA was synthesized using ThermoFisher GeneArt custom DNA synthesis service. (3) *ppk301*$^{3xP3\ dsRed}$ donor (4.6kb) was PCR amplified from *ppk301-T2A-QF2* HDR plasmid (Matthews et al., 2019). All three TC components were assembled according to NEBuilder Assembly Tool, which provided primer designs for appropriate ligation of fragments.

All products of the HiFi Assembly reaction were transformed in bacterial colonies and subsequently verified using Colony PCR. DNA extraction was done via Miniprep for verification or Midiprep for embryo microinjection. Details of each method were done according to commercial protocol, as listed previously in Lo, I. 2020.

3.2.3 Generation of *PiggyBac* Transposase mRNA

PiggyBac Transposase mRNA were generated and subsequently injected into *Ae. aegypti* embryos along with the TC. mRNA was made according to previously established protocol (Matthews, B. 2019) (https://www.protocols.io/view/transposase-injection-mix-protocol-e6nvw6772gmk/v1).

3.2.4 Gel Electrophoresis

All DNA samples were run in 1 – 2% agarose gel to ensure appropriate band size. HiFi Assembly samples were subsequently cleaned up using PCR Clean-up kit (New England Bio, T1030L).

3.2.5 Mosquito Rearing and Maintenance

Aedes aegypti mosquitoes were maintained according to standard protocol as described (Sun et al., 2022 ; Wohl & McMeniman, 2023). Mosquito eggs were hatched in a vacuum chamber (20 – 25 Psi) and kept in containers of dechlorinated water until pupation. All adult mosquito strains were kept at 25 – 28 °C in mesh cages (Bugdorm, 4M3030), with constant relative humidity of 70-80% and 12 : 12 light : dark photoperiod. 10% sucrose solution was provided in the mesh cages of mixed sex for strain maintenance. All females were blood fed on defibrillated sheep blood (Cedarlane Labs, DSB250) via a glass mosquito feeder (Chemglass, Cat# CG1836) with a layer of

parafilm spread across the feeder. Blood inside the feeder was warmed to 37.5°C. Blood fed mosquito cages were given 30% sucrose solution to minimize egg laying on 10% sucrose solution sugar wicks.

I utilised *Exu-Cas9* strain, which had a stable integration of *Exuprentia* promoter region expressing Cas9 sequence and a *DsRed* fluorescence body marker (Li et al., 2017). This strain was kindly provided and reared by Dr. Connor McMeniman and colleagues (Johns Hopkins Malaria Research Institute).

3.2.6 Embryo Microinjection

TC and *piggyBac* Transposase mRNA were co-injected into *Ae.aegypti* embryos. Injection was done according to Sun et al. (2022). All injections were done in the embryo injection station in Matthews Lab, UBC. 200 embryos were injected with 58 G_0s surviving to adulthood.

3.2.7 Fluorescence Screening and Crossing scheme

G0 larvae were screened for expression of both 3xP3 eye marker for *eCFP* and *dsRed.* Positive G_0s were kept and outcrossed to *LVP* strain mosquitoes of the opposite sex for three generations. All pupae were allowed to emerge individually in plastic cups covered in mesh to ensure females and males were not mated before outcrossing. G_3s were crossed to *ExuCas9* individually and established as individual strains. *ExuCas9* larvae were sorted for bright *dsRed* expression in the body to ensure high levels of Cas9 expression.

G_4 larvae and subsequent offspring were screened for expression of (i) Wildtype without fluorescence expression, (ii) eye fluorescence of dsRed only, (iii) eye

fluorescence of *dsRed* and *eCFP*, (iv) body fluorescence of *dsRed* only, (v) all fluorescence of eye and body markers and (vi) other expression patterns that did not fit these categories. Offspring with (v) all fluorescence expression were kept and outcrossed with *LVP* strain again. Outcrossing was done for three more generations.

3.2.8 Genomic DNA extraction

Genomic DNA of transgenic mosquitoes was individually extracted from G_4 adult tissue. Adults were collected after death and frozen in -74°C.Up to three females and three males were extracted for each individual strain. gDNA extraction was done using commercial gDNA kit and following their protocol (New England Bio, T3010L).

3.2.9 PCR and Sequencing

PCR amplification was done on *ppk301* to test for successful insertion of donor template $ppk301^{3xP3\ dsRed}$ from TC. Size of PCR amplicons were verified using gel electrophoresis. Insertion of $ppk301^{3xP3\ dsRed}$ would result in 5kb sequence, as oppose to 2.6kb in the unedited sequence. Primers for PCR amplification of the overhang region between *ppk301* and $ppk301^{3xP3\ dsRed}$ insert was designed to result in 1.37 kb and 1.8kb sequences. Insertion was considered successful if all three PCR amplicons were amplified and sequenced.

Sequencing primers were designed to target the *ppk301* gene, including upstream and downstream of the donor homology arms. Primers also targeted the 200 base pair area around the Cas9 cut site. Sequencing was done through the GENEWIZ Sanger Sequencing (https://www.genewiz.com/Public/Services/Sanger-Sequencing/) or

the UBC Sequencing + Bioinformatics Consortium (https://sequencing.ubc.ca/our-services-equipment/sanger-sequencing).

3.2.10 Splinkerette PCR

Splinkerette PCR was done to map the location of *piggyBac* mediated insertion of TC into the genome. Genomic DNA of G6 larvae was digested using BamHI, BglII or BstYI restriction enzymes. DNA fragments are ligated to the splinkerette oligo, and then PCR amplified for two rounds. Primers are designed to amplify the 5' or 3' region of the *piggyBac* insertion site. All PCR amplification was done using Q5 DNA Polymerase (New England Bio, Cat #M0491L) and purified with PCR clean-up. Amplicons were sent for sequencing and BLAST for matching nucleotide sequence in the *Ae.aegypti* genome. Detailed protocol was previously established by Potter and Luo (2010).

3.2.11 PCR Identification of NHEJ activity

Primers were designed 100 base pairs upstream and downstream of the proposed *ppk301* cut site with G4 genomic DNA. Mutations to the sequence act as a proxy to Non-Homologous End Joining activity. Sequences were PCR amplified, cleaned up and sent for Sanger sequencing. Synthego ICE analysis was used to compare edited sequences from wildtype sequence from *LVP* strain (https://ice.synthego.com/). Genetic sequences were compared at the proposed Cas9 cut site to check for percentages of reads containing insertion or deletion mutations, which acts as a proxy for NHEJ and Cas9 activity.

3.2.12 Data Analysis

R studio (Version 4.1.1) was used to analyze data in this chapter. Scatterpie plots and pie charts were generated with the ggplot() function. Scatterpie package was created by Yu, G. (2023). Schematics were created using Adobe Illustrator (2022).

3.2.13 Software Availability and Data Availability

DNA sequences were obtained from Vectorbase v. 66 (https://vectorbase.org/vectorbase/app/), Ensembl Metazoa v. 58 (https://metazoa.ensembl.org/index.html) and FlyBase FB2023_06 (https://flybase.org/). Genome Assembly AaegL5.0 was the reference genome for all analysis in this thesis (Matthews et al., 2018). All genic components were manually annotated on Benchling Vol. 12 (http://benchling.com).

Data is available upon request, contact: Benjamin Matthews (ben.matthews@zoology.ubc.ca)

3.3 Results

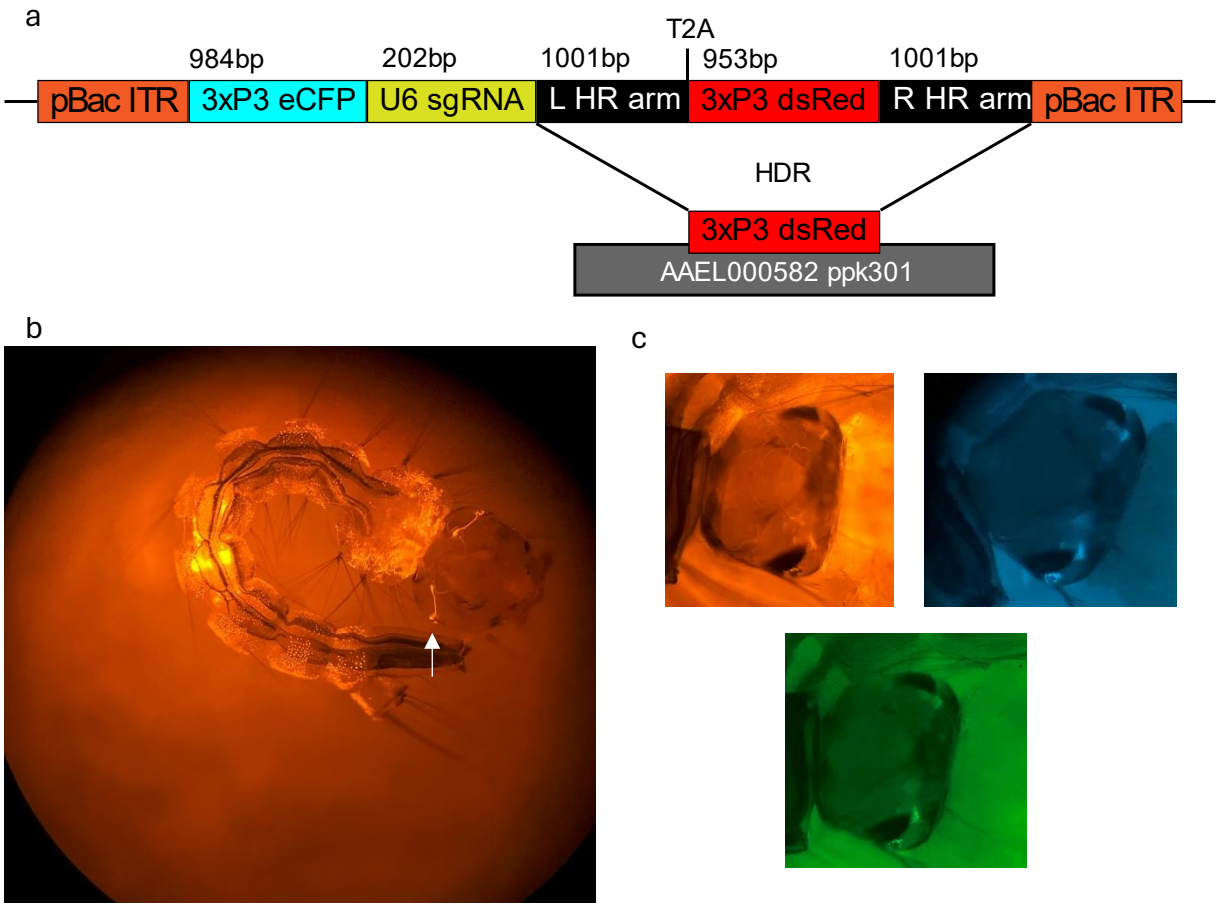

Figure 1. Transposon Cassette (TC) design
(a) Schematic representation of Transposon Cassette (TC) design that was injected to G_0 embryos. pBac ITR stands for *piggyBac* inverted terminal repeats. TC contains *3xP3 eCFP* which is the integration marker for successful *piggyBac* mediated integration. sgRNA targeting *ppk301* is expressed by a U6 promoter. Donor template includes 1Kb of homology arms flanking *3xP3 dsRed*, which is the marker for successful HDR integration. T2A is the ribosomal skip sequence. Successful HDR repair will integrate *3xP3 dsRed* but not *3xP3 eCFP* in the genome.
(b) Representation of *Ae. aegypti* larvae with *dsRed* expression of both body (*exuCas9*) and eye (*3xP3 dsRed*; arrow). **(c)** Repsentation of *Ae. aegypti* larvae with *3xP3 dsRed* (top right) and *3xP3 eCFP* (top left and bottom) expression.

3.3.1 Design of Transposon Cassette (TC) and fluorescence expression in larvae

To generate transgenic line that carries sgRNA and donor template, we designed a Transposon Cassette (TC) in between *piggyBac* inverted terminal repeats (ITR). *PiggyBac* transposase mRNA is co-injected into *LVP* embryos to generate random insertions of TC into the genome. Expression of the integration marker, *3xP3 eCFP* is inherited by Mendelian inheritance and signifies successful integration of TC into the genome. A sgRNA targeting *ppk301* expressed by a U6 promoter is adapted from Kistler, Vosshall and Matthews (2015), which has been used multiple times to generate *ppk301* mutants (Matthews, Younger and Vosshall, 2019). Finally, the donor template carries two1Kb homology arms for the *ppk301* cut site, as well as the *3xP3 dsRed* marker (**Fig. 1a**). The *3xP3* promoter restrict fluorescence expression in the eyes (Kokoza et al., 2001), which served as the indicator for successful integration or successful HDR repair. While both markers are expressed in a TC carrier, HDR events would lead to the inheritance of only the red but not blue eye marker (**Fig. 1c**). The separation of fluorescence marker expression allows HDR events to be identified through larval screening before the use of PCR and sequencing to validate successful HDR integration.

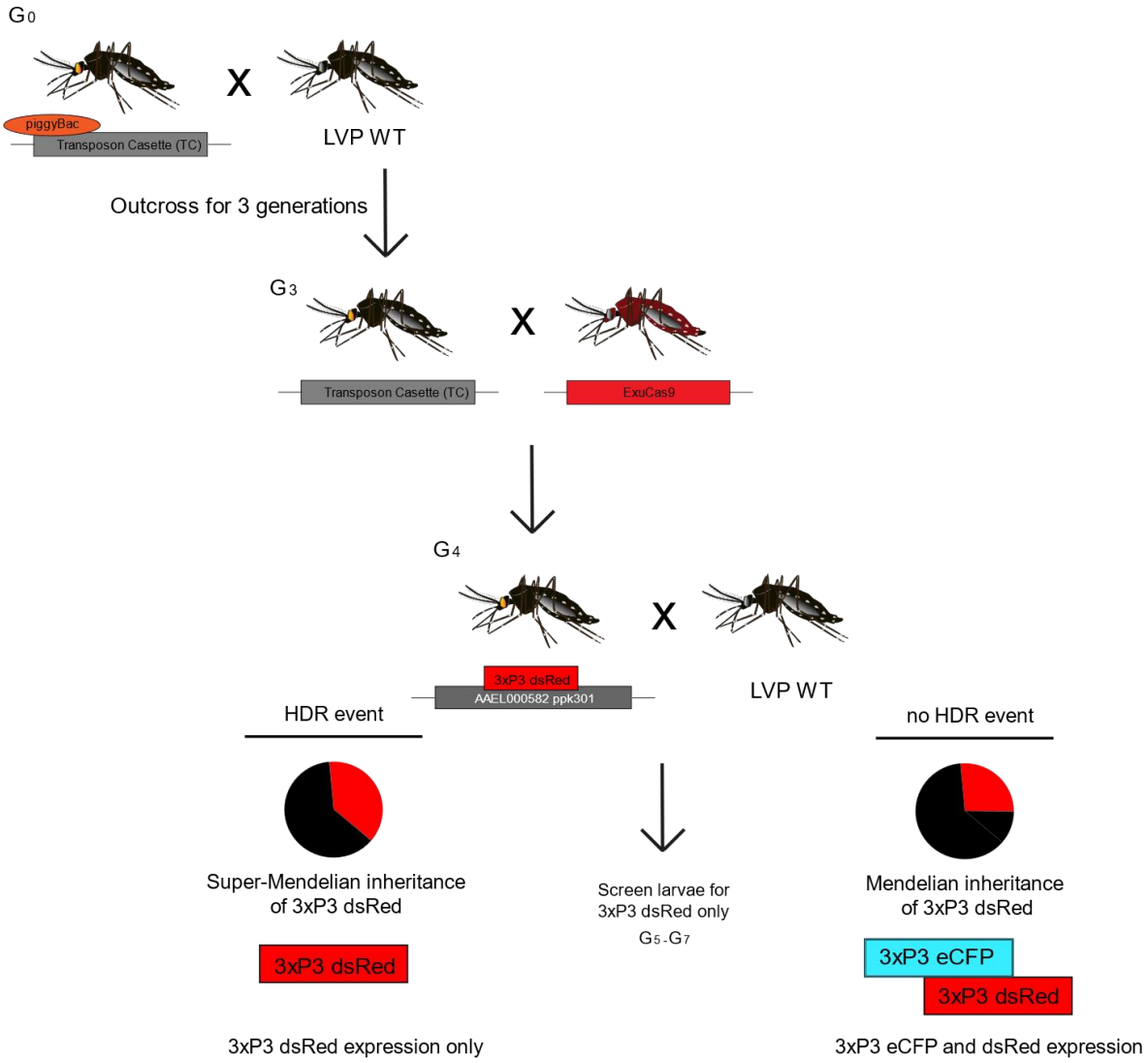

Figure 2. Overview of *Ae. aegypti* crosses to generate HDR events in after G_4s. G_0 *LVP* mosquitoes were injected with *piggyBac* transposase mRNA, which mediates the integration of TC into the genome. Founders were identified and outcrossed for 3 generations to WT *LVP* mosquitoes. In the G_3s, adults carrying TC were crossed to *exuCas9* adults. G_4 larvae were outcrossed again to *LVP* mosquitoes to separate TC carriers from transgenic larvae due to HDR repair. Larvae in the next 3 generations (G_5 – G_7) were sorted for their fluorescence expression. Successful HDR events could lead to Super-Mendelian like inheritance pattern of the red eye marker, as more larvae would express red eye marker only due to HDR repair. Lack of HDR events will lead to expected, Mendelian inheritance of markers, with larval inheritance and expression of both blue and red eye markers.

3.3.2 Generation of TC carriers

Of the 200 *LVP* embryos injected with TC plasmid and *piggyBac* transposase mRNA, 58 survived to adulthood (29% survival rate). 29 of these G_0 survivors gave offspring when outcrossed to *LVP* adults. A single transgenic strain was collected from the hatch of two possible founders (< 3.4% transgenic out of G_0 survivors), which resulted in 9 out of 27 larvae with expression of both blue and red eye marker (33% G_1 transgenic rate). A second strain resulted in 1 out of 59 with red eye marker expression only but failed to give further offspring when outcrossed. The following work was done with the single TC founding strain (**Fig. 2**).

3.2.3 Crossing scheme for TC and Cas9 in the G_3 cross

After three outcrosses of the TC carrier strain, G_3s were crossed to the *exuCas9* adults. G_4s should inherit all components of the split CRISPR/Cas9 system, including Cas9, sgRNA and donor template targeting *ppk301*. G_4s were screened for expression of all markers including the red body fluorescence from *exuCas9* (**Fig. 1b**). Offspring with positive expression of all markers were outcrossed again to separate inheritance of TC with HDR events that integrate the red eye marker only. We propagated each of these strains individually and outcrossed only those with eye marker expression only or expression of all markers. Larvae were continued to be screened for three more generations while outcrossed to *LVP* strain (**Fig. 3**).

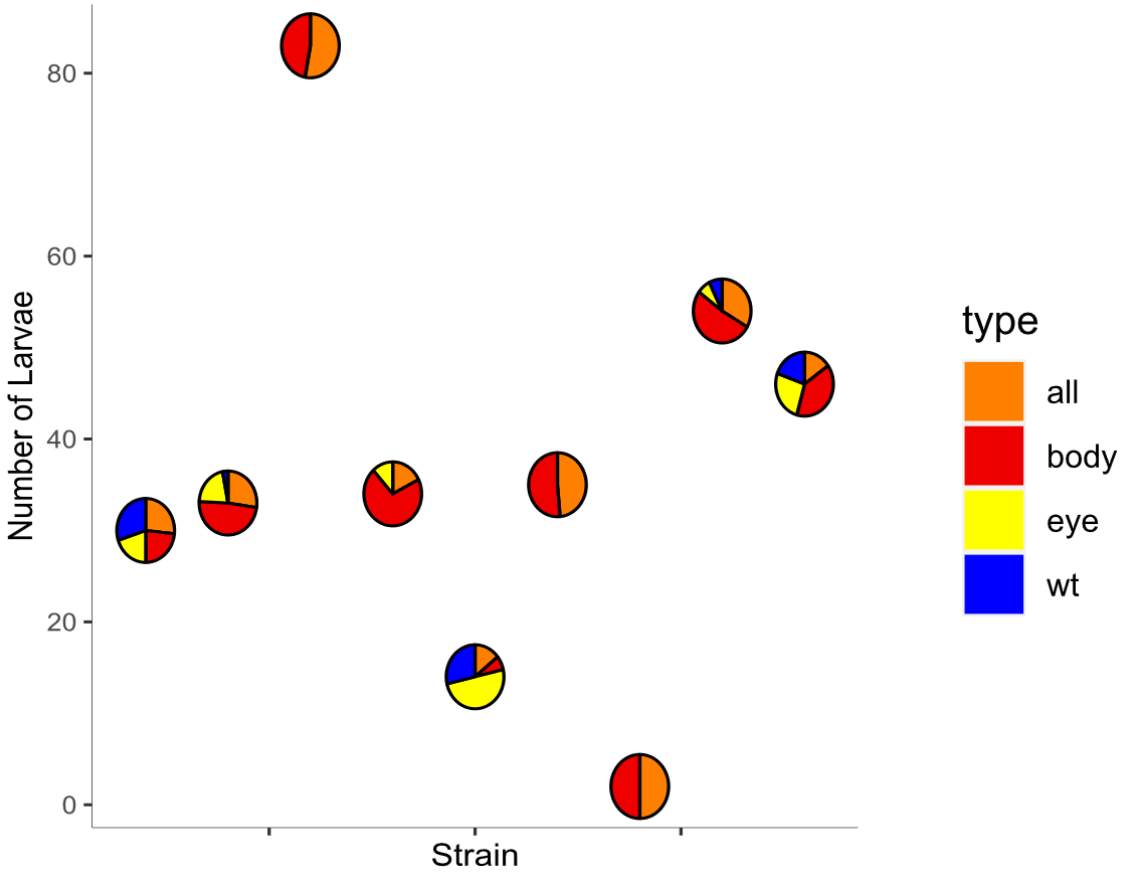

Figure 3. Scatterpie graph showing number of larvae in 9 G_4 strains and the proportion of fluorescence expression patterns in larvae
9 G_4 strains were recovered after crossing TC carriers (G_3) to *exuCas9* adults. “Type” refers to the fluorescence expression of larvae: “all” stands for red body, red eye and blue eye fluorescence; “body” stands for red body fluorescence from *exuCas9* only; “eye” stands for red and blue eye fluorescence from TC integration only; “wt” stands for wildtype without any fluorescence.

3.3.3 7 G_4 strains were recovered from G_3 x *exuCas9*

All components of the split system (TC and *exuCas9*) met in the G_4 generation. Nine G_4 strains were established in the G_3 cross to *exuCas9*, which should generate DSBs and allow HDR or NHEJ to happen. G_3 strains with less than 30 G_4 larvae hatched were discarded from further parental analysis, as the genotypes of these strains are unlikely to be a true representation of gene inheritance from their G_3 parental crosses. Two strains were discarded from analysis due to the low number of larvae hatched, with two and fourteen larvae respectively. We were unable to predict the genotype of their parental crosses. Out of nine G_3 crosses, seven of these G_4 strains had more than 30 larvae. We did not observe a super Mendelian inheritance like pattern of red eye markers in any of the G_4s. Red eye markers were not more represented in the G_4 larvae, which would be indicative of HDR events. In terms of inheritance patterns, two strains were inferred to be the offspring of heterozygous parents ($\frac{ExuCas9}{+}\ x\ \frac{+}{Casette\ (3xP3)}$), due to a 25% inheritance of all possible marker phenotypes; Two strains were inferred to be from homozygous parents ($\frac{ExuCas9}{ExuCas9}\ x \frac{+}{Casette\ (3xP3)}$), due to 50% inheritance of red body fluorescence only or all fluorescence markers; The remaining three strains did not follow these inheritance patterns and showed more than 50% of red body fluorescence inheritance. This signified that HDR events might not have occurred within the germline cells of the G_4s. We further outcrossed G_4s to clarify if HDR events and stable integration of red eye marker was masked by the expression of the TC cassette (**Fig. 3; Supp. Table 5**).

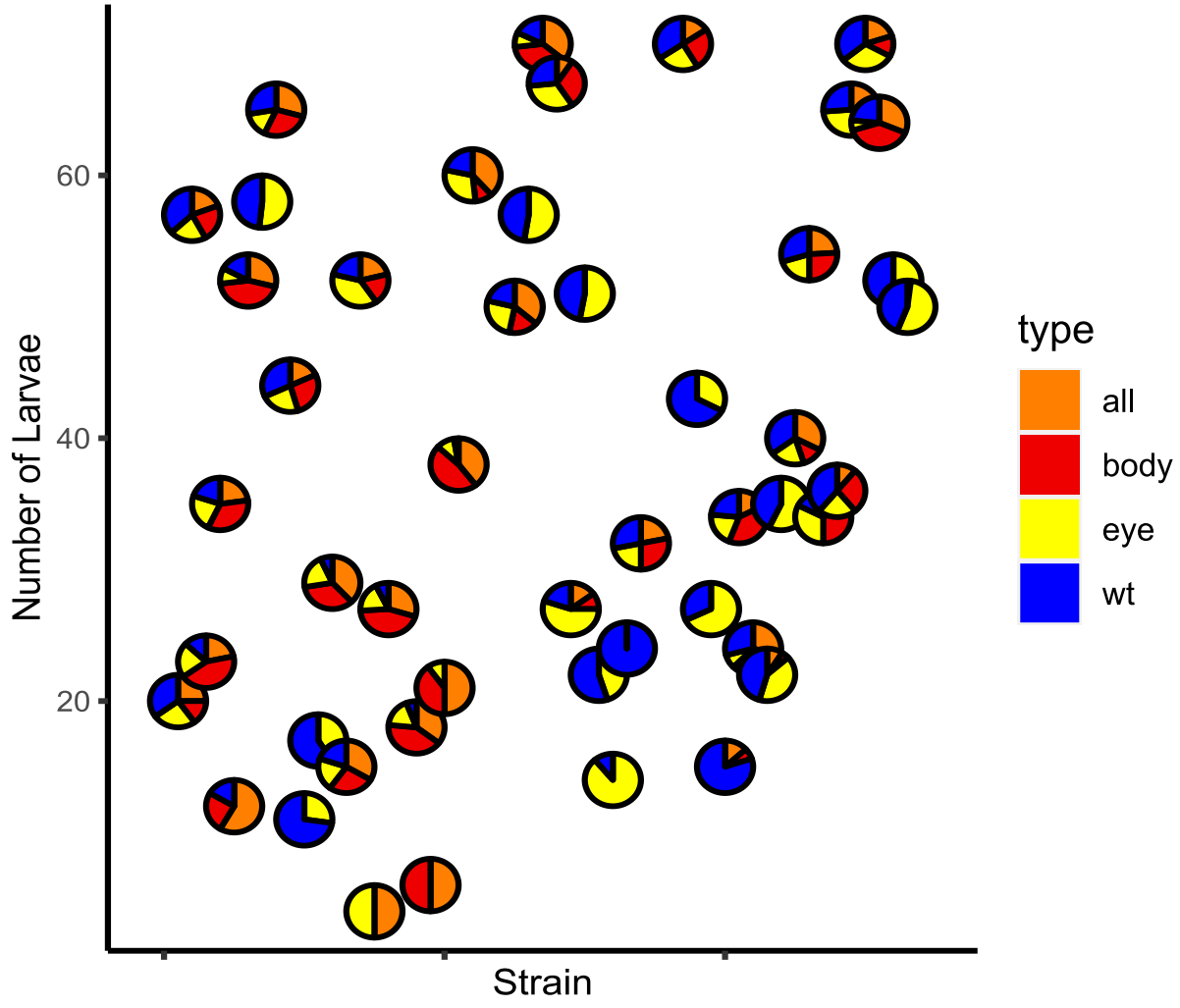

Figure 4. Scatterpie graph showing number of larvae in 53 G_5 strains and the proportion of fluorescence expression patterns in larvae
53 G_5 strains were recovered after outcross to *LVP* WT mosquitoes. “Type” refers to the fluorescence expression of larvae: “all” stands for red body, red eye and blue eye fluorescence; “body” stands for red body fluorescence from *exuCas9* only; “eye” stands for red and blue eye fluorescence from TC integration only; “wt” stands for wildtype without any fluorescence.

3.3.4 53 G_5 strains were screened for HDR but none were successfully identified

G_4s were separated where only those individuals carrying eye markers were further outcrossed to generate individual strains. HDR events would generate a red eye marker phenotype (which could be masked by TC expression). By outcrossing to *LVP*, we sought to separate these phenotypes by screening for offspring that showed inheritance of only red eye but not the other marker. 53 G_5 strains were established in this cross, while those with less than 30 larvae hatched were discarded from further analysis. 29 strains remained but did not result in any larvae with red eye marker only, indicating that HDR did not happen. Five of the G_5 strains had no larvae hatched, which accounted for 9.4% of the total number of G_5 strains. On average, 60% of larvae inherited both eye markers which could signify super Mendelian inheritance. We further outcrossed this strain to look for repeatable result and patterns of inheritance (**Fig 4; Supp. Table 6**).

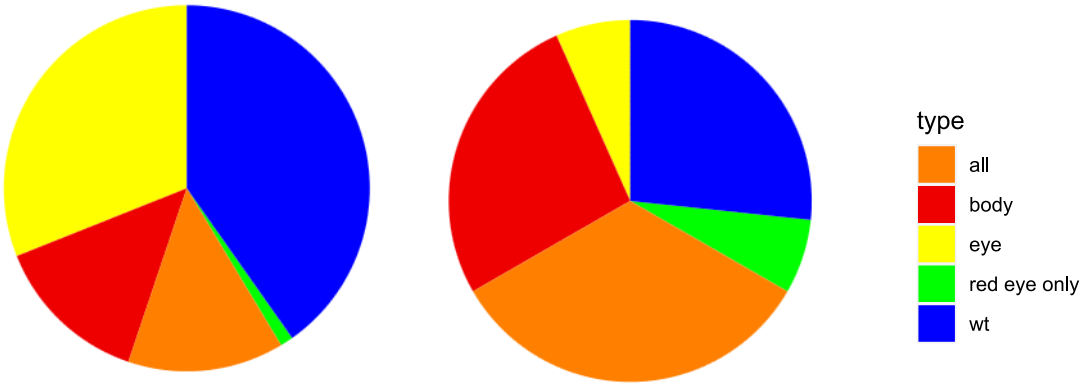

G6 R6M4 all+ Female

G6 R6M2 all+ Female

	red eye only	eye	all	wt	body	hatch rate
G6 R6M4 all+ female	1	27	12	35	12	0.44
G6 R6M2 all+ female	1	1	4	4	5	0.13

Figure 5. Pie chart showing distribution of larval expression where two larvae with red eyes only were identified in G_6s. Naming of strains are as follows: "R6M4" for initial G_4 strain founder of this strain, "all+ female" for female parent that had all fluorescence positive ("all" phenotype). Hatch rate and number of each phenotype are shown in the table. "Type" refers to the fluorescence expression of larvae: "all" stands for red body, red eye and blue eye fluorescence; "body" stands for red body fluorescence from *exuCas9* only; "eye" stands for red and blue eye fluorescence from TC integration only; "red eye only" stands for red eye fluorescence from possible HDR event only; "wt" stands for wildtype without any fluorescence.

3.3.5 Two G_6s showed possible HDR events but not in G_7s

Through continued outcrossing of G_5s, we found two possible larvae in G_6 with red eye marker only out of 25 strains (**Supp Fig. 1; Fig. 5; Supp. Table 7**). Five of the G_6 strains did not have any larvae hatched, which accounted for 17.9% of the total number of G_6 strains. "G6 R6M2 all+ female" strain had a low hatch rate and low number for each phenotype. Further outcross with the red eye only individual resulted in two larvae in the G_7s, with neither of them passing on red eyes only. Across all generations after G_4s, we observed delays in larval hatching of up to one month.

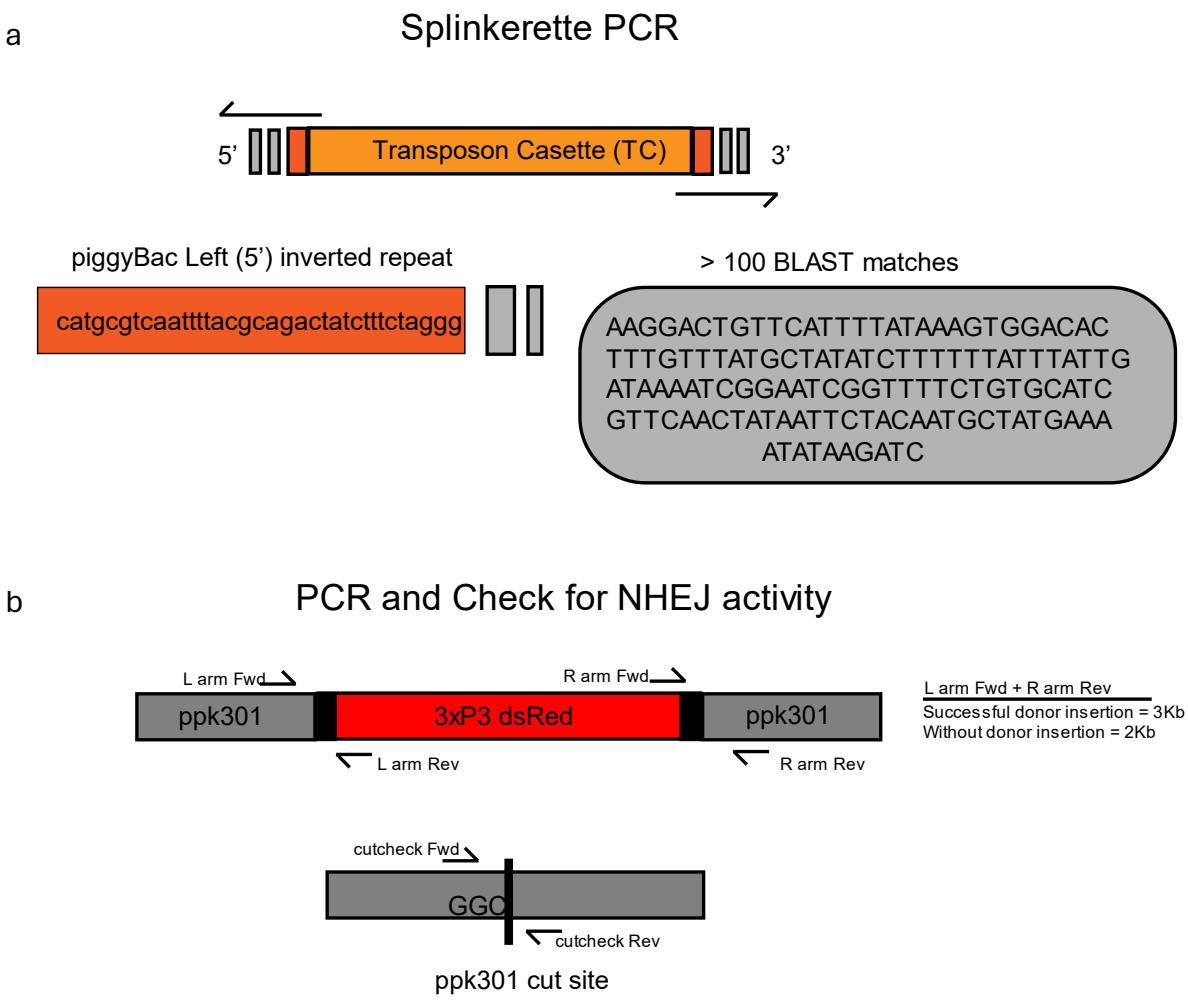

Figure 6. Schematic of Splinkerette PCR and check for NHEJ activity at the *ppk301* cut site, using G_4 genomic DNA. (a) Splinkerette PCR design and result from the (5') splinkerette. Orange sequence refers to sequence found in G_4 larvae showing 5' inverted repeat of the *piggyBac* transposon. Grey sequence refers to genomic DNA sequence upstream of the proposed TC integration site, that showed alignment to *Ae.aegypti* genome (AaegL_5). **(b)** Schematic for the PCR done to check for donor template integration at the *ppk301* cut site. Single headed arrows represent primer designs used for PCR and NHEJ check. PCR for successful integration results in 3Kb band while no integration shows 2Kb band. **(c)** NHEJ was checked via small PCR amplification at the proposed target site. PAM sequence is shown (GGC) on the reverse strand of *ppk301*, while primer pair (cutcheck Fwd and Rev) were used to amplify the cut site.

3.3.6 Mapping location of TC insertion

Since TC was integrated via *piggyBac* transposon, the location of integration can be mapped by using techniques such as inverse PCR (iPCR) or Splinkerette PCR (Potter and Luo, 2010). A total of 48 G_4 larvae had genomic DNA extracted, which represented all 7 G_4 strains established for analysis. After two rounds of nested PCRs, only the 5' inverted repeat resulted in successful sanger sequencing results. A BLAST search for this sequence in the *Ae. aegypti* genome returned more than 100 matches, suggesting that at least the 5' end of the TC landed in a highly repetitive sequence within the genome. The 3' inverted repeat did not result in informative sanger sequencing results, due to failure for PCR amplification in the second round of Splinkerette PCR. Thus, the site of TC insertion cannot be precisely located, nor can we confirm if there was more than one insertion of TC in the G_4s (**Fig. 5a**).

3.3.7 Check for NHEJ showed no Cas9 activity in G_4s

To further test for HDR activity in the G_4s, we used PCR to check for successful integration of donor template in the *ppk301* gene using genomic DNA from G_4s. Two sets of primers targeted part of *ppk301* and part of the donor template, which should only amplify where there is successful insertion. Both PCRs generated no amplicons, as confirmed by negative results in gel electrophoresis. Another round of PCR of the entire *ppk301* insertion region was around 2Kb instead of 3Kb, which confirmed that *3xP3 dsRed* was not inserted in this target site. This shows that HDR events did not occur in the G_4s (**Fig. 5b**). Without HDR activity, we further tested if Cas9 was active in the G_4s by measuring NHEJ activity. As DSBs are repaired by either repair pathway, NHEJ should act as a proxy for Cas9 activity at *ppk301* (Kistler, Vosshall and Matthews, 2015). Upon sequencing and comparison of sequences using ICE, we observed no insertion or deletion mutations at the proposed cut site (**Fig. 5c**). This indicates that Cas9 might not be actively cutting at *ppk301*. It is unlikely that all sequences were perfectly repaired by NHEJ, based on previous observations in **Chapter 2**.

3.4 Discussion

3.4.1 Design of TC and use of the *ExuCas9* strain

The design of TC and the use of *piggyBac* transposon mediated integration was built on the HACK system strategy by Lin and Potter (2016). The TC cassette carries two fluorescence markers, each indicating a different version of gene integration. The use of *exuCas9* adds an extra layer of visual marker to be screened for. Our results for checking NHEJ activity suggests that Cas9 did not actively make DSBs, at least in the G_4 cross. This is surprising as *exuCas9* has been shown to be highly active in generating mutations (Li et al., 2017; Li et al., 2022). Specifically, *exuCas9* strain injected with a version of the *U6* sgRNA promoter showed high rates of mutations (>90%) and super-Mendelian inheritance (>70%). As shown in the previous chapter, *exuCas9* was reliable in creating DSBs with the sgRNA targeting a different gene. Therefore, it is likely that sgRNA expression in this context was the reason for the lack of Cas9 activity. In future work, injection of sgRNAs in embryos can validate if Cas9 is active before attempting the G_4 crosses. The location of TC insertion could also affect the expression of the sgRNA, which could lead to the absence of Cas9 activity.

3.4.2 Genome of *Ae. aegypti* and the location of TC

The genome of *Ae. aegypti* could be another hurdle in the successful use of the TC strategy. The *Ae. aegypti* genome is approximately 1.22Gb (Matthews et al., 2018), and is about 5-fold larger than *An. gambiae* (Nene et al., 2017; Daron et al., 2024). When compared to other mosquitoes and *D. melanogaster*, *Ae. aegypti* genome is highly repetitive and compose of almost 40% Transposable elements (Arensburger et

al., 2011; De Melo and Wallau, 2020). This highly repetitive nature of the genome could be a possible reason for the failure to pinpoint the TC insertion through Splinkerette PCR. BLAST search revealed that the sequences upstream of the TC location is highly repetitive, with more than 100 matches to the *Ae. aegypti* genome.

3.4.3 HDR is affected by the proximity of the donor template

The exact location of TC has been shown to be important for successful HDR repair. Previous work in the HACK system showed that gene conversion is highly dependent on the position and proximity of the donor template in relation to the target (Lin and Potter, 2016). They mapped donor templates across the genome by using transposon mediated integration to map conversion efficiency. In summary, donor template insertion close to the target shows a 50-fold increase in conversion rates, but cold spots on the genome could reduce gene conversion activity. Thus, gene conversion by HDR depends on the distance of the donor from the target sequence (Chen et al., 2007). One limitation to our work was the lack of diversity in TC insertion outcomes. During the creation of G_0 founders, only one line was successful in carrying TC (3.4% G_0 transgenic rate). We cannot conclusively determine if the lack of Cas9 activity is due to the design of TC, or that the location of TC was not ideal for HDR repair. A possible improvement to our strategy would be to use *hyperactive piggyBac*, which can mediate integration in higher efficiency (Otte et al., 2018). The creation of multiple founder lines could benefit the conclusions we can draw from our work and has been shown to be successful in Anderson et al. (2024). The generation of TC strains was the major limiting step to our results.

The lack of HDR repair in out results could be further explained by the lack of localization of donor templates at the DSBs. In our work, we inserted TC to a random location of the genome and relied on homologous pairing between the donor template and DSB target. We predicted that donor template and sgRNAs should be present in the cell ubiquitously, and the expression of Cas9 would later induce DSB repair. However, it has been shown that DSB repair is highly dependent on the proximity of the donor template. When DSBs are repaired faithfully, homologous chromosomes can make contact at the site of DSBs which favors HDR repair (Lee et al., 2016; Lieber, M. R., 2010; Gandhi et al., 2012). If donor template was not localized at the site of DSB, it could decrease the efficiency of gene insertion through HDR. Although it is possible to link the donor template to the Cas9 protein (Savic et al., 2018) or use DNA in chromatin form as the donor template (Cruz-Becerra and Kadonaga, 2020), these strategies have not been attempted in systems other than mammalian cell lines. Future work in split systems like this could benefit from confirming location and proximity of donor templates before crossing to the Cas9 strain.

3.4.4 Maternal deposition of Cas9 in G_4 offspring

As noted in the previous chapter (**Chapter 2 – Discussion 2.4.6**), maternal deposition of Cas9 favors NHEJ and is a source of resistance to gene drives. Even in a split gene drive system, maternal inheritance of Cas9 induces mutations to the target site with sgRNA deposition. All embryos from the Cas9 strain would likely inherit Cas9 protein from their mother, which makes it more likely for NHEJ mutagenesis to disrupt HDR insertion (Champer et al., 2019; Kandul et al., 2020). The offspring after G_4s likely have Cas9 protein deposited in their germline cells, which makes it possible but

unfavorable for further HDR repair in subsequent generations. One strategy that might be able to bypass maternal deposition is “multiplexing”, which is the use of multiple sgRNAs targeting the same gene to achieve HDR repair in one of these sites. Multiple sgRNAs can target adjacent target sites so that NHEJ mutations generated at one target does not disrupt the overall possibility of HDR repair for that gene. This could possibly increase HDR efficiency at one target site, as shown by the recent sGD work in Anderson et al. (2024). One key advantage of the split system is the separation of sgRNA and donor from the Cas9 strain. Future work can separate Cas9 strains based on sex before crossing to TC, which should restrict deposition of Cas9 to only mothers and not fathers.

At the time of completing this work, a similar strategy of sGD homing system was attempted in *Ae. aegypti* with greater gene conversion rate by Anderson et al. (2024). They also utilized *piggyBac* insertions to generate five Cas9 strains. Combined with a previously characterized sgRNA/donor template carrying strain, this created a split system similar to our work. Their sGD utilized a new Cas9 driver from the *Drosophila bgcn* gene which is predicted to express in the germline and showed high HDR efficiency (>75%). In comparison, we relied on the *exuCas9* strain as the only source of Cas9. The difference of the Cas9 gene promoters could have resulted in differences between HDR repair rates.

Another key difference is their use of a homing donor template at the target site. This strategy converted the target gene to carry a donor template, which is subsequently used to convert future target genes in the offspring at much higher efficiency. This avoided the effect of template location, as donor template will always be

present on the other allele of the target site. Although our work did not involve the creation of a gene drive, it proposed a possible challenge for location specific activity that could be missed by gene drive studies. To study the location effect of the genome, more target sites will need to be compared for their HDR repair efficiency. The use of transposon mediated integration has the potential to create multiple transgenic lines before genetic cross for HDR integration at the gene of interest. Although our work does not involve self homing donor templates in gene drives, it showed the potential of using a split system to increase HDR efficiency.

3.4.5 Toxicity of Cas9 and lowered fitness

In the TC strategy, individuals in later generations (G_4 to G_7)s appeared to have lower fitness. One possibility is that this fitness cost was due to toxicity of Cas9 expression. As discussed in the previous chapter (**Chapter 2 – Discussion 2.4.7**), we observed similar trends in lowered fitness of transgenic mosquitoes. The elongated and high level of Cas9 endonuclease expression in the cell comes with possible negative impacts to the organism, even if the endonuclease is inactive (Jiang et al., 2014). We also observed heavily delayed hatching of eggs, which could be a previously not discussed sign of lowered fitness. Mosquitoes go through a process called diapause, which is a delay in development of the egg and larval stage due to environmental conditions (Lacour et al., 2015; Vinogradova, E. B., 2007). Diapause is a genetic process that alters expression of certain transcripts to help mosquitoes tolerate unfavorable conditions (Diniz et al., 2017). While it is unlikely that the (G_4 – G_7)s transgenic mosquitoes in our work was induced to dormancy during egg stage, we observed larvae that hatch from eggs up to one month after the initial hatching event.

This significant delay in egg hatch was unexpected and was not previously reported by work generating transgenic mosquitoes with integrated CRISPR/Cas9 components. We also noted that up to five strains failed to hatch in the G_5s and G_6s. The reason behind this hatch delay is currently unknown. This affected the rearing time needed to raise transgenic mosquitoes, especially if larvae could hatch after eggs are already discarded by researchers. Overall, we recommend counting the number of eggs before each hatch to account for hatch rate over each generation.

3.4.6 Cas9 activity and possible HDR event in G_6s

While initial screening and G_4 genomic DNA sequence analysis failed to recover successful NHEJ or HDR events, two possible HDR events could have happened in the G_6s. Since offspring after G_4s inherit the Cas9 cassette with TC, it is possible for HDR events to happen in any of the offspring germline cells. However, we expect that NHEJ mutations would be favored due to maternal deposition of Cas9. The two possibly transgenic G_6 larvae carried only the *3xP3 dsRed* marker without *eCFP*, which could indicate HDR repair. If HDR repair was successful, we would expect only the *3xP3 dsRed* marker to be passed on. However, both G_6s failed to give offspring with the same eye phenotype. As the G_7 larvae did not match this phenotype, we cannot conclude that HDR repair events led to *3xP3 dsRed* insertion. It is currently unclear as to why these two G_6s exhibited phenotypes resembling HDR repair events. Further sequencing and PCR validation can be done to genotype these two G_6s with red eye marker only phenotypes.

3.4.7 Limitations and Future Directions

The Transposon Transgene strategy aimed to induce HDR repair using a split system, which should reduce the time and effort required for G_0 embryo microinjection. Several improvements can be made to our current approach. First, the use of a *hyperactive piggyBac* transposon could increase the number of TC insertion events (Anderson et al., 2024; Otte et al., 2018). Having a TC insertion at different locations can help us identify expression cold spots in the genome. Second, other Cas9 strains in *Ae. aegypti* should be utilized to generate transgenic lines. As noted in the previous chapter and most gene drive work, germline gene promoter regions could impact Cas9 activity and HDR repair efficiency (Anderson et al., 2024; Li et al., 2017). We recommend testing multiple Cas9 strains with different gene promoter expression to generate transgenic strains.

3.4.8 Conclusion

To summarize, our transposon transgene strategy did not successfully produce stable HDR integration in the transgenic strain. While it is possible that HDR repair could be masked by TC expression, we did not observe any inheritable changes in the transgenic larvae. We cannot conclude that an endogenous, genomic source of sgRNA and donor template could promote HDR repair in *Ae. aegypti*. We cannot support nor reject our initial hypothesis. Multiple factors in our current system could limit HDR repair, including the lack of DSB generation, the location of TC insertions and the lowered fitness of transgenic offspring. While the lack of DSBs generated by *exuCas9* is the primary reason for the lack of transgenic offspring, DSBs could be made in the generations after G_4s. If HDR repair were to happen in these subsequent generations,

the location of TC insertion and lowered fitness of offspring would likely come into play. We also cannot conclude if sgRNA and donor template were present and localized during germline development, which could hinder the ability for Cas9 to make DSBs. The use of transposon mediated gene integration can still reduce the time and effort needed for generating transgenic strains. We recommend the use of multiple Cas9 promoters and multiple sgRNAs to ensure that HDR activity is not limited by the combination of each of these CRISPR components. Moreover, future efforts can be done to optimize expression of sgRNA and localize donor template to match the location of the target site.

4 Generation of a novel balancer chromosome

4.1 Introduction

4.1.1 Introduction to balancer chromosomes

Balancer chromosomes have long been used in model organisms to balance deleterious mutations, and acts as a vital part for the field of genetics. The idea of balancing lethal alleles was first proposed by Muller, H. J., (1918), where inversions in chromosomes were noted to enforce heterozygosity in *D. melanogaster* and limit homozygous offspring. A balancer chromosome is a region of inversion that suppresses recombination events, allowing mutations to be sustained in heterozygous individuals (Kaufman, T. C. 2017). During crossover events, chromosomal inversions have been shown to suppress recombination (Crown et al., 2018; Miller et al., 2016b). Balancers used in *D. melanogaster* have traditionally been created through ionizing radiation to generate multiple chromosome inversions randomly (Miller, Cook and Hawley, 2019; Miller et al., 2016a). Chromosomal breaks are sometimes repaired incorrectly, giving rise to inverted segments of the chromosome. Mutated organisms are then screened for changes in phenotype that could suggest possible inversion events. Not only is this method of non-selective mutagenesis random and unpredictable, but it also requires tremendous effort for researchers to create exact inversions (Stern, D. L., 2022). With the rising popularity of precise genetic editing, tailor designed balancer chromosomes have been generated in the past decade to balance specific mutations of interest.

4.1.2 Project approach and significance

CRISPR/Cas9 mediated genetic editing has the potential to generate precise inversions to the chromosome in *Ae. aegypti*. Previous work has used this transgenic tool to generate novel balancers in *D. melanogaster* (Muron et al., 2022; Stern, D. L., 2022) and *Caenorhabditis elegans* (Dejima et al., 2018; Iwata et al., 2016). Using simultaneous injection of two sgRNAs targeting separate genes on a chromosome, Cas9 can generate two DSBs and create junction points. With the addition of donor templates resembling both genes at the junction points, HDR repair has the potential to invert the region between DSBs. Serial inversions of these chromosomes can provide a strong balancer that suppress recombination of lethal or sterile mutations. Finally, visible phenotypes can be created through HDR insertion of fluorescent markers or disruption to certain genes. This allows researchers to maintain stocks of model organisms with relative ease. Moreover, the precise creation of balancers has the potential to cover regions that were previously missed by standard balancers, thereby maintaining more deleterious mutations (Iwata et al., 2016; Stern, D. L., 2022).

As *Ae. aegypti* has only peaked research interest as a non-traditional model organism as of the past few decades, balancer chromosomes are currently not a part of their genetic toolkit. Transgenic strains of *Ae. aegypti* are maintained through selecting positive individuals every few months and continued outcrossing. Many of these transgenes or mutations disrupt the function of the mosquito physiology and incur fitness costs. For example, mutants to CO2 detection (McMeniman et al., 2014), odor attraction (DeGennaro et al., 2013), vision (Zhan et al., 2021) and egg laying (Matthews, Younger & Vosshall, 2019) have all been created. These mutations are considered

deleterious and rely on the efforts of researchers maintain their stock. Other than the low efficiency of generating precise editing in *Ae. aegypti*, maintenance of transgenic strains is one of the biggest hurdles in mosquito genetics. Therefore, we proposed to adopt methods in precise balancer generation in *Ae. aegypti*.

We hypothesize that if “bi-genic” donor templates are present during DSBs, large chromosomal inversions can be generated via HDR in *Ae. aegypti*. (**Fig. 3**) “Bi-genic” refers to single-stranded oligodeoxynucleotides (ssODNs) that combines the sequence of two genes across the chromosome as a template for HDR repair to invert the chromosome. While ssODNs have been shown to be an effective donor template in *Ae. aegypti* (Kister, Voshall and Matthews, 2015), the efficiency of bi-genic ssODNs have not been attempted. We also made use of the visible phenotype generated by disruption to the *yellow* gene (Li et al., 2017), which can act as an indicator of possible novel balancers. It should be noted that the *Ae. aegypti* genome includes vast areas with low recombination rates, with up to 47% of the chromosome mapped in these recombination deserts. The most prominent area of extremely low recombination rate resides in the first chromosome, near the male-determining locus (Chen et al., 2022). Our choice of inversion at the distal part of the p arm of chromosome 1 should cover areas that avoid this recombination desert (**Fig 1**).

Not only will balancers be a much-needed addition to the *Ae. aegypti* genetic toolbox, this would also be the first instance of large-scale genetic engineering of structural variation in mosquitoes. Results generated from our work could have implications for mosquito genetics and gene drive applications, where large

chromosomal inversions could be implemented as an alternative to current standards of genetic manipulation.

4.2 Methods

4.2.1 Mosquito Strains

Aedes aegypti mosquitoes were maintained according to standard protocol as described (Sun et al., 2022; Wohl & McMeniman, 2023). Mosquito eggs were hatched in a vacuum chamber (20 – 25 Psi) and kept in containers of dechlorinated water until pupation. All adult mosquito strains were kept at 25 – 28 °C in mesh cages (Bugdorm, 4M3030), with constant relative humidity of 70-80% and 12 : 12 light : dark photoperiod. 10% sucrose solution was provided in the mesh cages of mixed sex for strain maintenance. All females were blood fed on defibrillated sheep blood (Cedarlane Labs, DSB250) via a glass mosquito feeder (Chemglass, Cat# CG1836) with a layer of parafilm spread across the feeder. Blood inside the feeder was warmed to 37.5°C. Blood fed mosquito cages were given 30% sucrose solution to minimize egg laying on 10% sucrose solution sugar wicks.

Exu-Cas9 strain had a stable integration of Cas9 sequence and an expression of *dsRed* in the body. *Yellow* strain was also created by mutation of the exon 2 of the *yellow* gene (AAEL016999) and has a visible yellow body phenotype (Li et al., 2017).

4.2.2 Identification of Possible Targets to Chromosomal Inversions

Chromosome arms in *Ae. aegypti* are denoted by “p” and “q” for the shorter and longer arms respectively. Seven candidate genes on the distal p arm on Chromosome 1 were identified to be possible targets for chromosomal inversion with *yellow*. These candidates have similar genic size with *yellow*. Gene sequences were exported from Vectorbase and approximate locations were mapped manually on a cytogenetic map

from Ensembl Metazoa. Information about the size, exon and intron number and possible phenotypes were collected. Previous mutations of gene orthologs in *Drosophila melanogaster* were collected from Flybase, as a possible indicator of mutation phenotypes. Of the seven candidate genes, three were selected for sgRNA activity validation which includes AAEL004193 (R), AAEL013840 (V) and AAEL012549 (F).

4.2.3 sgRNA Design and Transcription

CHOPCHOP v.3 was utilized to create sgRNA designs for the three candidates genes and *yellow*. For the three candidates, the top three sgRNA designs and their associated primers were used for validation. For *yellow*, sgRNA design from Li et al., 2017 was utilized as well as the top two designs from CHOPCHOP. sgRNA templates were produced using the HiScribe Quick T7 kit (New England Bio, Cat# E2050S). All procedures followed previously described protocol (Lo & Matthews, 2023). All sgRNA sequences are listed in **Supp. Table 1**.

4.2.4 Embryo Microinjection with sgRNA injection mix

One sgRNA of each of the targets and yellow were injected together as a single injection mix. Transcribed sgRNAs were purified and eluted in water separately, then combined in the same 1.5mL Microcentrifuge Tube. Injection mix was filtered through a SpinX centrifuge tube filter (CoStar, 8160) one minute in max speed in a centrifuge. 50 Exu-Cas9 embryos were injected for each sgRNA mix, for a total of 200 Exu-Cas9 embryos injected for sgRNA validation. All injections were done in the embryo injection station in Matthews Lab, UBC. Injection was done according to Sun et al. (2022).

4.2.5 Testing sgRNA Activity – ICE

Genomic DNA of injected Exu-Cas9 embryos was extracted in pools of three pupae and repeated for three samples. All pupae were frozen in -74°C before DNA extraction. DNA was sequenced at the cut site for all four targets. Gene sequences were compared to Exu-Cas9 sequence using Synthego ICE analysis. Mutations generated by NHEJ was used as a proxy for sgRNA activity. Of the pooled genomic DNA sequence, mismatch between AaegL5.0 genome used by CHOPCHOP and the Exu-Cas9 sequence caused some sgRNAs to have no activity at the cut site. Details for validation of sgRNA activity can be found in Lo and Matthews, 2023.

4.2.6 ssODN Repair Template Design

Chromosomal inversions are generated through simultaneous Homology Directed Repair events across two Double-strand breaks on the same chromosome. I designed two single-stranded oligodeoxynucleotides (ssODNs) as repair templates that have homology with both gene targets, following the design of Dejima et al. (2018).

For ssODN 1, 100 base pairs upstream of the *yellow* cut site was combined with the reverse compliment of 100 base pairs upstream of AAEL013840 (V) cut site. For ssODN 2, the reverse compliment of 100 base pairs downstream of the *yellow* cut site was combined with 100 base pairs downstream of AAEL013840 (V) cut site. ssODN 1 and 2 serve as the repair template of the inverted chromosome 1. ssODNs were synthesized commercially using the Integrated DNA Technologies Donor Oligos Synthesis service.

4.2.7 Embryo Microinjection of ssORNs to Generate Chromosomal Inversion

To generate chromosomal inversion, 559 Exu-Cas9 embryos were injected with sgRNA targeting AAEL013840 (V), sgRNA targeting *yellow* (40 ng/μL each) and the two ssODN repair templates (10.9 ng/μL each). Injection mix was combined and filtered as stated in **Embryo Microinjection with sgRNA injection mix**. All injections were done in the embryo injection station in Matthews Lab, UBC. Injection was done according to Sun et al. (2022).

4.2.8 Screening of Transgenic Mosquito and Outcross to *Yellow*

Injected Exu-Cas9 embryos were hatched and reared to adulthood. Male G0s were mated with a *yellow* virgin female; Female G0s were batch mated with *yellow* males. Five days post bloodmeal, females were separated into individual egg laying vials. G1 embryos are scored for their color during melanisation, at least one hour after they are laid. Embryos with yellow phenotype are noted and dried for one week before hatching.

4.2.9 Data Analysis

R studio (Version 4.1.1) was used to analyze data in this chapter. Bar graph was generated with the ggplot() function. Schematics were created using Adobe Illustrator (2022).

4.3 Results

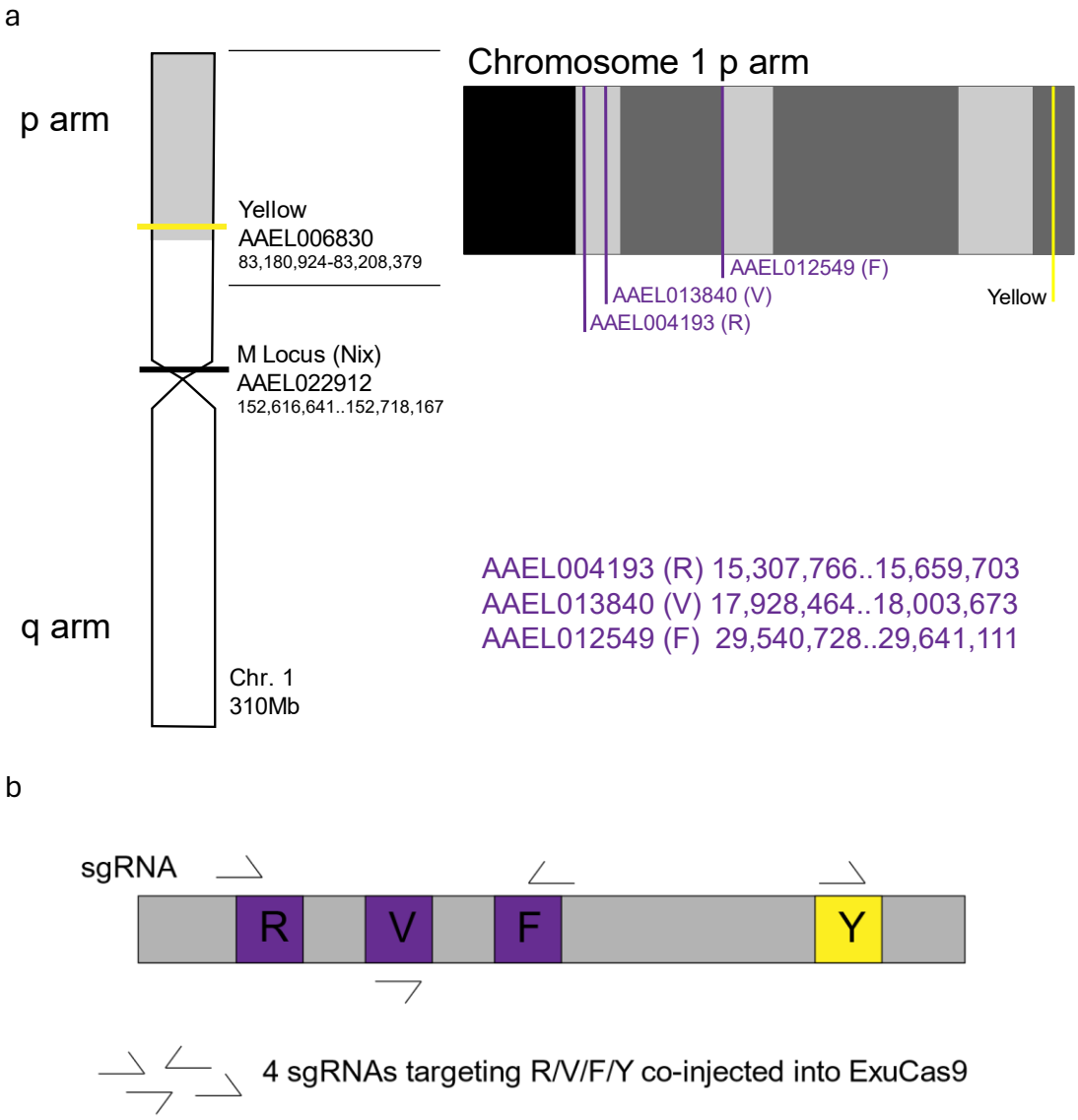

Figure 1. Schematic of four genic targets in Chr. 1 of *Ae. aegypti* to generate chromosomal inversions. (a) Schematic of the entire chromosome 1 with *AAEL006830* (yellow) and *AAEL022912* (Nix) mapped. Part of the distal p arm chromosome 1 enlarged showing the location of the four genic targets chosen for sgRNA testing. Physical genome map recreated from Timoshevskiy et al. (2014). *AAEL004193*, *AAEL013840*, *AAEL012549* and *AAEL006830* (yellow) are mapped from distal to proximal to the centromere of Chr. 1. **(b)** Schematic representation of testing four sgRNAs for each genic target during testing for sgRNA efficiency. Single headed arrow represent sgRNAs.

4.3.1 Identification of possible targets to generate chromosomal inversions

We identified four genic targets that can act as possible sites for chromosomal inversions. *AAEL006830 yellow* was chosen, as disruption of this gene causes a recessive, visible yellow phenotype in eggs and adults (Li et al., 2017). Genes on the p arm of chromosome 1 were screened to pair with yellow during inversions. 14 gene targets were identified by manually scanning Ensembl Metazoa gene map of chromosome 1. We then searched for possible phenotypes if genes were mutated on VectorBase and associated research on their orthologs in *D. melanogaster* on FlyBase. Three genes from the distal to proximal end of p arm were picked: *AAEL004193*, *AAEL013840* and *AAEL012549*. *AAEL004193* (R) is Rhophilin and has an ortholog in *D. melanogaster* involved in stress fiber regulation; *AAEL013840* (V) has an ortholog in *D. melanogaster* called VEGF-related factor 1 and is involved in cell migration; *AAEL012549* (F) is an ATPase and orthologs in *D. melanogaster* regulate flippase activity. All gene targets were mapped onto a physical genome map from Timoshevskiy et al. (2014) to recreate approximate distances between targets (**Fig. 1a**).

Using CHOPCHOP design tool, we designed three sgRNAs for each genic target to validate their activity. As seen in Kistler, Vosshall and Matthews (2015), the activity of sgRNAs can vary greatly within the same target site area. We injected an injection mix of four sgRNAs, one for each target, into *exuCas9* embryos. Genomic DNA was extracted from a pool of three pupae for three replicates. At least 50 *exuCas9* eggs were injected for each sgRNA injection mix with an average hatch rate of 22% (**Supp. Table 8**).

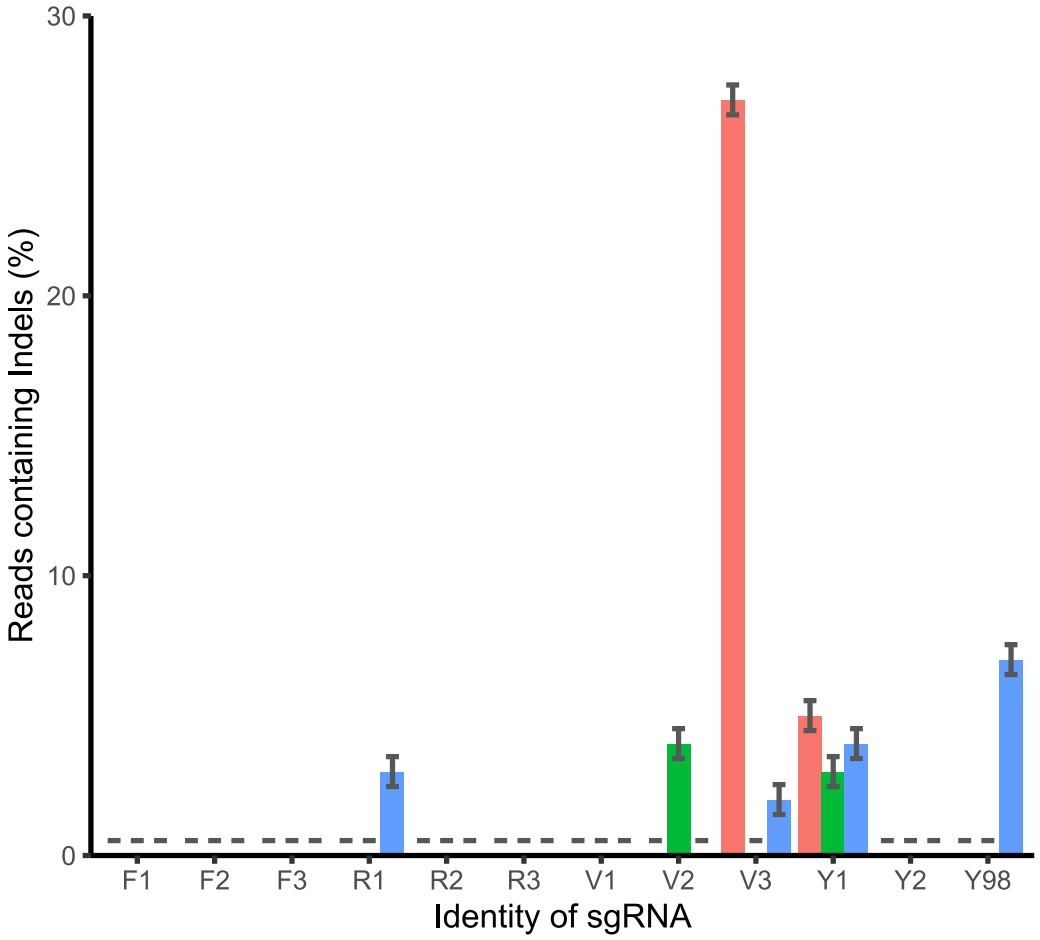

sgRNA	F1	F2	F3	R1	R2	R3	V1	V2	V3	Y1	Y2	Y98
Length (bp)	23	23	23	23	23	23	23	23	23	23	23	23
Indels (%)	0,0,0	0,0,0	0,0,0	0,0,3	0,0,0	0,0,0	0,0,0	0,4,0	27,0,2	5,3,4	0,0,0	0,0,7
Target	Exon 7			Exon 8			Exon 1			Exon 2		

Figure 2. Percentage of reads containing indels for all sgRNA designs across four genic targets. Each bar represents an average of sequence data from three G_0 pupae for a total of three replicates. Error bar represents standard error. Length of each sgRNA and percent indels across reads are shown in the table. All three sgRNAs targets the same approximate location on the gene within 200bp of each design.

4.3.2 Validation of sgRNA designs

sgRNA designs were validated by ICE analysis, which compared sequences at the target site to determine the percentage of reads that contain insertion or deletion (indel) mutations. *ExuCas9* expresses Cas9 endogenously, which can interact with injected sgRNAs to generate mutations. All sgRNAs were 23 bp in length. For F, all three sgRNA designs did not result in mutations and was not chosen as the inversion target. For R, only one sgRNA design resulted in 3% of mutation in one pooled sample (three pupae genomic DNA). We also did not choose R as an inversion target. All V sgRNA designs target exon 1 of the V gene, with V3 showing the highest sgRNA activity of 27%. We chose V3 as the sgRNA for generating DSB at the V gene. Upon comparisons between *ExuCas9* sequences with sequence from R3 and V1, we found that target sites were not identified. As the *LVP* genome (AaegL_5) was used to design sgRNAs, single nucleotide polymorphism in the *exuCas9* likely affected target site sequences. Thus, both designs of sgRNA were unable to bind to the target site and resulted in no mutations and no Cas9 activity. As the four genic targets were spread across the p arm, it is possible for deletions between two DSBs to occur that are missed by our sequencing analysis. However, the distance between these targets render it unlikely for large scale deletions to occur.

For *yellow*, we compared two sgRNA designs (Y1 and Y2) with the original sgRNA sequence Y98 used in Li et al. (2017). While Y98 did have the highest percentage of indels in one of the samples, Y1 showed activity across all three replicates. We chose V and *yellow* as our gene targets to generate inversion, with V3 and Y1 as the sgRNAs used for this work.

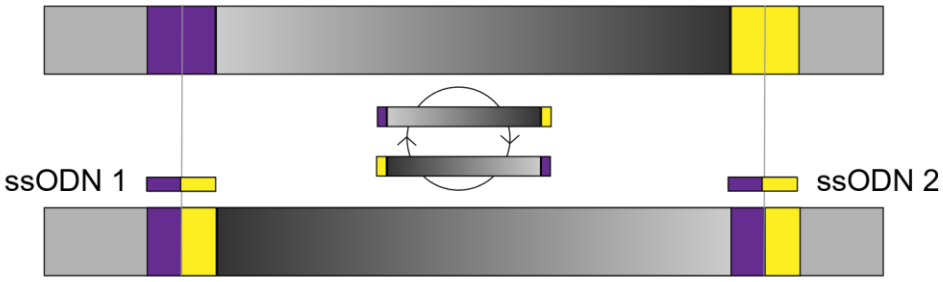

Figure 3. Schematic representation of chromosomal inversions generated by two DSBs, and repaired according to two "bi-genic" ssODN templates. All genes in the gradient regions are inverted and considered balanced.

4.3.3 Design of bi-genic ssODNs

HDR templates were created according to Iwata et al. (2016) and Dejima et al. (2018). ssODNs were created by combining the two ends of V and *yellow* together, creating a bi-genic ssODN (**Supp. Table 10**). The 100bp upstream region of both genes were combined into ssODN 1, while the 100bp downstream region of both genes were combined into ssODN 2. When a DSB is generated at both cut sites, HDR repair can use ssODNs as templates and repair these sites with the inverted chromosome (**Fig. 3**). All genes in between the two inverted sites are considered balanced, as recombination of any these genes will cause inviable offspring. The inversion between V and *yellow* is 65 Mb in size.

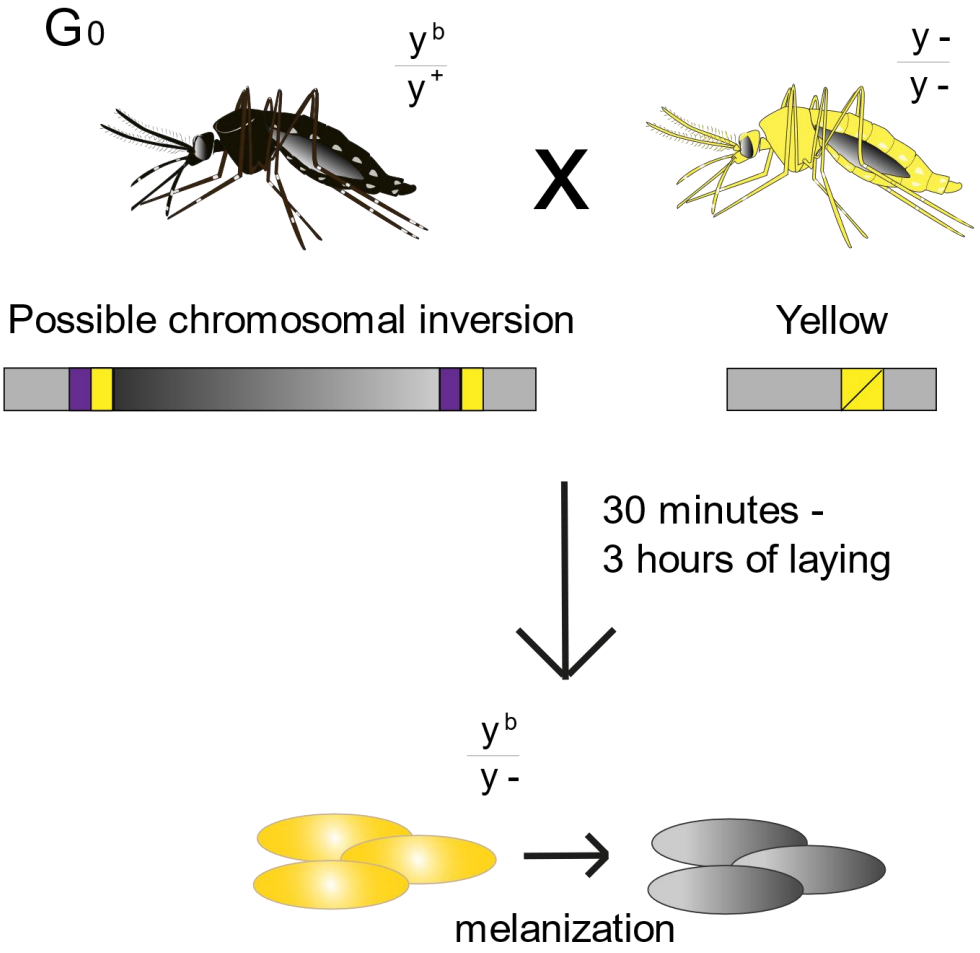

Figure 4. Schematic of crossing scheme for G_0s to identify possible chromosomal inversion. G_0 adults were crossed with yellow adults individually to lay eggs. Disruption to *yellow* gene due to NHEJ or HDR results in heterozygous G_0s. Eggs carrying possible inversion will be yellow in the first 30 minutes to 3 hours within egg laying, before melanization to black. Yellow eggs were screened at this time window for possible transgenic G_1s.

Table 1. Total count for G_0s injected with bi-genic ssODNs targeting V and *yellow*. "Yellow eggs" refer to number of G_0 crosses that laid yellow eggs before melanization. Transgenic rate is the number of G_0s that laid yellow eggs against total number of G_0s that survived to adulthood. All crosses that laid yellow eggs were from male G_0s.

	Eggs injected	Total Hatch	Survive to adulthood	Hatch Rate (%)	Yellow Eggs	Transgenic Rate (%)
Total	559	58	45	0.10	11	0.24

Table 2. Total counts for G_0s x *yellow* cross that gave eggs between female and male G_0s. "Laid eggs" refer to G_0 females that laid eggs individually, or *yellow* females that mated with G_0 males to lay eggs. "Yellow eggs" refers to the number of individuals that gave yellow eggs during melanization. "Yellow (%)" is the percentage of egg papers collected that had yellow eggs compared to total number of egg papers.

	Total number	Laid eggs	Laid eggs (%)	Yellow eggs	Yellow (%)
Females	31	8	25.81	0	0.00
Males	14	12	85.71	11	91.67

4.3.4 Screening eggs laid by G_0 x Yellow crosses to determine possible chromosomal inversion events

559 *ExuCas9* embryos were injected with V3 sgRNA, Y1 sgRNA and ssODN repair templates, across seven injections. Of note, only 58 embryos hatched successfully and 45 of which survived to adulthood (**Table 1**). All adult G_0s were treated as possible carriers of the balancer and crossed to *yellow* adults of the opposite sex. As the balancer should disrupt the copy of *yellow*, offspring carrying chromosomal

inversion should be recessive for *yellow* mutations and show a yellow phenotype. Mosaicism is possible as some G_0s might not have germline cells disrupted by chromosomal inversions. Those that laid yellow eggs were counted as possible inversion events. The yellow phenotype was only present during the first 30 minutes to 3 hours of eggs being laid (**Fig. 4**).

Of the 45 G_0s that were crossed to *yellow* and allowed to lay eggs, only 20 G_0s gave offspring. 25.81% of female G_0s laid eggs, where none of which were yellow. Surprisingly, 85.71% of *yellow* females crossed to G_0 males laid eggs, where 91.67% of egg laying events had yellow eggs during melanization. All eggs were observed to be yellow within the first 30 minutes of egg laying. We identified these 11 G_0 males as those carrying possible chromosomal inversions (**Table 2; Supp. Table 9**).

4.4 Discussion

4.4.1 *Yellow* phenotype restricted to egg development only

Our results shown here are promising first steps in generating possible balancers in *Ae. aegypti*, which to our knowledge is the first attempt for this type of work in mosquito genetics. Our work modeled the protocol by Dejima et al. (2018) in *C. elegans* and optimised the system for *Ae. aegypti*. We generated a 200bp ssODN template, as opposed to the 66bp template in *C. elegans*, to promote homology of the donor to the target site. The generation of a chromosomal inversion simultaneously disrupted *yellow*, which led to visible phenotypes that allowed effective screening. It should be noted that yellow phenotype was only observed in the eggs during melanization and not in adulthood. This differed from the generation of the original *yellow* mutants, which made use of NHEJ mutations at the *yellow* target site (Li et al., 2017). Egg melanization in *Ae. aegypti* is a complex process orchestrated by multiple proteins to ensure egg viability and prevent desiccation (Isoe et al., 2023). The possible inversion generated in our work could be a different mutation than the original yellow mutants, which explains the varying patterns of adult expression. Future work will make use of sequencing analysis at the target site to validate the types of mutations at *yellow*. Nonetheless, the generation of yellow eggs in the G_0 outcross still showed promise in creating chromosomal inversions.

4.4.2 All possible G_0 founders were males, majority of females did not give offspring

All yellow eggs were laid by outcrosses with G_0 males. This indicates that the possible inversion events that disrupted *yellow* likely happened in males only. It should be noted that the male determining region *Nix* and the *M* locus are also located near the centromere of Chromosome 1 (Turner et al., 2018), which is on the same chromosomal arm as *yellow*. It has been shown that disruption to *Nix* create male like offspring (Hall et al., 2015), and the positions near the centromere has lowered recombination rate (Juneja et al., 2014). In our work, we proposed to create chromosomal inversion in the p arm of Chromosome 1. These inversions are unlikely to be linked and inherited with *Nix*, due to a 69Mb distance between *yellow* and *Nix*. Thus, the explanation of this strong male bias could lie with the lowered fitness of females.

As noted in **Chapter 2**, we observed a strong male bias partly due to an overrepresentation of viable male founders. Cas9 toxicity could have affected the fecundity of female G0s but not males. While only 26% of females laid eggs, 86% of males gave offspring with the majority being yellow. Possible chromosomal inversion could have strongly impacted female fitness, leaving them unable to past on mutations to their offspring. This observation is supported by the sGD system that noted a disproportionate representation of males with less transgene expression (Anderson et al., 2024). Although the reason for a fitness cost to transgenic female remain unknown, it could affect how genetics work in *Ae. aegypti*. Further confirmation is needed to see if this male bias is inherited past G1s, and how this relates to chromosomal inversions.

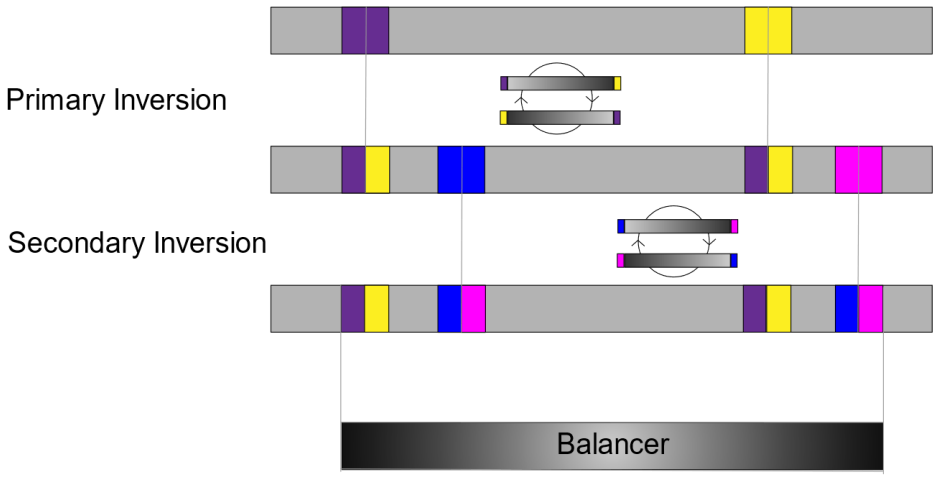

Figure 5. Schematic representation of primary and secondary inversions to generate a balancer. The first inversion involved the purple and yellow genes, while the second inversion involved the blue and pink genes. Note that one of the secondary inversion targets should be in between the primary inversions. All genes in the gradient regions are inverted and considered balanced.

4.4.3 Current work and future directions

At the time of completing this thesis, we have only collected the G_0 eggs and are outcrossing G_1s. To validate chromosomal inversions, we plan to use PCR to confirm bi-genic target sites. Sanger sequencing will then be done to ensure that HDR repair created inversions as expected by our design. We will be able to confirm our hypothesis for this work, which is that bi-genic donor template allows chromosomes to be inverted by HDR in *Ae. aegypti*. Once a primary inversion is sustained, a secondary inversion that inverts one of the target sites will be created (**Fig 5**). Visual fluorescence markers can then be integrated into the balancer to allow ease of screening by researchers. It is our hope that a balancer chromosome with double inversions can be created for *Ae. aegypti* and effectively balance mutations in Chromosome 1.

5 Overall conclusions

5.1.1 Conclusions for the genetic toolbox of Ae. aegypti

Our work in this thesis seek to expand the genetic toolbox of *Ae. aegypti*, which could benefit researchers studying these fascinating and potentially dangerous organisms. Across our results, we noticed a strong male bias in founders that led to the successful creation of transgenic strains. It is currently unknown whether males simply had a higher fitness, or if maternal deposition of Cas9 could potentially impact transgenes inheritance. Male mosquitoes are able to be batch mated with a pool of females, which provides an advantage over the number of offspring a male founder can give rise to in comparison to female founders. While female founders can be blood-fed multiple times, this is time- and effort- prohibitive and proved difficult in practise.

Across our work, we can now highlight a few key improvements that can be made to current workflow for transgenic mosquito generation. First, the screening of transient expression of the donor template in larvae can significantly reduce screening effort. This initial screening step can help discard individuals that are not likely to be founders, which reduces subsequent rearing effort and time. Second, we recommend separating transgenic crosses between males and female in the case of strong sex bias. We suggest focusing screening efforts on crosses with male founders that have given rise to offspring by outcrossing to multiple females. This can lower the risk of a transgene being lost if females with lowered fitness do not lay eggs. Third, advancements in endogenous Cas9 promoters should be used to maximize the chances of generating transgenic G0s. The *bgcn*-Cas9 transgenic strain (Anderson et

al., 2024) could be a promising successor to *exuCas9* (Li et al., 2017) in generating transgenic *Ae. aegypti* strains. Our work in the generation of a novel balancer chromosome shows great promise. A balancer chromosome can provide a new genetic tool with great ease of use to researchers generating and maintaining deleterious mutations in the mosquito. This can not only benefit the field, but also demonstrate the power of CRISPR/Cas9 in *Ae. aegypti* for large scale genome engineering.

5.1.2 Future work in *Ae. aegypti* genetics

Ae. aegypti has been an increasingly popular non-model organism in the past decade. While some work aimed to understand and alter the behavior of these mosquitoes, other effort has been made to improve gene drive systems and control their population. The history of precise CRISPR gene editing in *Ae.* aegypti ranges from the first instance of CRISPR/Cas9 adaptation in *Ae. aegypti* (Kistler, Vosshall and Matthews, 2015), the first effective gene drive system (Li et al., 2020) to the latest improvements to a split gene drive (Anderson et al., 2024). Gene drive work has also recently been an active area of development in the private, biotechnology sector with the emergence of Biocentis and continued efforts of Oxitec Ltd. These works have shown that CRISPR/Cas9 gene editing for *Ae. aegypti* remains a hugely complex area of active research. While some novel techniques like ReMOT control (Chaverra-Rodriguez et al., 2018) and DIPA-CRISPR (Shira et al., 2023) are proving to be potential contenders to traditional methods of gene editing, much work is still needed for their HDR repair to be optimised.

While the creation of robust gene drives has been successful in *Drosophila* and *Anopheles*, *Ae. aegypti* gene drive research is still restricted by their low HDR efficiency. Our results also show that strategies to improve gene drive in other systems do not directly translate to *Ae. aegypti*. This could be due to the unique nature of the *Ae. aegypti* genome. Not only is the *Ae. aegypti* genome is much larger than other Diptera, a recent study has shown that this large genome size is due to a high rate of propagation and low rate of elimination of TEs (Daron et al., 2024). It is unclear why Ae. aegypti has accumulated these excess copies of TEs in their genome. There are also vast areas of recombination deserts observed in the *Ae. aegypti* genome, where regions in all three chromosomes display a much lower recombination rate than expected (Chen et al., 2022). This large genome is filled with TEs but restrictive to recombination events, which could be a hurdle to gene editing and gene drive optimization. While some of these features might go under-appreciated in most gene drive work, they could have far-reaching consequences to how DNA damage can be repaired by *Ae. aegypti.* We believe that future work in gene drive application can uncover what makes the *Ae. aegypti* genome particularly challenging for HDR repair during DNA damage. While the yellow fever mosquitoes remain one of the most challenging non-model organisms to study, gene editing and gene drive applications is increasingly feasible.

Bibliography

Adelman, Z. N., Jasinskiene, N., Onal, S., Juhn, J., Ashikyan, A., Salampessy, M., MacCauley, T., & James, A. A. (2007). Nanos gene control DNA mediates developmentally regulated transposition in the yellow fever mosquito Aedes aegypti. *Proceedings of the National Academy of Sciences of the United States of America*, *104*(24), 9970–9975. https://doi.org/10.1073/pnas.0701515104

Alphey, L. (2014). Genetic control of mosquitoes. *Annual Review of Entomology*, *59*, 205–224. https://doi.org/10.1146/annurev-ento-011613-162002

Anderson, M. A. E., Gonzalez, E., Ang, J. X. D., Shackleford, L., Nevard, K., Verkuijl, S. A. N., Edgington, M. P., Harvey-Samuel, T., & Alphey, L. (2023). Closing the gap to effective gene drive in Aedes aegypti by exploiting germline regulatory elements. *Nature Communications*, *14*(1). https://doi.org/10.1038/s41467-023-36029-7

Anderson, M. A. E., Gonzalez, E., Edgington, M. P., Ang, J. X. D., Purusothaman, D. K., Shackleford, L., Nevard, K., Verkuijl, S. A. N., Harvey-Samuel, T., Leftwich, P. T., Esvelt, K., & Alphey, L. (2024). A multiplexed, confinable CRISPR/Cas9 gene drive can propagate in caged Aedes aegypti populations. *Nature Communications*, *15*(1). https://doi.org/10.1038/s41467-024-44956-2

Arensburger, P., Hice, R. H., Wright, J. A., Craig, N. L., & Atkinson, P. W. (2011). The mosquito Aedes aegypti has a large genome size and high transposable element load but contains a low proportion of transposon-specific piRNAs. *BMC Genomics*, *12*(1), 606. https://doi.org/10.1186/1471-2164-12-606

Aryan, A., Anderson, M. A. E., Myles, K. M., & Adelman, Z. N. (2013). TALEN-Based Gene Disruption in the Dengue Vector Aedes aegypti. *PLoS ONE*, *8*(3). https://doi.org/10.1371/journal.pone.0060082

Aryan, A., Myles, K. M., & Adelman, Z. N. (2014). Targeted genome editing in Aedes aegypti using TALENs. *Methods*, *69*(1), 38–45. https://doi.org/10.1016/j.ymeth.2014.02.008

Barrangou, R., & van Pijkeren, J. P. (2016). Exploiting CRISPR-Cas immune systems for genome editing in bacteria. *Current Opinion in Biotechnology*, *37*, 61–68. https://doi.org/10.1016/j.copbio.2015.10.003

Barrett, A. D. T., & Higgs, S. (2007). Yellow fever: A disease that has yet to be conquered. *Annual Review of Entomology*, *52*, 209–229. https://doi.org/10.1146/annurev.ento.52.110405.091454

Bassett, A. R., Tibbit, C., Ponting, C. P., & Liu, J. L. (2013). Highly Efficient Targeted Mutagenesis of Drosophila with the CRISPR/Cas9 System. *Cell Reports*, *4*(1), 220–228. https://doi.org/10.1016/j.celrep.2013.06.020

Burt, A. (2003). Site-specific selfish genes as tools for the control and genetic engineering of natural populations. *Proceedings of the Royal Society B: Biological Sciences*, *270*(1518), 921–928. https://doi.org/10.1098/rspb.2002.2319

Calvo, E., Walter, M., Adelman, Z. N., Jimenez, A., Onal, S., Marinotti, O., & James, A. A. (2005). Nanos (nos) genes of the vector mosquitoes, Anopheles gambiae, Anopheles stephensi and Aedes aegypti. *Insect Biochemistry and Molecular Biology*, *35*(7), 789–798. https://doi.org/10.1016/j.ibmb.2005.02.007

Champer, J., Buchman, A., & Akbari, O. S. (2016). Cheating evolution: Engineering gene drives to manipulate the fate of wild populations. *Nature Reviews Genetics*, *17*(3), 146–159. https://doi.org/10.1038/nrg.2015.34

Champer, J., Chung, J., Lee, Y. L., Liu, C., Yang, E., Wen, Z., Clark, A. G., & Messer, P. W. (2019). Molecular safeguarding of CRISPR gene drive experiments. *ELife*, *8*, 1–10. https://doi.org/10.7554/ELIFE.41439

Champer, J., Reeves, R., Oh, S. Y., Liu, C., Liu, J., Clark, A. G., & Messer, P. W. (2017). Novel CRISPR/Cas9 gene drive constructs reveal insights into mechanisms of resistance allele formation and drive efficiency in genetically diverse populations. *PLoS Genetics*, *13*(7), 1–18. https://doi.org/10.1371/journal.pgen.1006796

Chang, N., Sun, C., Gao, L., Zhu, D., Xu, X., Zhu, X., Xiong, J. W., & Xi, J. J. (2013). Genome editing with RNA-guided Cas9 nuclease in Zebrafish embryos. *Cell Research*, *23*(4), 465–472. https://doi.org/10.1038/cr.2013.45

Chaverra-Rodriguez, D., Macias, V. M., Hughes, G. L., Pujhari, S., Suzuki, Y., Peterson, D. R., Kim, D., McKeand, S., & Rasgon, J. L. (2018). Targeted delivery of CRISPR-Cas9 ribonucleoprotein into arthropod ovaries for heritable germline gene editing. *Nature Communications*, *9*(1), 1–11. https://doi.org/10.1038/s41467-018-05425-9

Chen, J. M., Cooper, D. N., Chuzhanova, N., Férec, C., & Patrinos, G. P. (2007). Gene conversion: Mechanisms, evolution and human disease. *Nature Reviews Genetics*, *8*(10), 762–775. https://doi.org/10.1038/nrg2193

Chen, S., Lee, L., Naila, T., Fishbain, S., Wang, A., Tomkinson, A. E., Lees-Miller, S. P., & He, Y. (2021). Structural basis of long-range to short-range synaptic transition in NHEJ. *Nature*, *593*(7858), 294–298. https://doi.org/10.1038/s41586-021-03458-7

Coates, C. J., Jasinskiene, N., Miyashiro, L., & James, A. A. (1998). Mariner transposition and transformation of the yellow fever mosquito, Aedes aegypti.

Proceedings of the National Academy of Sciences of the United States of America, *95*(7), 3748–3751. https://doi.org/10.1073/pnas.95.7.3748

Cobb, R. E., Wang, Y., & Zhao, H. (2015). High-Efficiency Multiplex Genome Editing of Streptomyces Species Using an Engineered CRISPR/Cas System. *ACS Synthetic Biology*, *4*(6), 723–728. https://doi.org/10.1021/sb500351f

Cong, L., Ran, F. A., Cox, D., Lin, S., Bareetto, R., Habib, N., … Zhang, F. (2013). Multiplex Genome Engineering Using CRISPR/Cas Systems. Science, 286(5446 (Dec.), 1893–1897.

Crown, K. N., Miller, D. E., Sekelsky, J., & Hawley, R. S. (2018). Local Inversion Heterozygosity Alters Recombination throughout the Genome. *Current Biology*, *28*(18), 2984-2990.e3. https://doi.org/10.1016/j.cub.2018.07.004

Crucs, S., Chatterjee, S. & Gavis, E. G. (2000). Overlapping but Distinct RNA Elements Control Repression and Activation of *nanos* Translation. *Cell, 5*(3), 457-467. https://doi.org/10.1016/S1097-2765(00)80440-2

Daron, J., Bergman, A., Lpez-Maestre, H. & Lambrechts, L. (2024) Atypical Landscape of Transposable Elements in the Large Genome of *Aedes aegypti*. *bioRxiv*. https://doi.org/10.1101/2024.02.07.579293

de Melo, E. S., & Wallau, G. L. (2020). Mosquito genomes are frequently invaded by transposable elements through horizontal transfer. *PLoS Genetics*, *16*(11), 1–26. https://doi.org/10.1371/journal.pgen.1008946

Degennaro, M., Mcbride, C. S., Seeholzer, L., Nakagawa, T., Dennis, J., Goldman, C., Jasinskiene, N., James, A. A. & Leslie, B.,Genetics, M. (2013). *HHS Public Access*. *498*(7455), 487–491. https://doi.org/10.1038/nature12206.orco

Dejima, K., Hori, S., Iwata, S., Suehiro, Y., Yoshina, S., Motohashi, T., & Mitani, S. (2018). An Aneuploidy-Free and Structurally Defined Balancer Chromosome Toolkit for Caenorhabditis elegans. *Cell Reports*, *22*(1), 232–241. https://doi.org/10.1016/j.celrep.2017.12.024

Diniz, D. F. A., De Albuquerque, C. M. R., Oliva, L. O., De Melo-Santos, M. A. V., & Ayres, C. F. J. (2017). Diapause and quiescence: Dormancy mechanisms that contribute to the geographical expansion of mosquitoes and their evolutionary success. *Parasites and Vectors*, *10*(1), 1–13. https://doi.org/10.1186/s13071-017-2235-0

Dong, S., Lin, J., Held, N. L., Clem, R. J., Passarelli, A. L., & Franz, A. W. E. (2015). Heritable CRISPR/Cas9-mediated genome editing in the yellow fever mosquito,

Aedes aegypti. *PLoS ONE*, *10*(3), 1–13. https://doi.org/10.1371/journal.pone.0122353

Doudna, J. A., & Charpentier, E. (2014). The new frontier of genome engineering with CRISPR-Cas9. *Science*, *346*(6213). https://doi.org/10.1126/science.1258096

Fuller, H. S. (1961). Aedes Aegypti: The Yellow Fever Mosquito. The American Journal of Tropical Medicine and Hygiene, 10(1), 112–113. https://doi.org/10.4269/ajtmh.1961.10.112

Gandhi, M., Evdokimova, V. N., Cuenco, K. T., Nikiforova, M. N., Kelly, L. M., Stringer, J. R., Bakkenist, C. J., & Nikiforov, Y. E. (2012). Homologous chromosomes make contact at the sites of double-strand breaks in genes in somatic G 0/G 1-phase human cells. *Proceedings of the National Academy of Sciences of the United States of America*, *109*(24), 9454–9459. https://doi.org/10.1073/pnas.1205759109

Gantz, V. M., Jasinskiene, N., Tatarenkova, O., Fazekas, A., Macias, V. M., Bier, E., & James, A. A. (2015). Highly efficient Cas9-mediated gene drive for population modification of the malaria vector mosquito Anopheles stephensi. *Proceedings of the National Academy of Sciences of the United States of America*, *112*(49), E6736–E6743. https://doi.org/10.1073/pnas.1521077112

Gratz, S. J., Cummings, A. M., Nguyen, J. N., Hamm, D. C., Donohue, L. K., Harrison, M. M., Wildonger, J., & O'connor-Giles, K. M. (2013). Genome engineering of Drosophila with the CRISPR RNA-guided Cas9 nuclease. *Genetics*, *194*(4), 1029–1035. https://doi.org/10.1534/genetics.113.152710

Gutschner, T., Haemmerle, M., Genovese, G., Draetta, G. F., & Chin, L. (2016). Post-translational Regulation of Cas9 during G1 Enhances Homology-Directed Repair. *Cell Reports*, *14*(6), 1555–1566. https://doi.org/10.1016/j.celrep.2016.01.019

Halstead, S. B. (2008). Dengue virus-mosquito interactions. *Annual Review of Entomology*, *53*, 273–291. https://doi.org/10.1146/annurev.ento.53.103106.093326

Hammond, A., Galizi, R., Kyrou, K., Simoni, A., Siniscalchi, C., Katsanos, D., Gribble, M., Baker, D., Marois, E., Russell, S., Burt, A., Windbichler, N., Crisanti, A., & Nolan, T. (2016). A CRISPR-Cas9 gene drive system targeting female reproduction in the malaria mosquito vector Anopheles gambiae. *Nature Biotechnology*, *34*(1), 78–83. https://doi.org/10.1038/nbt.3439

Hammond, A., Karlsson, X., Morianou, I., Kyrou, K., Beaghton, A., Gribble, M., Kranjc, N., Galizi, R., Burt, A., Crisanti, A., Nolan, T. (2021) Regulating the expression of gene drives is key to increasing their invasive potential and the mitigation of resistance. *PLoS Genet*,17(1):e1009321. https://doi.org/10.1371/journal.pgen.1009321

Handler, A. M., & Harrell, R. A. (1999). Germline transformation of Drosophila melanogaster with the piggyBac transposon vector. *Insect Molecular Biology*, *8*(4), 449–457. https://doi.org/10.1046/j.1365-2583.1999.00139.x

Hay, B. A., Chen, C. H., Ward, C. M., Huang, H., Su, J. T., & Guo, M. (2010). Engineering the genomes of wild insect populations: Challenges, and opportunities provided by synthetic Medea selfish genetic elements. *Journal of Insect Physiology*, *56*(10), 1402–1413. https://doi.org/10.1016/j.jinsphys.2010.05.022

Howden, S. E., McColl, B., Glaser, A., Vadolas, J., Petrou, S., Little, M. H., Elefanty, A. G., & Stanley, E. G. (2016). A Cas9 Variant for Efficient Generation of Indel-Free Knockin or Gene-Corrected Human Pluripotent Stem Cells. *Stem Cell Reports*, *7*(3), 508–517. https://doi.org/10.1016/j.stemcr.2016.07.001

Isoe, J., Simington, C. J., Oscherwitz, M. E., Peterson, A. J., Rascón, A. A., Massani, B. B., Miesfeld, R. L., & Riehle, M. A. (2023). Characterization of essential eggshell proteins from Aedes aegypti mosquitoes. *BMC Biology*, *21*(1), 1–24. https://doi.org/10.1186/s12915-023-01721-z

Iwata, S., Yoshina, S., Suehiro, Y., Hori, S., & Mitani, S. (2016). Engineering new balancer chromosomes in C. Elegans via CRISPR/Cas9. *Scientific Reports*, *6*, 1–8. https://doi.org/10.1038/srep33840

Jasinskiene, N., Coates, C. J., Benedict, M. Q., Cornel, A. J., Rafferty, C. S., James, A. A., & Collins, F. H. (1998). Stable transformation of the yellow fever mosquito, Aedes aegypti, with the Hermes element from the housefly. *Proceedings of the National Academy of Sciences of the United States of America*, *95*(7), 3743–3747. https://doi.org/10.1073/pnas.95.7.3743

Jiang, W., Brueggeman, A. J., Horken, K. M., Plucinak, T. M., & Weeks, D. P. (2014). Successful transient expression of Cas9 and single guide RNA genes in Chlamydomonas reinhardtii. *Eukaryotic Cell*, *13*(11), 1465–1469. https://doi.org/10.1128/EC.00213-14

Jinek, M., Chylinski, K., Fonfara, I., Hauer, M., Doudna, J. A., & Charpentier, E. (2012). *A Programmable Dual-RNA – Guided*. *337*(August), 816–821.

Juneja, P., Osei-Poku, J., Ho, Y. S., Ariani, C. V., Palmer, W. J., Pain, A., & Jiggins, F. M. (2014). Assembly of the Genome of the Disease Vector Aedes aegypti onto a Genetic Linkage Map Allows Mapping of Genes Affecting Disease Transmission. *PLoS Neglected Tropical Diseases*, *8*(1), 8. https://doi.org/10.1371/journal.pntd.0002652

Kandul, N. P., Liu, J., Bennett, J. B., Marshall, J. M., & Akbari, O. S. (2021). A confinable home-and-rescue gene drive for population modification. *ELife*, *10*, 1–25. https://doi.org/10.7554/eLife.65939

Kandul, N. P., Liu, J., Buchman, A., Gantz, V. M., Bier, E., & Akbari, O. S. (2020). Assessment of a split homing based gene drive for efficient knockout of multiple genes. *G3: Genes, Genomes, Genetics*, *10*(2), 827–837. https://doi.org/10.1534/g3.119.400985

Kaufman, T. C. (2017). A short history and description of Drosophila melanogaster classical genetics: Chromosome aberrations, forward genetic screens, and the nature of mutations. *Genetics*, *206*(2), 665–689. https://doi.org/10.1534/genetics.117.199950

Kistler, K. E., Vosshall, L. B., & Benjamin J M. (2017). Genome-engineering with CRISPR-Cas9 in the mosquito Aedes aegypti. *Physiology & Behavior*, *176*(12), 139–148. https://doi.org/10.1016/j.physbeh.2017.03.040

Kokoza, V., Ahmed, A., Wimmer, E. A., & Raikhel, A. S. (2001). Efficient transformation of the yellow fever mosquito Aedes aegypti using the piggyBac transposable element vector pBac[3xP3-EGFP afm]. *Insect Biochemistry and Molecular Biology*, *31*(12), 1137–1143. https://doi.org/10.1016/S0965-1748(01)00120-5

Koreman, G. T., Xu, Y., Hu, Q., Zhang, Z., Allen, S. E., Wolfner, M. F., Wang, B. & Han, C. (2021) Upgraded CRISPR/Cas9 Tools for Tissue-Specific Mutagenesis in *Drosophila. Proc Natl Acad Sci U S A*, *118*(14). https//doi.org/10.1073/pnas.2014255118

Krafsur, E. S. (1998). Sterile insect technique for suppressing and eradicating insect population: 55 years and counting. *Journal of Agricultural and Urban Entomology*, *15*(4), 303–317.

Krejci, L., Altmannova, V., Spirek, M., & Zhao, X. (2012). Homologous recombination and its regulation. *Nucleic Acids Research*, *40*(13), 5795–5818. https://doi.org/10.1093/nar/gks270

Kyrou, K., Hammond, A. M., Galizi, R., Kranjc, N., Burt, A., Beaghton, A. K., Nolan, T., & Crisanti, A. (2018). A CRISPR–Cas9 gene drive targeting doublesex causes complete population suppression in caged Anopheles gambiae mosquitoes. *Nature Biotechnology*, *36*(11), 1062–1071. https://doi.org/10.1038/nbt.4245

Labbe, G. M.C., Scaife, S., Morgan, S. A., Curtis, Z. H. and Alphey, L. (2012) Female-Specific Flightless (fsRIDL) Phenotype for Ctonrol of *Aedes albopictus*. *PLoS Nehl Top Dis*, *6*(7): e1724. http://doi.org/10.1371/journal.pntd.0001724

Lacour, G., Chanaud, L., L'Ambert, G., & Hance, T. (2015). Seasonal Synchronization of Diapause Phases in Aedes albopictus (Diptera: Culicidae). *PLoS ONE*, *10*(12), 1–16. https://doi.org/10.1371/journal.pone.0145311

Lee, C. S., Wang, R. W., Chang, H. H., Capurso, D., Segal, M. R., & Haber, J. E. (2016). Chromosome position determines the success of double-strand break repair. *Proceedings of the National Academy of Sciences of the United States of America*, *113*(2), E146–E154. https://doi.org/10.1073/pnas.1523660113

Li, G., Liu, D., Zhang, X., Quan, R., Zhong, C., Mo, J., Huang, Y., Wang, H., Ruan, X., Xu, Z., Zheng, E., Gu, T., Hong, L., Li, Z., Wu, Z., & Yang, H. (2018). Suppressing Ku70/Ku80 expression elevates homology-directed repair efficiency in primary fibroblasts. *International Journal of Biochemistry and Cell Biology*, *99*(January), 154–160. https://doi.org/10.1016/j.biocel.2018.04.011

Li, M., Bui, M., Yang, T., Bowman, C. S., White, B. J., & Akbari, O. S. (2017). Germline Cas9 expression yields highly efficient genome engineering in a major worldwide disease vector, Aedes aegypti. *Proceedings of the National Academy of Sciences of the United States of America*, *114*(49), E10540–E10549. https://doi.org/10.1073/pnas.1711538114

Li, M., Yang, T., Kandul, N. P., Bui, M., Gamez, S., Raban, R., Bennett, J., Sánchez C, H. M., Lanzaro, G. C., Schmidt, H., Lee, Y., Marshall, J. M., & Akbari, O. S. (2020). Development of a confinable gene drive system in the human disease vector aedes aegypti. *ELife*, *9*, 1–22. https://doi.org/10.7554/eLife.51701

Lieber, M. R. (2011). The mechanism of DSB repair by the NHEJ. *Annual Review of Biochemistry*, *79*(3), 181–211. https://doi.org/10.1146/annurev.biochem.052308.093131.The

Liesch, J., Bellani, L. L., & Vosshall, L. B. (2013). Functional and Genetic Characterization of Neuropeptide Y-Like Receptors in Aedes aegypti. *PLoS Neglected Tropical Diseases*, *7*(10). https://doi.org/10.1371/journal.pntd.0002486

Lin, C. C., & Potter, C. J. (2016). Editing transgenic DNA components by inducible gene replacement in Drosophila melanogaster. *Genetics*, *203*(4), 1613–1628. https://doi.org/10.1534/genetics.116.191783

Lin, S., Staahl, B. T., Alla, R. K., & Doudna, J. A. (2014). Enhanced homology-directed human genome engineering by controlled timing of CRISPR/Cas9 delivery. *ELife*, *3*, e04766. https://doi.org/10.7554/eLife.04766

Liu, M., Rehman, S., Tang, X., Gu, K., Fan, Q., Chen, D., & Ma, W. (2019). Methodologies for improving HDR efficiency. *Frontiers in Genetics*, *10*(JAN), 1–9. https://doi.org/10.3389/fgene.2018.00691

Lo, I. (2021). Improving genetic efficiency in *Aedes aegypti* mosquitoes via germline Cas9. *UBC Honors Animal Biology*. http://mosquitolab.zoology.ubc.ca/assets/pdf/IvanLo-Honours-2021.pdf

Lo, I. H. Y. and Matthews, B. J. Design and validation of guide RNAs for CRISPR-Cas9 genome editing in mosquitoes. *Cold Spring Harb Protoc.* http://doi.org/10.1101/pdb.top107688

Lobo, N. F., Hua-Van, A., Li, X., Nolen, B. M., & Fraser, M. J. (2002). Germ line transformation of the yellow fever mosquito, Aedes aegypti, mediated by transpositional insertion of a piggyBac vector. *Insect Molecular Biology*, *11*(2), 133–139. https://doi.org/10.1046/j.1365-2583.2002.00317.x

López Del Amo, V., Bishop, A. L., Sánchez C, H. M., Bennett, J. B., Feng, X., Marshall, J. M., Bier, E., & Gantz, V. M. (2020). A transcomplementing gene drive provides a flexible platform for laboratory investigation and potential field deployment. *Nature Communications*, *11*(1). https://doi.org/10.1038/s41467-019-13977-7

Ma, H., Tu, L.-C., Naseri, A., Huisman, M., Zhang, S., Grunwald, D., & Pederson, T. (2016). CRISPR-Cas9 nuclear dynamics and target recognition in living cells. J Cell Biol, 214(5), 529–537. https://doi.org/10.1083/JCB.201604115

Marshall, J. M., Buchman, A., Sánchez, C. H. M., & Akbari, O. S. (2017). Overcoming evolved resistance to population-suppressing homing-based gene drives. *Scientific Reports*, *7*(1), 1–12. https://doi.org/10.1038/s41598-017-02744-7

Marshall, J. M., Raban, R. R., Kandul, N. P., Edula, J. R., León, T. M., & Akbari, O. S. (2019). Winning the tug-of-war between effector gene design and pathogen evolution in vector population replacement strategies. *Frontiers in Genetics*, *10*(OCT), 1–12. https://doi.org/10.3389/fgene.2019.01072

Matthews, B. J., Dudchenko, O., Kingan, S. B., Koren, S., Antoshechkin, I., Crawford, J. E., Glassford, W. J., Herre, M., Redmond, S. N., Rose, N. H., Weedall, G. D., Wu, Y., Batra, S. S., Brito-Sierra, C. A., Buckingham, S. D., Campbell, C. L., Chan, S., Cox, E., Evans, B. R., … Vosshall, L. B. (2018). Improved reference genome of Aedes aegypti informs arbovirus vector control. *Nature*, *563*(7732), 501–507. https://doi.org/10.1038/s41586-018-0692-z

McBride, C. S., Baier, F., Omondi, A. B., Spitzer, S. A., Lutomiah, J., Sang, R., Ignell, R. and Vosshall, L. B. (2014) Evolution of mosquito preference for humans linked to an odorant receptor. *Nature*, 515(7526): 222 – 7. https://doi.org/10.1038/nature13964

McMeniman, C. J., Corfas, R. A., Matthews, B. J., Ritchie, S. A., & Vosshall, L. B. (2014). Multimodal integration of carbon dioxide and other sensory cues drives

mosquito attraction to humans. *Cell*, *156*(5), 1060–1071. https://doi.org/10.1016/j.cell.2013.12.044

Miller, D. E., Cook, K. R., Arvanitakis, A. V., & Hawley, R. S. (2016a). Third chromosome balancer inversions disrupt protein-coding genes and influence distal recombination events in Drosophila melanogaster. *G3: Genes, Genomes, Genetics*, *6*(7), 1959–1967. https://doi.org/10.1534/g3.116.029330

Miller, D. E., Cook, K. R., Kazemi, N. Y., Smith, C. B., Cockrell, A. J., Hawley, R. S., & Bergman, C. M. (2016b). Rare recombination events generate sequence diversity among balancer chromosomes in Drosophila melanogaster. *Proceedings of the National Academy of Sciences of the United States of America*, *113*(10), E1352–E1361. https://doi.org/10.1073/pnas.1601232113

Miller, D. E., Cook, K. R., & Scott Hawley, R. (2019). The joy of balancers. *PLoS Genetics*, *15*(11), 1–8. https://doi.org/10.1371/journal.pgen.1008421

Moreira, L. A., Iturbe-Ormaetxe, I., Jeffery, J. A., Lu, G., Pyke, A. T., Hedges, L. M., Rocha, B. C., Hall-Mendelin, S., Day, A., Riegler, M., Hugo, L. E., Johnson, K. N., Kay, B. H., McGraw, E. A., van den Hurk, A. F., Ryan, P. A., & O'Neill, S. L. (2009). A Wolbachia Symbiont in Aedes aegypti Limits Infection with Dengue, Chikungunya, and Plasmodium. *Cell*, *139*(7), 1268–1278. https://doi.org/10.1016/j.cell.2009.11.042

Mota, M. B. S., Carvalho, M. A., Monteiro, A. N. A., & Mesquita, R. D. (2019). DNA damage response and repair in perspective: Aedes aegypti, Drosophila melanogaster and Homo sapiens. *Parasites and Vectors*, *12*(1), 1–20. https://doi.org/10.1186/s13071-019-3792-1

Muller, H. J. (1918). Genetic Variability, Twin Hybrids and Constant Hybrids, in a Case of Balanced Lethal Factors. *Genetics*, *3*(5), 422–499. https://doi.org/10.1093/genetics/3.5.422

Muron, S., Kucera, S., Oliver, B., & Benner, L. (2022). Creation of a new Drosophila melanogaster X chromosome balancer, First Multiple 8 (FM8), using the CRISPR/Cas9 gene-editing system. *MicroPublication Biology*, *8*(Muller 1918), 9–12. http://hpc.nih.gov

Nambiar, T. S., Baudrier, L., Billon, P., & Ciccia, A. (2022). CRISPR-based genome editing through the lens of DNA repair. *Molecular Cell*, *82*(2), 348–388. https://doi.org/10.1016/j.molcel.2021.12.026

Nene, V., Wortman, J. R., Lawson, D., Haas, B., Kodira, C., Tu, Z., Loftus, B., Xi, Z., Megy, K., Grabherr, M., Ren, Q., Zdobnov, E. M., Lobo, N. F., Campbell, K. S., Brown, S. E., Bonaldo, M. F., Zhu, J., Sinkins, S. P., Hogenkamp, D. G., …

Severson, D. W. (2007). Genome sequence of Aedes aegypti, a major arbovirus vector. *Science*, *316*(5832), 1718–1723. https://doi.org/10.1126/science.1138878

Otte, M., Netschitailo, O., Kaftanoglu, O., Wang, Y., Page, R. E., & Beye, M. (2018). Improving genetic transformation rates in honeybees. *Scientific Reports*, *8*(1), 1–6. https://doi.org/10.1038/s41598-018-34724-w

Paix, A., Folkmann, A., Goldman, D. H., Kulaga, H., Grzelak, M. J., Rasoloson, D., … Seydoux, G. (2017). Precision genome editing using synthesis-dependent repair of Cas9-induced DNA breaks. *Proceedings of the National Academy of Sciences of the United States of America*, 114(50), E10745–E10754. https://doi.org/10.1073/pnas.1711979114

Phuc, H., Andreasen, M. H., Burton, R. S., Vass, C., Epton, M. J., Pape, G., Fu, G., Condon, K. C., Scaife, S., Donnelly, C. A., Coleman, P. G., White-Cooper, H., & Alphey, L. (2007). Late-acting dominant lethal genetic systems and mosquito control. *BMC Biology*, *5*, 1–11. https://doi.org/10.1186/1741-7007-5-11

Reid, W., Williams, A. E., Sanchez-Varga, I., Lin, J., Juncu, R., Olson, K. E., & Franz, A. W. E. (2022). Assessing single-locus CRISPR/Cas9-based gene drive variants in the mosquito Aedes aegypti via single-generation crosses and modeling. *G3: Genes, Genomes, Genetics*, *12*(12). https://doi.org/10.1093/g3journal/jkac280

Ren, X., Sun, J., Housden, B. E., Hu, Y., Roesel, C., Lin, S., Liu, L. P., Yang, Z., Mao, D., Sun, L., Wu, Q., Ji, J. Y., Xi, J., Mohr, S. E., Xu, J., Perrimon, N., & Ni, J. Q. (2013). Optimized gene editing technology for Drosophila melanogaster using germ line-specific Cas9. *Proceedings of the National Academy of Sciences of the United States of America*, *110*(47), 19012–19017. https://doi.org/10.1073/pnas.1318481110

Richardson, C. D., Ray, G. J., DeWitt, M. A., Curie, G. L., & Corn, J. E. (2016). Enhancing homology-directed genome editing by catalytically active and inactive CRISPR-Cas9 using asymmetric donor DNA. *Nature Biotechnology*, *34*(3), 339–344. https://doi.org/10.1038/nbt.3481

Rozen-Gagnon, K., Yi, S., Jacobson, E., Novack, S., & Rice, C. M. (2021). A selectable, plasmid-based system to generate CRISPR/Cas9 gene edited and knock-in mosquito cell lines. *Scientific Reports*, *11*(1), 1–14. https://doi.org/10.1038/s41598-020-80436-5

Ryazansky, S.S., Chen, C., Potters, M., Naumenko, A. N., Lukyanchikova, V., Masri, R. A., Brusentosov, I. I., Karagodin, D. A., Yuchenko, A. A., dos Anjos, V. L., Haba, Y., Rose, N. H., Hoffman, J., Guo, R., Menna, T., Kelley, M., Ferrill, E., Schultz, K. E., Qi, Y., Sharma, A., Deschamps, S., Llaca, V., Mao, C., Murphy, T. D. …

Sharakhova, M.V. (2024) The chromosome-scale genome assembly for the West Nile vector Culex quinquefasciatus uncovers patterns of genome evolution in mosquitoes. *BMC Biol,* 22, 16. https://doi.org/10.1186/s12915-024-01825-0

Savic, N., Ringnalda, F. C. A. S., Lindsay, H., Berk, C., Bargsten, K., Li, Y., Neri, D., Robinson, M. D., Ciaudo, C., Hall, J., Jinek, M., & Schwank, G. (2018). Covalent linkage of the DNA repair template to the CRISPR-Cas9 nuclease enhances homology-directed repair. *ELife*, *7*, 1–18. https://doi.org/10.7554/eLife.33761

Scott, T. W., & Takken, W. (2012). Feeding strategies of anthropophilic mosquitoes result in increased risk of pathogen transmission. *Trends in Parasitology*, *28*(3), 114–121. https://doi.org/10.1016/j.pt.2012.01.001

Sekelsky, J. (2017). DNA repair in Drosophila: Mutagens, models, and missing genes. *Genetics*, *205*(2), 471–490. https://doi.org/10.1534/genetics.116.186759

Sentmanat, M. F., Peters, S. T., Florian, C. P., Connelly, J. P., & Pruett-Miller, S. M. (2018). A Survey of Validation Strategies for CRISPR-Cas9 Editing. *Scientific Reports*, *8*(1), 1–8. https://doi.org/10.1038/s41598-018-19441-8

Shankar, S., Tauxe, G. M., Spikol, E. D., Li, M., Akbari, O. S., Giraldo, D., & McMeniman, C. J. (2021). Synergistic Coding of Carbon Dioxide and a Human Sweat Odorant in the Mosquito Brain. *BioRxiv*, 2020.11.02.365916. https://www.biorxiv.org/content/10.1101/2020.11.02.365916v2%0Ahttps://www.biorxiv.org/content/10.1101/2020.11.02.365916v2.abstract

Shirai, Y., Piulachs, M. D., Belles, X., & Daimon, T. (2022). DIPA-CRISPR is a simple and accessible method for insect gene editing. *Cell Reports Methods*, *2*(5), 100215. https://doi.org/10.1016/j.crmeth.2022.100215

Shirai, Y., Takahashi, M., Ote, M., Kanuka, H., & Daimon, T. (2023). DIPA-CRISPR gene editing in the yellow fever mosquito Aedes aegypti (Diptera: Culicidae). *Applied Entomology and Zoology*, *58*(3), 273–278. https://doi.org/10.1007/s13355-023-00831-y

Song, F., & Stieger, K. (2017). Optimizing the DNA Donor Template for Homology-Directed Repair of Double-Strand Breaks. *Molecular Therapy Nucleic Acids*, *7*(June), 53–60. https://doi.org/10.1016/j.omtn.2017.02.006

Srivastava, M., Nambiar, M., Sharma, S., Karki, S. S., Goldsmith, G., Hegde, M., Kumar, S., Pandey, M., Singh, R. K., Ray, P., Natarajan, R., Kelkar, M., De, A., Choudhary, B., & Raghavan, S. C. (2012). An inhibitor of nonhomologous end-joining abrogates double-strand break repair and impedes cancer progression. *Cell*, *151*(7), 1474–1487. https://doi.org/10.1016/j.cell.2012.11.054

Stern, D. L. (2022). Transgenic tools for targeted chromosome rearrangements allow construction of balancer chromosomes in non-melanogaster Drosophila species. *G3: Genes, Genomes, Genetics*, *12*(4). https://doi.org/10.1093/g3journal/jkac030

Sternberg, S. H., Redding, S., Jinek, M., Greene, E. C., & Doudna, J. A. (2014). DNA interrogation by the CRISPR RNA-guided endonuclease Cas9. *Nature*, 507: 62-67. https://doi.org/ 10.1038/nature13011

Sun, D., Guo, Z., Liu, Y., & Zhang, Y. (2017). Progress and prospects of CRISPR/Cas systems in insects and other arthropods. *Frontiers in Physiology*, *8*(SEP), 1–22. https://doi.org/10.3389/fphys.2017.00608

Sun, P., Nie, K., Zhu, Y., Liu, Y., Wu, P., Liu, Z., Du, S., Fan, H., Chen, C. H., Zhang, R., Wang, P., & Cheng, G. (2020). A mosquito salivary protein promotes flavivirus transmission by activation of autophagy. *Nature Communications*, *11*(1), 1–15. https://doi.org/10.1038/s41467-019-14115-z

Suzuki, H., Saba, R., Sada, A. & Saga, Y. (2010). The Nanos3-3'UTR is required for germ cell specific NANOS3 expression in mouse embryos. *PLoS One*, 18, *5(2)*:e9300. https://doi.org/10.1371/journal.pone.0009300

Tang, X. D., Gao, F., Liu, M. J., Fan, Q. L., Chen, D. K., & Ma, W. T. (2019). Methods for enhancing clustered regularly interspaced short palindromic repeats/Cas9-mediated homology-directed repair efficiency. Frontiers in Genetics, 10(JUN). https://doi.org/10.3389/fgene.2019.00551

Taning, C. N. T., Van Eynde, B., Yu, N., Ma, S., & Smagghe, G. (2017). CRISPR/Cas9 in insects: Applications, best practices and biosafety concerns. *Journal of Insect Physiology*, *98*, 245–257. https://doi.org/10.1016/j.jinsphys.2017.01.007

Tantowijoyo, W., Tanamas, S. K., Nurhayati, I., Setyawan, S., Budiwati, N., Fitriana, I., Ernesia, I., Wardana, D. S., Supriyati, E., Arguni, E., Meitika, Y., Prabowo, E., Andari, B., Green, B. R., Hodgson, L., Rancès, E., Ryan, P. A., O'neill, S. L., Anders, K. L., … Simmons, C. P. (2022). Aedes aegypti abundance and insecticide resistance profiles in the Applying Wolbachia to Eliminate Dengue trial. *PLoS Neglected Tropical Diseases*, *16*(4), 1–16. https://doi.org/10.1371/journal.pntd.0010284

Tazuke, S. I., Schulz, C., Gilboa, L., Fogarty, M., Mahowald, A. P., Guichet, A., Ephrussi, A., Wood, C. G., Lehmann, R., Fuller, M. T., Biologie, L. De, & Monod, I. J. (2002). *2002Cancer Y Cx43*. *2539*, 2529–2539.

Terradas, G., Buchman, A. B., Bennett, J. B., Shriner, I., Marshall, J. M., Akbari, O. S., & Bier, E. (2021). Inherently confinable split-drive systems in Drosophila. *Nature Communications*, *12*(1). https://doi.org/10.1038/s41467-021-21771-7

Timoshevskiy, V. A., Kinney, N. A., deBruyn, B. S., Mao, C., Tu, Z., Severson, D. W., Sharakhov, I. V., & Sharakhova, M. V. (2014). Genomic composition and evolution of Aedes aegypti chromosomes revealed by the analysis of physically mapped supercontigs. *BMC Biology*, *12*, 1–13. https://doi.org/10.1186/1741-7007-12-27

Timoshevskiy, V. A., Severson, D. W., deBruyn, B. S., Black, W. C., Sharakhov, I. V., & Sharakhova, M. V. (2013). An Integrated Linkage, Chromosome, and Genome Map for the Yellow Fever Mosquito Aedes aegypti. *PLoS Neglected Tropical Diseases*, *7*(2). https://doi.org/10.1371/journal.pntd.0002052

Turner, J., Krishna, R., Van'T Hof, A. E., Sutton, E. R., Matzen, K., & Darby, A. C. (2018). The sequence of a male-specific genome region containing the sex determination switch in Aedes aegypti. *Parasites and Vectors*, *11*(1), 3–7. https://doi.org/10.1186/s13071-018-3090-3

Vinogradova, E. B. (2007). Diapause in Aquatic Insects, with Emphasis on Mosquitoes. *Diapause in Aquatic Invertebrates Theory and Human Use*, *1987*, 83–113. https://doi.org/10.1007/978-1-4020-5680-2_5

Wakiyama, M., Matsumoto, T. & Yokoyama, S. (2005) *Drosophila* U6 Promoter-driven Short Hairpin RNAs Effectively Induce RNA Interference in Shneider 2 Cells, *Biochemical and Biophysical Research Communications, 331*(4), 1163-1170. https://doi.org/10.1016/j.bbrc.2005.03.240

Wang, G., Gamez, S., Raban, R. R., Marshall, J. M., Alphey, L., Li, M., Rasgon, J.L. Akbari, O. S. (2021) Combating Mosquito-borne Diseases Using Genetic Control Technologies. *Nature Communications*, *12*(4388). https://doi.org/10.1038/s41467-021-24654-z

Wang, H., Yang, H., Shivalila, C. S., Dawlaty, M. M., Cheng, A. W., & Zhang, F. (2013). Resource One-Step Generation of Mice Carrying Mutations in Multiple Genes by CRISPR / Cas-Mediated Genome Engineering. https://doi.org/10.1016/j.cell.2013.04.025

Wendt, K. E., Ungerer, J., Cobb, R. E., Zhao, H., & Pakrasi, H. B. (2016). CRISPR/Cas9 mediated targeted mutagenesis of the fast growing cyanobacterium Synechococcus elongatus UTEX 2973. *Microbial Cell Factories*, *15*(1), 1–8. https://doi.org/10.1186/s12934-016-0514-7

Wohl, M. P., & McMeniman, C. J. (2023). Batch Rearing Aedes aegypti. *Cold Spring Harbor Protocols*, *2023*(3), 172–181. https://doi.org/10.1101/pdb.prot108017

Xue, W., Chen, S., Yin, H., Tammela, T., Papagiannakopoulos, T., Joshi, N. S., … Jacks, T. (2014). CRISPR-mediated direct mutation of cancer genes in the mouse liver. Nature, 514(7522), 380–384. https://doi.org/10.1038/nature13589

Yang, D., Scavuzzo, M. A., Chmielowiec, J., Sharp, R., Bajic, A., & Borowiak, M. (2016). Enrichment of G2/M cell cycle phase in human pluripotent stem cells enhances HDR-mediated gene repair with customizable endonucleases. *Scientific Reports*, *6*(January), 1–15. https://doi.org/10.1038/srep21264

Yu, Guangchuang, (2023). Scatterpie. GitHub repository. https://github.com/GuangchuangYu/scatterpie

Zhan, Y., Alberto, D. A. S., Rush, C., Riffell, J. A. and Montell, C. (2021) Elimination of vision-guided target attraction in *Aedes aegypti* using CRISPR. *Current Biology*, (31), 4180 – 4187. https://doi.org/10.1016/j.cub.2021.07.003

Zhao, Z., Tian, D. & McBride, C. S. (2021) Development of a Pan-neuronal Genetic Driver in *Aedes aegypti* mosquitoes. *Cell Reports Methods, 1*(100042). https://doi.org/10.1016/j.crmeth.2021.100042

Appendix

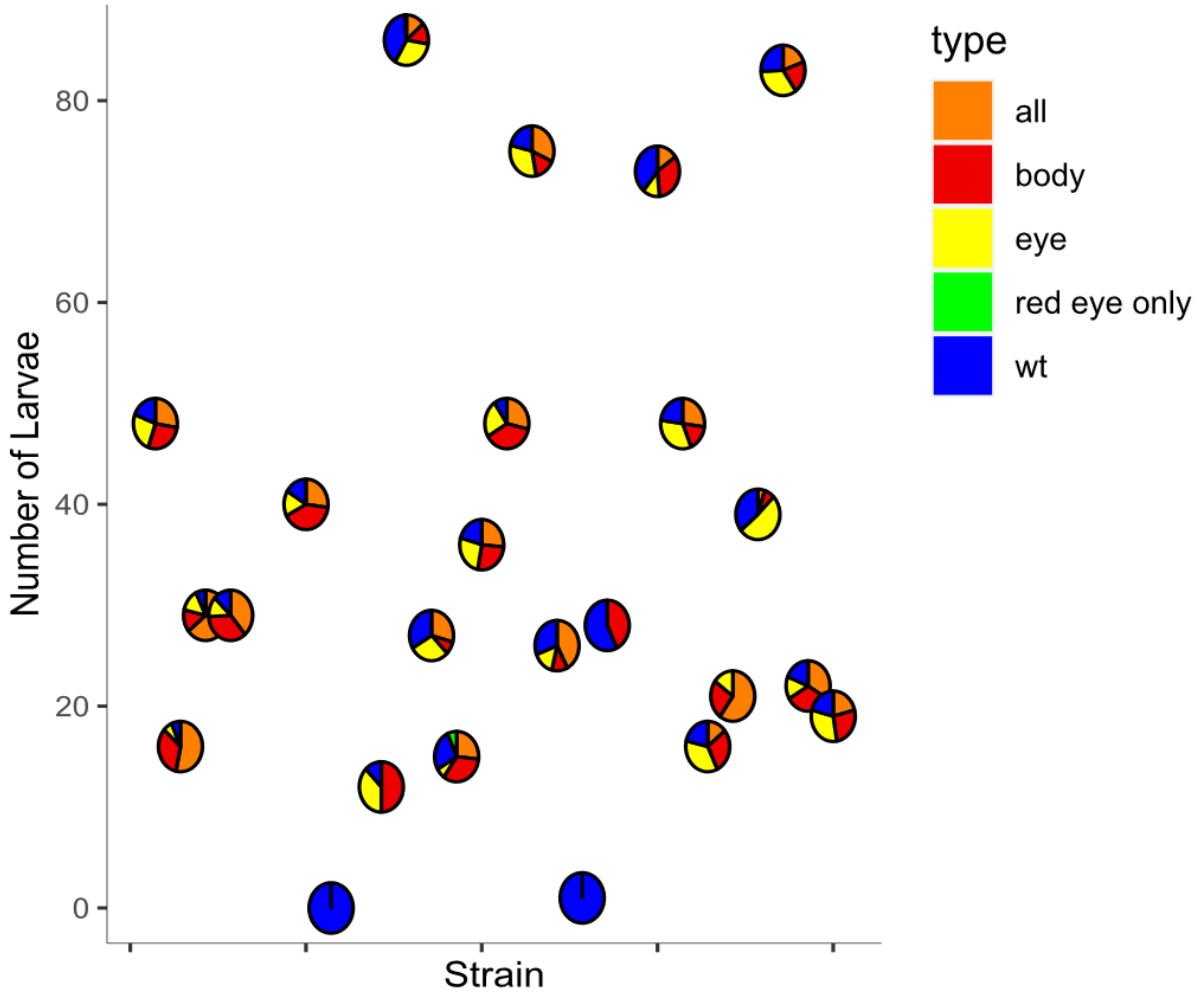

Supplementary Figure 1. Scatterpie chart showing distribution of larval expression in G6s. “Type” refers to the fluorescence expression of larvae: “all” stands for red body, red eye and blue eye fluorescence; “body” stands for red body fluorescence from *exuCas9* only; “eye” stands for red and blue eye fluorescence from TC integration only; “red eye” stands for red eye fluorescence from possible HDR event only; “wt” stands for wildtype without any fluorescence.

Supplementary Table 1. Primer sequences used in Chapter 2, 3 and 4

Chapter 2 primers	Sequence (5'-3')
sgRNAw (IR8a)	GGTGCGATCTTGACCCCCGGAGG

Chapter 3 primers	Sequence (5'-3')
Gibson U6 sgRNA fwd	GATCAATTCGTTAACAGATCGAATGAAATCGCCCATCG
Gibson U6 sgRNA rev	GACGAACACAAAAAAAGCACCGACTCGG
Gibson donor fwd	GTGCTTTTTTTGTGTTCGTCGGATTTCG
Gibson donor rev	GCCGCAGATCAGTGTCGATCCCGTATGAAATTATC
Gibson pBAC fwd	GATCGACACTGATCTGCGGCCGCGGCTC
Gibson pBAC rev	GATCTGTTAACGAATTGATCCCCCGATCTGTTAAC
Ppk301 Larm Fwd	GTGAGGGTGGTGTCGAATTAACTCTT
Ppk301 Rarm Rev	CCAGCTCAAAGTCCAAAAACGAAACC
Cutcheck Fwd	TCACAGTATGGTGGAAGCTTGT
Cutcheck Rev	CTAGAACGACCGTGAGACCC
L arm Fwd	CTGGACATCACCTCCCACAAC
L arm Rev	CCTGTTTCTGGCGTCCATTC
R arm Fwd	GCTACTCAACCGTGTCACAG
R arm Rev	GCTGTATTCCGTCGCATTTCTC
Ppk301 sgRNA	GGTTGGCAGTTGAGTCCCGG

Chapter 4 primers	Sequence (5'-3')
F1 sgRNA	AACGTGTACAGATCCGTTCG
F2 sgRNA	CAGGCACGAGATGACCAGCG
F3 sgRNA	GGATCTGGAGCTGTACGACG
R1 sgRNA	CGTGTGCAACATCTCCGATG
R2 sgRNA	TTCTGCAGACGGATACACCG
R3 sgRNA	ACCCCAACCAGAGATGTCCA
V1 sgRNA	TGCGAACACGAAACGCACCT
V2 sgRNA	CAGTAAGGACGTGAAACGGG
V3 sgRNA	TAGTAGGCGTTGCCTTCCAG
Y1 sgRNA	GTACCCGACTGGGAGCAGGGTGG
Y2 sgRNA	TGTGTACCCGACTGGGAGCA

Y98 sgRNA	GGCCAGTCACCGTGAATTCA
F1 seq Fwd	CGGAGGATAAGCTGCATACTTT
F1 seq Rev	TCATTTTGTTGCTCACCATCTT
F2 seq fwd	GAACGGATCTGTACACGTTCAA
F2 seq Rev	TCATTTTGTTGCTCACCATCTT
F3 seq Fwd	TACAACGATCGCTACAATCAGG
F3 seq Rev	TCCTCGTTAATATCCGAGGTGT
R1 seq Fwd	CCAGTGCAACAAGACCAACTAC
R1 seq Rev	AACCGTCCTACTTCAAGGAACA
R2 seq Fwd	CCAAGTTTACGATCTCCCTGAC
R2 seq Rev	TTCCGTTCTGTTCGCTATTGTA
R3 seq Fwd	CATCACCGATACGAGACAGGTA
R3 seq Rev	AAGTAGACCCCCAGACTTCGAT
V1 seq Fwd	GCATGGCTAATTGGTTCAAGAT
V1 seq Rev	CTTGCTTTGTGCACTTGAAATC
V2 seq Fwd	GCTGGTCCTGATCAGTGTTTTT
V2 seq Rev	CTTAGGTTGAAGCGAAGGTCTC
V3 seq Fwd	GATTTCAAGTGCACAAAGCAAG
V3 seq Rev	CCTTACTGATGACGTTGTAGCG
Y1 seq Fwd	TGGACTACAGCGATGTCAACTT
Y1 seq Rev	CTGTGTACTTGGTGACAGGGG
Y2 seq Fwd	TGGACTACAGCGATGTCAACTT
Y2 seq Rev	CTGTGTACTTGGTGACAGGGG
Y98 seq Fwd	CGGTTCGAGCATAGTTTCTTCT
Y98 seq Rev	GGTGAACTTGTGGAAGCTCTCT

Supplementary Table 2. Number of hatched G0s and Number of transient larvae in Chapter 2 Helper Plasmid. Egg and larvae counted over multiple injection events for helper strain and *exuCas9* strain. Number of transients refers to larvae with tail transient expression. Rates were counted as hatched larvae or transient expression larvae over total number of larvae.

IR8a sg1w gRNA/Donor > exu-Cas9 strain	Number of eggs	Number of Larvae	Hatch rate (%)	Number of transient	Numer of non-transient	Transient rate (%)
1	127	36	28%	14	22	39%
2	111	17	15%	15	2	88%
3	127	44	35%	15	29	34%
4	137	37	27%	26	11	70%
5	98	7	7%	3	4	43%
6	83	19	23%	9	10	47%
Total	683	160	23.43%	82	78	51%
IR8a sg1w gRNA/Donor + Nos helper > LVPib12	**Number of eggs**	**Number of Larvae**	**Hatch rate (%)**	**Number of transient**	**Numer of non-transient**	**Transient rate (%)**
1	100	25	25%	12	13	48%
2	119	25	21%	13	12	52%
3	169	62	37%	31	31	50%
4	104	17	16%	4	13	24%
Total	492	129	26.22%	60	69	47%
IR8a sg1w gRNA/Donor + Zpg helper > LVPib12	**Number of eggs**	**Number of Larvae**	**Hatch rate (%)**	**Number of transient**	**Numer of non-transient**	**Transient rate (%)**
1	101	24	24%	8	16	33%
2	113	40	35%	7	33	18%
3	204	54	26%	9	45	17%
4	25	1	4%	0	1	0%
Total	443	119	26.86%	24	95	20%

Supplementary Table 3. Count for larval expression pattern in generation of transgenic G1s from *exuCas9* G0 founders.

Cross	Eggs	Hatched	DsRed + CFP -	DsRed + CFP +	Tail DsRed	Body DsRed	hatch rate (%)	positive rate (%)
1	62	15	0	0	0	0	24.19	0.0
2	117	24	0	0	0	0	20.51	0.0
3	98	11	5	0	0	4	11.22	45.5
4	112	4	0	0	0	0	3.57	0.0
5	N/A	N/A	N/A	N/A	N/A	N/A	N/A	N/A
6	92	17	6	0	4	3	18.48	35.3
7	N/A	N/A	N/A	N/A	N/A	N/A	N/A	N/A
8	21	3	2	0	2	0	14.29	66.7
9	N/A	N/A	N/A	N/A	N/A	N/A	N/A	N/A
10	78	2	0	0	0	0	2.56	0.0
11	57	0	0	0	0	0	0.00	N/A
12	114	35	0	0	0	33	30.70	0.0
13	117	10	0	0	0	5	8.55	0.0
14	111	2	0	0	0	0	1.80	0.0
15	44	1	0	0	0	0	2.27	0.0
16	116	7	0	0	0	4	6.03	0.0
17	114	4	0	0	0	2	3.51	0.0
18	118	33	0	0	0	28	27.97	0.0
19	137	65	0	0	0	65	47.45	0.0
20	103	5	0	0	0	2	4.85	0.0
21	122	7	0	0	0	7	5.74	0.0
22	127	1	0	0	0	1	0.79	0.0
23	13	0	0	0	0	0	0.00	N/A
24	117	6	0	0	0	4	5.13	0.0
25	111	1	0	0	0	0	0.90	0.0
26	78	4	0	0	0	2	5.13	0.0
27	N/A	N/A	N/A	N/A	N/A	N/A	N/A	N/A
28	109	27	0	0	0	18	24.77	0.0
29	130	7	0	0	0	3	5.38	0.0
30	125	15	0	0	0	10	12.00	0.0
31	143	24	0	0	0	24	16.78	0.0
32	N/A	N/A	N/A	N/A	N/A	N/A	N/A	N/A
33	73	0	0	0	0	0	0.00	N/A
34	70	1	0	0	0	1	1.43	0.0
35	85	6	0	0	0	6	7.06	0.0
36	102	1	0	0	0	1	0.98	0.0
37	76	0	0	0	0	0	0.00	N/A
38	91	16	0	0	0	15	17.58	0.0
39	146	10	0	0	0	10	6.85	0.0
40	140	21	0	0	0	21	15.00	0.0
41	N/A	N/A	N/A	N/A	N/A	N/A	N/A	N/A
42	N/A	N/A	N/A	N/A	N/A	N/A	N/A	N/A
43	N/A	N/A	N/A	N/A	N/A	N/A	N/A	N/A
44	N/A	N/A	N/A	N/A	N/A	N/A	N/A	N/A
45	65	14	0	0	0	14	21.54	0.0
46	91	25	0	0	0	25	27.47	0.0
47	140	18	0	0	0	17	12.86	0.0
48	N/A	N/A	N/A	N/A	N/A	N/A	N/A	N/A
49	130	12	0	0	0	12	9.23	0.0
50	124	1	0	0	0	0	0.81	0.0
51	136	6	0	0	0	1	4.41	0.0
52	108	3	0	0	0	0	2.78	0.0
53	78	0	0	0	0	0	0.00	0.0
54	104	17	0	0	0	13	16.35	0.0
55	N/A	N/A	N/A	N/A	N/A	N/A	N/A	N/A
56	151	11	0	0	0	11	7.28	0.0
57	N/A	N/A	N/A	N/A	N/A	N/A	N/A	N/A
58	100	36	0	0	0	33	36.00	0.0
59	N/A	N/A	N/A	N/A	N/A	N/A	N/A	N/A
60	N/A	N/A	N/A	N/A	N/A	N/A	N/A	N/A
61	139	28	0	0	0	24	20.14	0.0
62	N/A	N/A	N/A	N/A	N/A	N/A	N/A	N/A
63	111	4	0	0	0	2	3.60	0.0

Supplementary Table 4. Identity of parental crosses in Supplementary Table 3.

G0 parent identity	Cross
non dsRed , Transient G0 male (4) x WT female (20)	**1-10**
dsRed , Transient G0 male (27) x WT female (50)	**11-38**
dsRed , Transient G0 female (22) x WT male (50)	**39-57**
non dsRed , Transient G0 female (9) x WT male (50)	**58-63**

Supplementary Table 5. Larval expression pattern and number of hatch in G4s.
G4s are named as follows: G4, Female/Male which is the sex of the G3 parent and F/M which is the sex of the G2 parent, followed by the number of this offspring

G4 identity	all +	body	eye	WT	Number of hatch
G4 Male F1	8	7	6	9	30
G4 Male F2	9	16	7	1	33
G4 Female F5	44	39	0	0	83
G4 Male M13	6	24	4	0	34
G4 Male M2	2	1	7	4	14
G4 Male M1	17	18	0	0	35
G4 Female M5	1	1	0	0	2
G4 Female M4	18	28	4	4	54
G4 Female F7	7	18	12	9	46

Supplementary Table 6. Larval expression pattern in G5s. Besides phenotypes previously mentioned," adults" refer to larvae that have already emerged as adult and di not show specific fluorescence pattern; "thorax green" refers to green fluorescence patterns in the thorax of larvae; "blue tail" refers to blue fluorescence in the tail area of larvae; hatch rate was calculated by total number of larvae divided by number of eggs. Naming of G5 identity include name of G5 and parent identity shown in brackets.

G5 identity	eye	all +	WT	body +	adults	thorax green	blue tail	special	total	# of eggs	hatch rate
R1M5 (G4mF2all+)	5	5	7	3	0	0	0	0	20	31	0.65
R1F7 (G4mF2all+)	12	11	21	13	0	0	0	0	57	106	0.54
R1F14 (G4fF5all+)	5	5	3	10	0	0	0	0	23	32	0.72
R2F3 (G4fF5all+)	8	8	7	12	0	0	0	0	35	42	0.83
R2M11 (G4mM1 all+)	0	7	2	3	0	0	0	0	12	32	0.38
R2F21 (G4mM1all+)	5	15	9	23	0	0	0	0	52	54	0.96
R1F3 (EG4MF1)	30	0	11	0	0	17	0	0	58	66	0.88
R1F17 (G4mM2all+)	10	19	17	18	0	1	0	0	65	115	0.57
R2F7 (G4mM2all+)	10	8	8	12	0	6	0	0	44	83	0.53
R2M2 (EG4mF2)	3	0	7	0	0	0	0	1	11	31	0.35
R2F9 (EG4mM2)	7	0	10	0	0	0	0	0	17	30	0.57
R3F1 (G4mF1)	6	11	1	10	0	1	0	0	29	71	0.41
R3M4 (G4fM5)	3	5	3	4	0	0	0	0	15	31	0.48
R3F2 (G4mM13)	20	11	10	10	0	1	0	0	52	65	0.80
R2M1 (G4mF2)	2	2	0	0	0	0	0	0	4	40	0.10
R2M18 (G4mF2)	5	8	0	12	0	1	0	1	27	37	0.73
R2F4 (G4fF5)	0	0	0	0	0	0	0	0	0	13	0.00
R2M19 (G4mF2)	3	6	1	7	1	0	0	0	18	30	0.60
R2F13 (G4mM1)	0	2	0	2	2	0	0	0	6	11	0.55
R2F14 (G4mM1)	2	10	0	8	1	0	0	0	21	57	0.37
R2F15 (G4mM1)	4	15	1	18	0	0	0	0	38	42	0.90
R2F8 (G4mM2)	18	23	13	6	0	0	0	0	60	94	0.64
R4F14 (G4fM4)	0	0	0	0	0	0	0	0	0	71	0.00
R4F15 (G4fM4)	0	0	0	0	0	0	0	0	0	96	0.00
R4F17 (G4fF7)	12	17	8	8	3	2	0	0	50	76	0.66
R4F20 (EG4fF7)	30	0	12	0	0	15	0	0	57	142	0.40
R2F17 (G4mM1)	6	24	3	25	3	9	0	0	70	93	0.75
R3F3 (EG4M13)	21	6	5	20	0	12	3	0	67	88	0.76
R4M11 (EG4M13)	11	3	4	2	7	0	0	0	27	35	0.77
R5F3 (EG4M4)	27	0	10	0	0	14	0	0	51	91	0.56
R7M5 (EG4M4)	9	0	11	0	0	0	2	0	22	66	0.33
R4F2 (EG4F1)	8	0	1	0	5	0	0	0	14	19	0.74
R4F3 (EG4F1)	0	0	17	0	0	7	0	0	24	51	0.47
R4F19 (G4mF2)	7	7	6	9	0	3	0	0	32	63	0.51
R4F4 (G4fF5)	0	0	0	0	0	0	0	0	0	35	0.00
R4F6 (G4fF5)	0	0	0	0	0	0	0	0	0	70	0.00
R4F18 (G4fF7)	17	11	12	18	0	12	0	0	70	86	0.81
R5M4 (EG4fF7)	14	0	20	0	0	7	0	2	43	47	0.91
R5M6 (EG4fF7)	17	0	3	0	0	5	2	0	27	46	0.59
R4F7 (G4fF5)	0	2	9	1	0	3	0	0	15	33	0.45
R4F8 (G4fF5)	7	6	6	13	0	1	0	1	34	56	0.61
R4F10 (G4fF5)	2	7	7	8	0	0	0	0	24	62	0.39
R5F2 (G4fM4)	9	2	10	1	0	0	0	0	22	36	0.61
R5M7 (EG4fF7)	20	0	15	0	0	0	0	0	35	43	0.81
R7M1 (G4fM4)	8	13	14	5	0	0	0	0	40	96	0.42
R7M2 (G4fM4)	11	13	16	14	0	0	0	0	54	90	0.60
R6M2 (G4fF7)	11	6	6	11	0	0	0	0	34	62	0.55
R6M3 (G4fF7)	8	4	12	10	0	2	0	0	36	40	0.90
R6M4 (G4fF7)	22	12	17	14	0	0	0	0	65	87	0.75
R5F8 (EG4fF7)	22	14	23	9	0	2	0	0	70	93	0.75
R5F9 (EG4fF7)	4	20	11	25	0	4	0	0	64	131	0.49
R6F5 (EG4fF7)	26	0	23	0	0	3	0	0	52	152	0.34
R7M4 (EG4fF7)	27	1	22	0	0	0	0	0	50	89	0.56

Supplementary Table 7. Larval expression pattern of G6s. Explanation of the phenotypes can be referred to Supp. Table 6.

G6 identity	red eyes	eyes	all +	WT	body +	adult (N/A)	thorax green	blue tail	special	total	# of eggs	hatch rate
R3F1 all+ M	0	12	13	9	13	0	3	0	0	48	88	0.55
R2F3 all+ F	0	0	0	0	0	0	0	0	0	0	45	0.00
R1F14 all+ F	0	0	0	0	0	0	0	0	0	0	40	0.00
R1M5 all+ F	0	4	11	8	3	0	0	0	0	26	26	1.00
R2F17 all+ F	0	1	8	1	5	0	0	0	1	16	66	0.24
R3F3 all+ M	0	21	21	14	10	0	9	0	0	75	136	0.55
R5F2 all+ F	0	5	2	3	4	0	3	0	0	16	161	0.10
R4F17 all+ M	0	0	0	0	0	0	0	0	0	0	37	0.00
R4F8 all+ M	0	6	10	6	15	0	3	0	0	40	91	0.44
R3F13 all+ F	0	4	18	2	4	0	1	0	0	29	117	0.25
R4F18 all+ F	0	3	0	1	4	0	2	1	0	12	14	0.86
R7M1 all+ inbred	0	3	12	0	5	0	1	0	0	21	272	0.08
R7M1 all+ M	0	20	2	14	3	0	0	0	0	39	47	0.83
R7M1 all+ F	0	28	16	21	17	0	1	0	0	83	174	0.48
R2F13 all+ F	0	4	12	4	11	0	0	0	0	29	43	0.67
R3M4 all+ F	0	9	11	28	24	0	1	0	0	73	197	0.37
R3M4 all+ M	0	16	13	11	8	0	0	0	0	48	48	1.00
R1F7 all+ F	0	0	0	1	0	0	0	0	0	1	25	0.04
R1F7 all+ M	0	0	0	16	12	0	0	0	0	28	28	1.00
R2M18 all+ F	0	0	0	0	0	0	0	0	0	0	32	0.00
R3F2 all+ F	0	9	9	7	9	0	2	0	0	36	135	0.27
R3F2 all+ M	0	10	12	4	16	0	6	0	0	48	72	0.67
R1F14 all+ M	0	0	0	27	0	0	0	0	0	0	37	0.00
R6M4 all+ F	1	27	12	35	12	0	3	0	0	86	196	0.44
R6M4 all+ M	0	7	7	8	2	0	3	0	0	27	138	0.20
R6M2 all+ F	1	1	4	4	5	0	0	0	0	15	120	0.13
R7M2 all+ F	0	3	7	4	7	0	1	0	0	22	146	0.15
R7M2 all+ M	0	6	4	4	5	0	0	0	0	19	125	0.15

Supplementary Table 8. Injection of mix of sgRNA in *exuCas9* to validate their activity.

ExuCas9	Eggs injected	Larvae hatched	Pupae collected	Hatch rate (%)	Identity
sgRNA mix 1	50	11	9	22	Y98 R1 F1 V1
sgRNA mix 2	50	21	18	42	Y1 R2 F2 V2
sgNRA mix 3	50	19	15	38	Y2 R3 F3 V3
sgRNA mix 2 repeat	50	4	0	8	Y1 R2 F2 V2
sgNRNA mix 3 repeat	25	0	0	0	Y2 R3 F3 V3
Total	225	55	42		
Average				22	

Supplementary Table 9. Number of eggs hatched and subsequently gave yellow eggs during outcross for injection of bi-genic templates to generate chromosomal inversion.

Injection Number	Eggs injected	Hatch	Survive to adulthood	Hatch Rate (%)	Yellow Eggs	Transgenic Rate (%)
1	100	14	14	14.00	4	0.29
2	50	1	1	2.00	0	0
3	56	1	1	1.79	1	1
4	47	1	0	2.13	0	N/A
5	100	2	0	2.00	0	N/A
6	100	29	29	29.00	6	0.21
7	106	10	0	9.43	0	N/A
Total	559	58	45		11	0.24

Supplementary Table 10. ssODN template sequences used for yellow and V2

ssODN	Sequence (5'-3')
ssODN1	TACGCTGGAGCGGCTGTGTACTTGGTGACAGGGGCAACGGTTGG GGCGTACGAGGACGGGGTATAGCTGATGGGTTGTGTGTACCCGAC TGGGAGCAGGGCTGGAAGGCAACGCCTACTATGGGCGACGCATC CGTGGTGGCGGTAACAGTGCCAACCGCATGGTATACCCCAACGAA AATGAACGCTACAACGTCATCA
ssODN2	TACGCTGGAGCGGCTGTGTACTTGGTGACAGGGGCAACGGTTGG GGCGTACGAGGACGGGGTATAGCTGATGGGTTGTGTGTACCCGAC TGGGAGCAGGGCTGGAAGGCAACGCCTACTATGGGCGACGCATC CGTGGTGGCGGTAACAGTGCCAACCGCATGGTATACCCCAACGAA AATGAACGCTACAACGTCATCA